Abstract

The pipeline-riser systems needed to transport oil to the production facilities gives rise to an undesired flow regime known as slug flow. Slug flow usually occurs when you have a low point in the pipeline topography followed by an inclining section of pipe. These slugs can grow very large and often cause severe problems when they reach the production facility.

A lab scale Miniloop had been build to simulate severe slugging by a previous student.
A simple PI controller using the downstream pressure as measurement stabilized the process and eliminated the slugging. However this measurement can in many cases be unavailable.

A controllability analysis will show that the process can be stabilized by using a cascade configuration with a flow measurement in the inner loop and the upstream pressure in the outer loop. This thesis will document the changes done to the Miniloop in order to obtain the measurements needed for the cascade controller. To document this better a user manual has been written.

Two different cascade structures were tested on the Miniloop and simulated on the simplified slug model. A cascade controller using mass flow in the inner loop and downstream pressure in the outer loop managed to stabilize the process and eliminate the slugging. The cascade controller using only upstream measurement, with mass flow in the inner loop and the upstream pressure in the outer loop failed to stabilize the Miniloop. However it stabilized the system in the simulations. The reason the cascade controller failed to stabilize the Miniloop was because of the disturbances and the noise picture associated with the flow measurement. The result obtained from the experiments verifies the simplified slug model as a useful tool for control purposes.

Acknowledgement

Various people have been of assistance during the work and experiments on the Miniloop, as well as in the writing of this final report. I would therefore wish to thank the following people for their invaluable help and support.

- Supervisors Espen Storkaas and Heidi Sivertsen, for being there and for all the invaluable help they provided during the experimental phase of the thesis. A special thanks to Espen, for providing and assisting me with the simplified slug model.
- Professor Sigurd Skogestad, for all the tips and hints provided.
- Ingvald Bårdsen, for help in understanding the Miniloop.
- Torgrim Aas, for demonstrating the Miniloop build at Statoil.
- Ole Ivar Hovin, for reparing equipment that broke.
- Jan Ole Sundli, for updating the field point modules.

Table of contents

Table of figures

1 Introduction

1.1 Background

The diploma thesis brings the education as a chemical engineer at the Norwegian University of Science and Technology (NTNU) to a close. It has been carried out at the Department of Chemical Engineering. The title for the thesis is "Anti-slug control. Experimental testing and verification", and can be considered as a continuation of the project "Anti-slug control for a two phase flow. Experimental verification" by Bårdsen[3].

1.2 History

Multiphase pipelines connecting remote wellhead platforms and sub-sea wells are a common feature of offshore oil production in the North Sea, and the signs are that even more of them will be laid in the coming decades [8]. This makes the problem connected to multiphase transport of gas, oil and water an increasingly important topic for the offshore oil industry. Underwater installations allow the untreated well streams from different well cluster and wellhead platforms to be collected and transported into the production platforms. The trend towards more satellite wells means that the multiphase flow has to be transported over greater distances. In addition to the increased length, greater depths provide additional challenges for multiphase transport and control.

The pipeline-riser systems needed to transport the oil to the production facilities gives rise to an undesired flow regime known as slug flow. Slug flow usually occurs when you have a low point in the pipeline topography. The liquid will accumulate at the low point, blocking the pipe and result in the forming of a liquid slug. The slug will continue to grow until enough upstream pressure has developed to overcome the weight of the liquid slug. These slugs can grow very large and often cause severe problems when they reach the production facility. Severe slugging can in the worst case lead to a plant shutdown. More frequently the large and rapid variation in flow leads to poor separation and unwanted flaring.

Severe slugging can be avoided by increasing the pressure drop over the top side choke valve. Early solutions involved closing the top side choke valve to avoid the slugging. This solution is far from optimal as it will result in a reduced oil recovery. Other solutions include installation of slug catchers. By applying active feedback control it is possible to stabilize the flow at a pressure drop that would normally lead to severe slugging. This reduces the need for additional topside equipment and allows a higher rate of oil recovery.

There are currently several successful implementations of control systems that stabilize the system under conditions that would normally lead to slug flow. They are briefly discussed in Storkaas [4] and are all based on experiments and rigorous simulators like OLGA. In Storkaas [2,4] the need for a simpler model is made evident and a simplified linear slug model with only three states is developed.

Bårdsen[3] constructed a lab scale Miniloop to experimentally verify the simplified slug model. The Miniloop successfully verified the simplified slug model as a useful tool for analysis and control purposes. A simple pressure controller using the upstream pressure as measurement managed to stabilize the flow. This measurement can in many cases be unreliable or unavailable so the use of alternative measurements will be explored in this thesis.

1.3 Scope of the thesis

This thesis can be considered as a continuation of the work done by Bårdsen [3].
The main part of the thesis was experimental work and the overall goal was to stabilize the Miniloop using alternative measurements as proposed Storkaas[4]. This meant that a lot of additional work had to be done on the Miniloop. Additional equipment had to be bought and installed. The measurements and sensors needed to be analyzed and adjusted. The miniloop program (user interface) also had to be rewritten from scratch to obtain the new measurements and to allow other control configurations.

Because an experimental approach was chosen the different controllers were tuned experimentally. The controller would be tuned until satisfactory control was achieved. In this case satisfactory control meant that the slugging is eliminated by stabilizing the system at a valve opening that would normally result in severe slugging for open loop.

During the work on this thesis great emphasis was put on the fact that a third party should be able to continue the work with as little effort as possible. The miniloop program was constructed so that it should be easy to use for a third party. Text boxes etc. were added to the code to explain the function of the most important components. This was also emphasized in this report by including a detailed description of the work done. A user manual was also written for the Miniloop.

1.4 Notation

The word miniloop will be used frequently in this thesis. However it will be used in two different contexts.

Miniloop written with a Capital M refers to the lab scale Miniloop, while miniloop spelled with a small m refers to the LabVIEW program written to control it. Hence Miniloop is the physical equipment setup, and the miniloop program is the user interface.

2 Theory

2.1 Slug flow

Slug flow is characterized by intermittent axial distribution of liquid and gas. The bulk of the liquid is transported as slugs of oil and water, while the gas is transported as bubbles in between the slugs. Slug flow can be divided into two main types, hydrodynamic and gravity induced slugging. Hydrodynamic slugging occurs in horizontal pipelines because of velocity differences between the phases and will not be a topic in this thesis.

2.1.1 Gravity induced slugging

Gravity induced slug flow is induced by a low point in the pipeline topography followed by an inclining section of the pipe. The prerequisite for this to occur are low pipeline pressure and flow rates. A sufficiently large volume upstream of the slug is also needed to allow the build up of gas. The slug cycle can be divided into four stages as shown by figure 2.1. It is initiated by an accumulation of liquid in the low point of the pipe (stage 1). This will eventually block the flow of gas and lead to a build up of pressure upstream the liquid slug. The pressure and liquid slug will continue to grow (stage 2) until the pressure is high enough to overcome the weight of the liquid in the riser. At this point the gas will start to penetrate the liquid and push the slug all the way out of the riser (stage 3). This will result in a drop of pressure and the gas will no longer be able to drag the liquid up the raiser. Some of the liquid will therefore fall back down the riser(stage 4) and accumulate at the low point and initiate the cycle again.

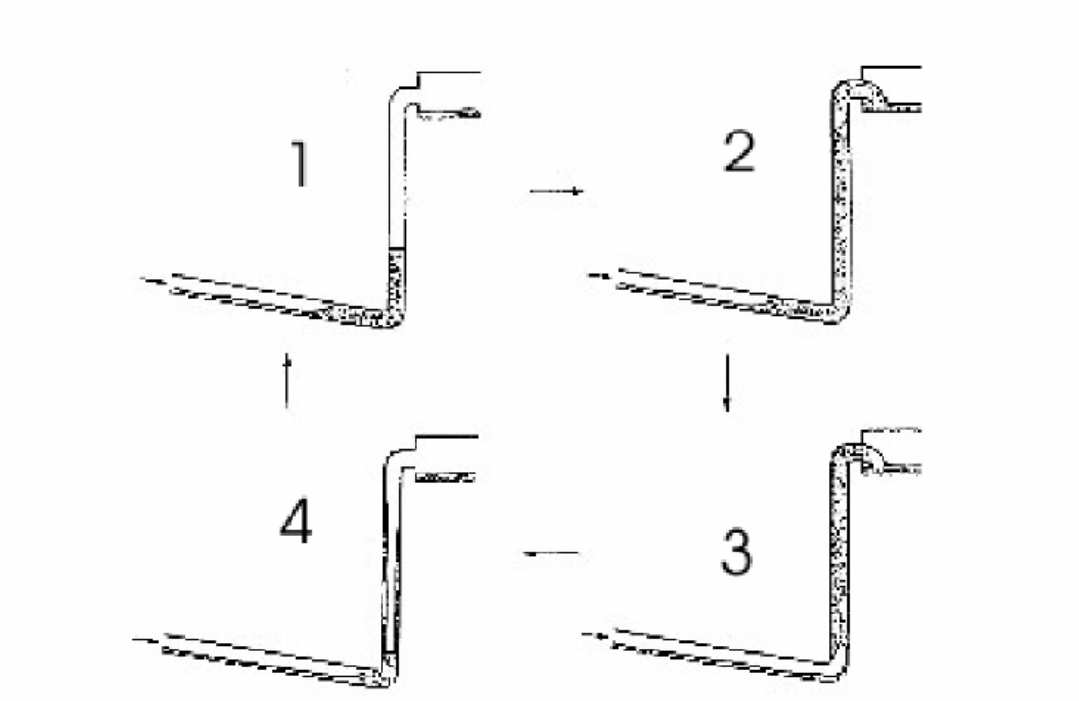

Figure 2.1 The slug flow cycle.

2.2 Flow through chokes

Knowledge about the behaviour of flow through chokes is important in production systems where flow rates are controlled by choke valves. Different phases like gas, water and oil have different flow behaviour through choke valves and other restrictions.

2.2.1 Single phase liquid flow through chokes

The flow rate through a valve depends on the size of the valve, the pressure drop over the valve and the fluids properties according to the following equation [11].

$$Q_l = C_v z \sqrt{\frac{\Delta P_v}{\rho}} \tag{2-1}$$

Where:

Q_l = Liquid flow rate [l/min]
C_v = Valve constant
Z = Valve opening [$0 \leq z \leq 1$]
ΔP = Pressure drop over the valve
ρ = Density of fluid

2.2.2 Gas Flow through chokes

Gas flow through chokes is more complex then fluids because of its compressibility and pressure temperature changes. Therefore corrections have to be made to the equation for expansion and temperature. A correlation for the gas choke is given by [1].

$$Q_{g,sc} = 6.85 \cdot 10^{-2} \frac{c_d A_2}{Z_1 T_1 \gamma_g} p_1 \sqrt{\left(\frac{k}{k-1}\right)\left[(y)^{\frac{2}{k}} - (y)^{\frac{k+1}{k}}\right]} \tag{2-2}$$

Where:
$q_{g,sc}$ = *Gas rate, standard conditions [Sm3 / s]*
c_d = *Discharge coefficient*
A_2 = *Choke area [m2]*
Z_1 = *Z-factor at choke inlet*
T_1 = *Temperature at inlet [ºK]*
ãg = *Specific gas gravity relative to air*
p_1 = *Inlet pressure [Pa]*
k = *Adiabatic gas constant*
y = *Expansion ratio*

2.2.3 Multiphase flow through choke

When two or more phases flow together in a pipe many different flow regimes may occur. The different phases will also exhibit different behaviour when passing through a valve. Correlations need to predict both critical and non-critical flow for all phases, and several assumptions needs to be done.

Because of this complexity, valve sizing and characteristics are usually based on experimental results.

2.3 Modelling

Storkaas [2] has developed a simplified dynamic model of multiphase flow for systems where severe slugging occurs. The model covers both the stable limit cycle known as slug flow, and even more importantly, the unstable but preferred stationary slug regime. This makes it suitable for controller design. The model focuses on describing the observed macro-scale behaviour rather then the detailed physics that governs the flow. For more details about the model see Storkaas [2].

The macro-scale behaviour described by the model is:

- The stability of the solutions and the operational conditions as a function of choke valve opening.
- The nature of the transition to instability.
- An unstable stationary solution at the same choke valve opening as those corresponding to severe slugging.
- The amplitude/frequency of the oscillations.

Storkaas model is based on the following assumptions:

- Constant liquid level in the feed pipe, witch implies:
  - Constant upstream gas volume.
- Only one liquid control volume.
- Two gas control volumes, separated by the low point, and connected through a pressure-flow relationship.
- Ideal gas behaviour.
- Stationary pressure balance between riser and feed section.
- Simplified choke model for gas and liquid leaving the riser.
- Constant system temperature.

2.4 Controllability analysis

The following theory is found in [7].

2.4.1 Limitations imposed by RHP-zeros and unstable poles.

A linear dynamic system can be represented as $\dot{x} = Ax + Bu$. The system is stable if and only if all the poles are in the left half plane(LHP), $\mathrm{Re}\{_i(A)\} \prec 0 \ \ \forall$ i.
Unstable poles can be stabilized by feed back control. Right half plane (RHP)-poles impose a lower bound on the bandwidth w_c for a system. [7] provides the following lower bound for RHP poles.

$$W_c \succ 2p \tag{2-3}$$

and for imaginary poles

$$W_c \succ 1.15 \mid p \mid \tag{2-4}$$

RHP-zeros results in an inverse response and impose an upper bound on the bandwidth for any system using feedback control. When a system is using feedback control the closed loop poles will approach the open loop poles as the gain approches infinity. This makes the system unstable and limits the bandwidth for high gains. The bound on the upper bandwidth for a system with real RHP-zeros is

$$W_b \approx W_c \prec \frac{z_n}{2} \tag{2-5}$$

And for complex zeros

$$W_b \approx W_c \prec \begin{cases} \mid z_n \mid /4 & \mathrm{Re}(z) >> \mathrm{Im}(z) \\ \mid z_n \mid /2.8 & \mathrm{Re}(z) = \mathrm{Im}(z) \\ \mid z_n \mid & \mathrm{Re}(z) << \mathrm{Im}(z) \end{cases} \tag{2-6}$$

RHP-zeros close to the origin of coordinates impose the largest constraints on the bandwidth. Control is more difficult if the zeros are located close to the origin of coordinates compared to zeros close to the imaginary axis. When both RHP-poles and zeros are present in the same system, the given upper and lower bounds on the bandwidth will make the stabilizing of the system impossible.

In order to fulfil the limitations imposed on the bandwidth and achieve a satisfactory performance and resilience the following is demanded

$$Z_n > 2.4|p| \tag{2-7}$$

3 Experimental testing and verification

3.1 Apparatus

Figure 3.1 shows an overview of the lab-scale Miniloop that was used during the experimental face of this thesis. The Miniloop was originally constructed by Bårdsen [3] as a part of his fifth grade project with the Department of Chemical Engineering at NTNU. Some changes have been made to the original Miniloop, including purchase and installation of additional equipment. These changes will be addressed later on in this chapter.

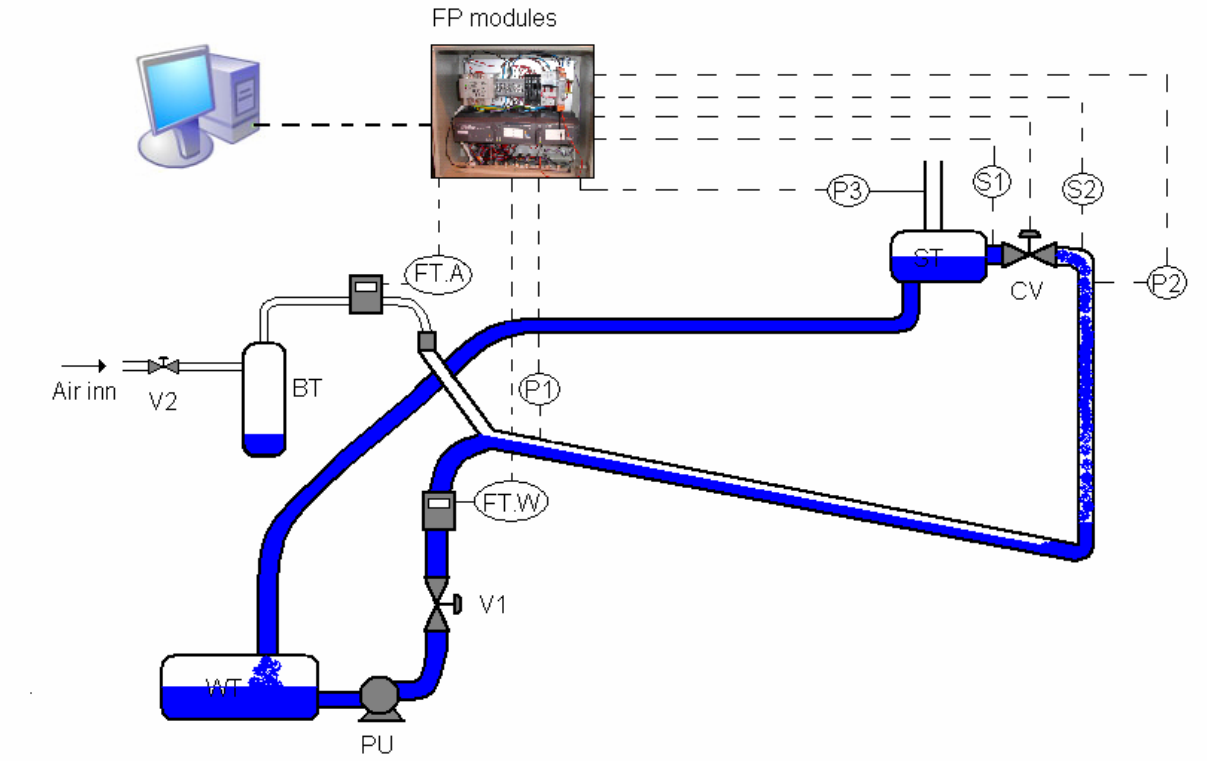

Figure 3.1 Flow sheet for the Miniloop.

As can be seen from the figure the Miniloop has a water (WT) and an air source. The water is pumped from the reservoir into the system, while the air is let into the system from a pressurized air outlet in the wall. The flow rate of water and air is controlled by manually adjusting valves V1 and V2. The pipeline system is constructed of several connecting sections of transparent plastic tubes. The pipeline is meant to imitate the pipeline topography where gravity induced slugging occurs, which is a low point connected to an inclined section of the pipe. At the top of the riser the multiphase flow passes the control valve before it enters the separator. At this point the air is released out of the system through an open hole in the separator, while the water is returned to the reservoir. To monitor the behaviour of the system a combination of pressure measurements and slug sensors are used. As can be seen from Figure 3.1 the water has a blue colour. This is a necessity and not a just a cosmetic issue. The reason is that the slug sensors are optical in nature and the water had to be a colour that allowed it to absorb the light emitted from the sensors. This will be addressed more thoroughly in chapter 3.4.1.

3.1.1 Equipment

Table 3.1 lists the different equipment used in the Miniloop. Consult table A.1 in the user manual appended to this thesis for more info about the distributors and prises. More detailed information about the different equipment can be found in the user manual, appendix B.

Table 3.1List of equipment.

Notation	Equipment
FT.W	Rate meter for water(Gemu 3021)
FT.A	Rate meter for Air
P1	Pressure sensor (MPX5100DP) Feed inlet
P2	Pressure sensor (MPX5100DP) Valve
P3	Pressure sensor (MPX5100DP) Separator air outlet
S1	Slug sensor (E3X-DA-N)
S2	Slug sensor (E3X-DA-N)
PU	Pump (Eheim 1060)
WT	Reservoir
BT	Buffer tank
ST	Separator
CV	Control valve

The rate meter for water (Figure 3.2) is placed in front of the mixing point of water and air. The digital display shows the rate of water in l/min. It provides a signal between 4-20mA, depending on the rate of flow, which is send to the computer.

Figure 3.2 Rate meter for water

The rate meter for air (Figure 3.3) is placed in front of the mixing point of water and air. It has a digital display that shows the rate of air in percent of its operating area, witch is 0-2.2 l/min. The rate meter also provides a signal between 0-5 V which is send to the computer.

Figure 3.3 Rate meter for air

The pressure sensors (Figure 3.4) is one of Motorola's differential pressure sensors that delivers a signal between 0.2-4.5 V. The relationship between voltage and pressure is linear and its operating area is between 0-100kPa.

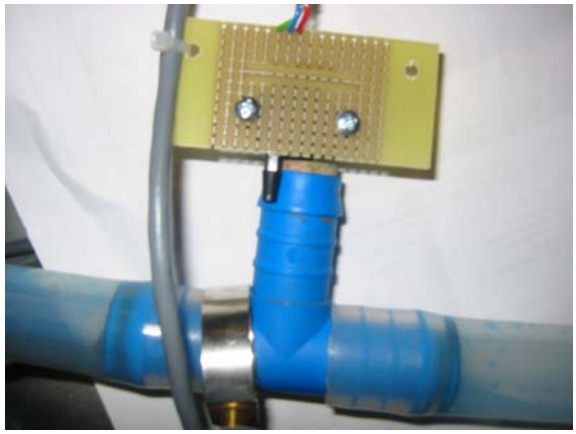

Figure 3.4 Pressure sensor

The slug sensors (Figure 3.5) are fibre optical sensors. Each slug sensor is made up of two fibre optical cables connected to a sensor. The light emitted from the senor will travel out through one of the cables and back through the other. The device will provide a signal between 1-5 V depending on how much light is transmitted between the two cables.

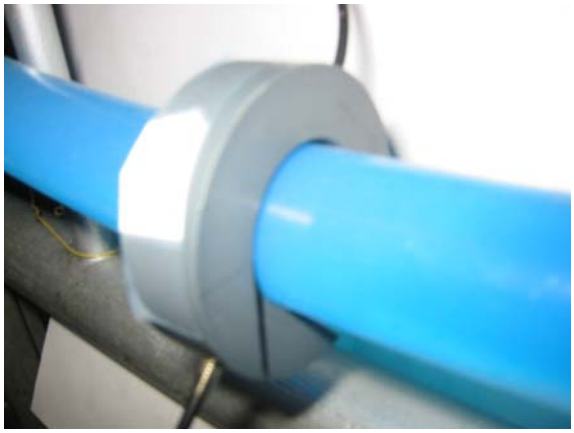

Figure 3.5 Slug sensor

The pump used is a standard aquarium pump. It can deliver up to 38 l/min and work against a head of 3.1 m. Special care must be taken to make sure it doesn't pump air as this can damage the pump.

Figure 3.6 Pump

The reservoir (Figure 3.7) is a cylindrical container made of transparent glass. It serves as the water source for the Miniloop, and the water is returned to the tank from the separator.

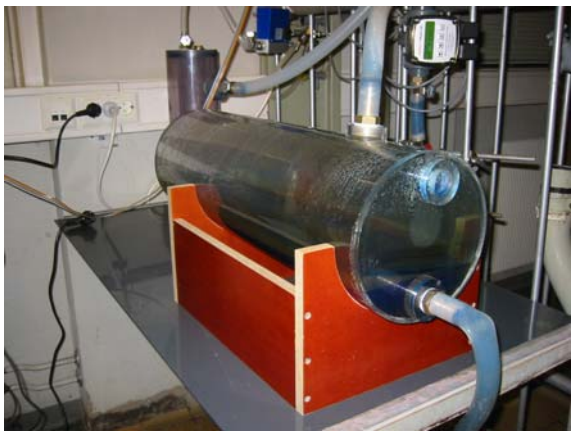

Figure 3.7 Reservoir

The buffer tank (Figure 3.8) is a cylindrical container made of transparent glass.
For slugs to appear the system needs a sufficiently large air volume. The air volume in the tank can be altered by adding water to the tank.

Figure 3.8 Buffer tank

The separator is also a cylindrical glass container with one inlet and two outlets. The air is released to the surroundings through an open hole in the top, while the water is returned to the reservoir.

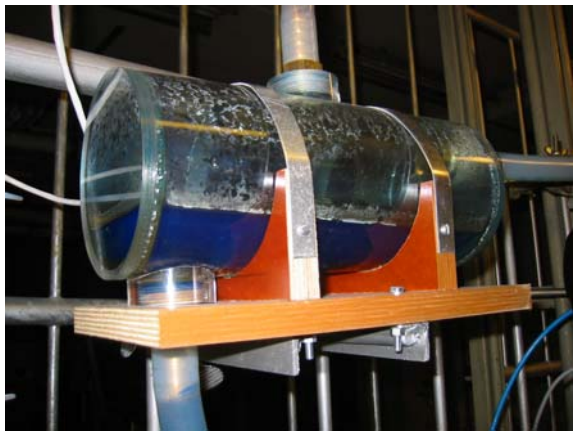

Figure 3.9 Separator

The control valve is located at the top of the riser before the separator inlet. The valve requires a 24V power supply and is controlled by a signal to the actuator between 4-20 mA. The relationship between the valve's actuator an the valve opening is linear. To operate the actuator an external pressurized air source of 4-8 bar is required to counteract the spring power. The lab has its own pressurized air source, which was used for this purpose.

Figure 3.10 Control Valve

3.1.2 Changes to the Miniloop

As mentioned above some changes have been made to the Miniloop since it was constructed by Bårdsen. These changes include modification of existing equipment and purchase of new parts.

In the original loop permanganate was used to dye the water red. The Miniloop had been out of use for some months, so the colouring matter used had stained the pipes. These stains created problems for the optical sensors. For reasons that will be made obvious in chapter 3.4.1 all the tubes were replaced and a more water-soluble colouring matter was added. The new colouring matter added is called Vulcanosol-Blau 684.

The original brackets used to attach the slug sensors to the pipe had a couple of flaws. In the original bracket there was no way to adjust the distance between the two optical cables. There was also some concern that the metal used in the brackets could reflect some of the light and create an error in the measurement. After some consideration a new design was chosen. The new bracket (figure 3.5) was drilled out of a PVC pipe to resemble a horseshoe. With this design the distance between the two cables could be altered depending on how far into the material the cables were screwed.

One of the biggest problems with the original loop was that we had no way of ensuring the same operating conditions each time an experiment was conducted. There was a flow meter installed to measure the flow of water, but we lacked a way to measure the flow of air. For this reason a flow meter for air was purchased and installed. An additional pressure sensor was also installed at the air outlet of the separator. The purpose of this sensor was to estimate the air flow through the control valve.

3.2 Data Flow and Data logging

The data measured by the devices installed on the Miniloop had to be recorded, analyzed and stored. To accomplish this, the different devices are connected to a lap top computer through the Field Point modules (Figure 3.11). The Field Point modules are mounted on a terminal base inside a water proof locker. The different analogue transducers are connected to the FP input module (middle), while the control valve is connected to the FP output module (right). The computer is connected to the communication module to the left.

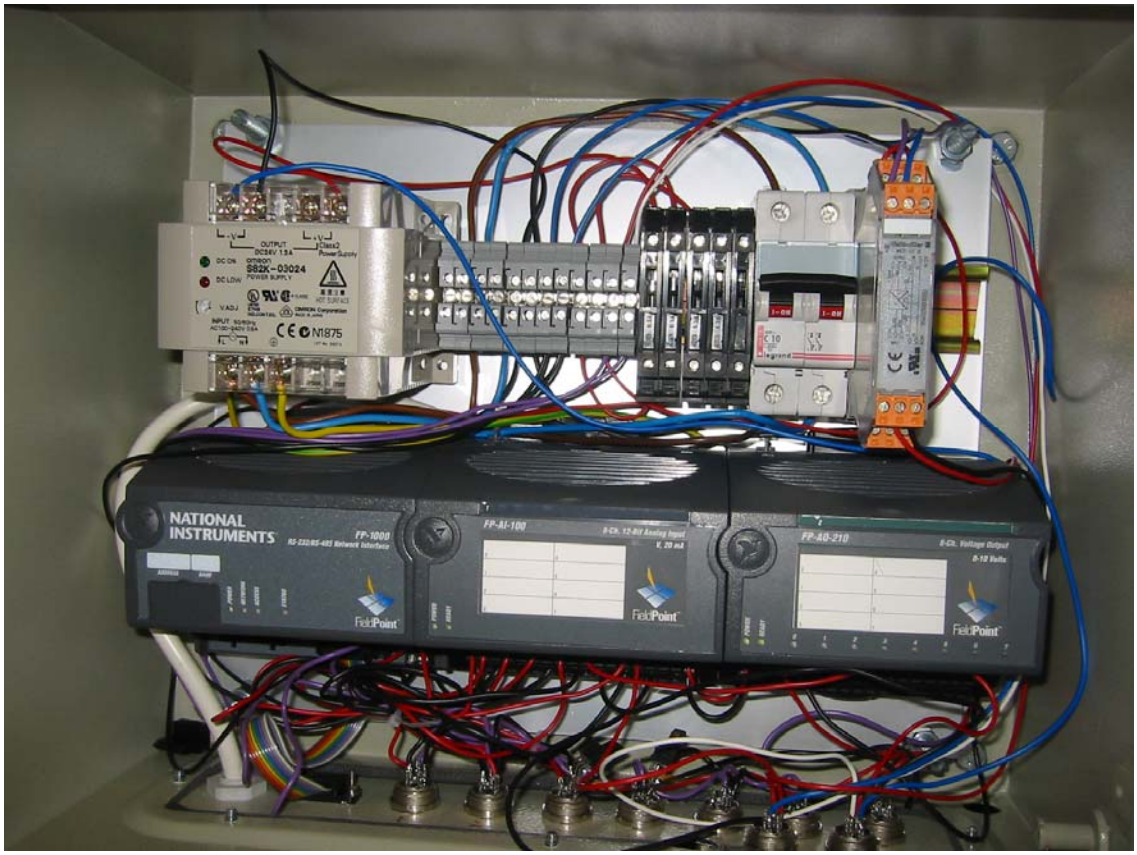

Figure 3.11 Picture of the FP modules mounted on the termination card.

3.2.1 Software and drivers

The hardware (FP modules) and software required to analyze, store and display the data are delivered by National Instruments (NI).

The software needed is LabView with the following additional content installed :

- PID control toolset.
- Fieldpoint explorer version 3.01 drivers (FP module drivers)

3.3 LabView

> *"LabVIEW delivers a powerful graphical development environment for signal acquisition, measurement analysis, and data presentation, giving the flexibility of a programming language without the complexity of traditional development tools."[12]*

The user interface in LabVIEW is called a Virtual Instrument (VI). These VI's have to be made for the specific measuring set-up, in this case for the Mini-Loop. The programming language used in LabVIEW is called G, and is a graphical drag-and-drop programming. This programming language is based on C+, and LabVIEW supports additional code both in C+, Visual Basic and Matlab Scripts.

LabView consists of three main parts. The front panel is the interactive user interface of a VI, so named because it simulates the panel of a physical instrument. The front panel can contain knobs, push buttons, graphs and many other controls (user inputs) and indicators (program outputs). Data or control can be input by a mouse or a keyboard, and results can be viewed by the program on the screen.

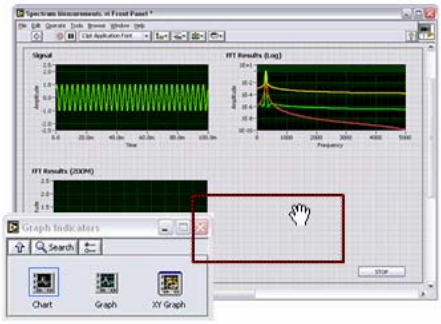

LabVIEW includes a wide array of visualization features, including tools for charting and graphing. This makes it easy to visualize data. The user simple drags and drops the desired controls or indicators from the build-in control palette to the front panel.

Figure 3.12 Labview Front Panel.

The second part of LabVIEW is the block diagram. Its in the block diagram that the data is acquired, analyzed and generated. While the front panel is the user interface, the block diagram is the VI's source code. It is constructed in LabVIEW's graphical programming language, G. The block diagram is the actual executable program. The components of a block diagram are lower-level VIs, built-in functions, constants, and program execution control structures. You draw wires to connect the appropriate objects together to indicate the flow of data between them. Front panel objects have corresponding terminals on the block diagram so that data can pass from the user to the program and back to the user.

The hierarchy window displays a graphical representation of the calling hierarchy for all VIs in memory, including type definitions and global variables. This hierarchy window shows the relationship between the subVIs in a program. This is a good insight to the structure of the program. The power of G programming lies in the hierarchical nature of VIs. After creating a VI, one can use it as a subVI in the block diagram of a higher level VI.

3.3.1 Miniloop front panel

Figure 3.13 shows the front panel for the LabVIEW program miniloop. The original program created by Bårdsen [3] were abandoned, and a new one was created from scratch to accommodate better flexibility and different control structures. The front panel serves as the interface between the user and the lab scale Miniloop.

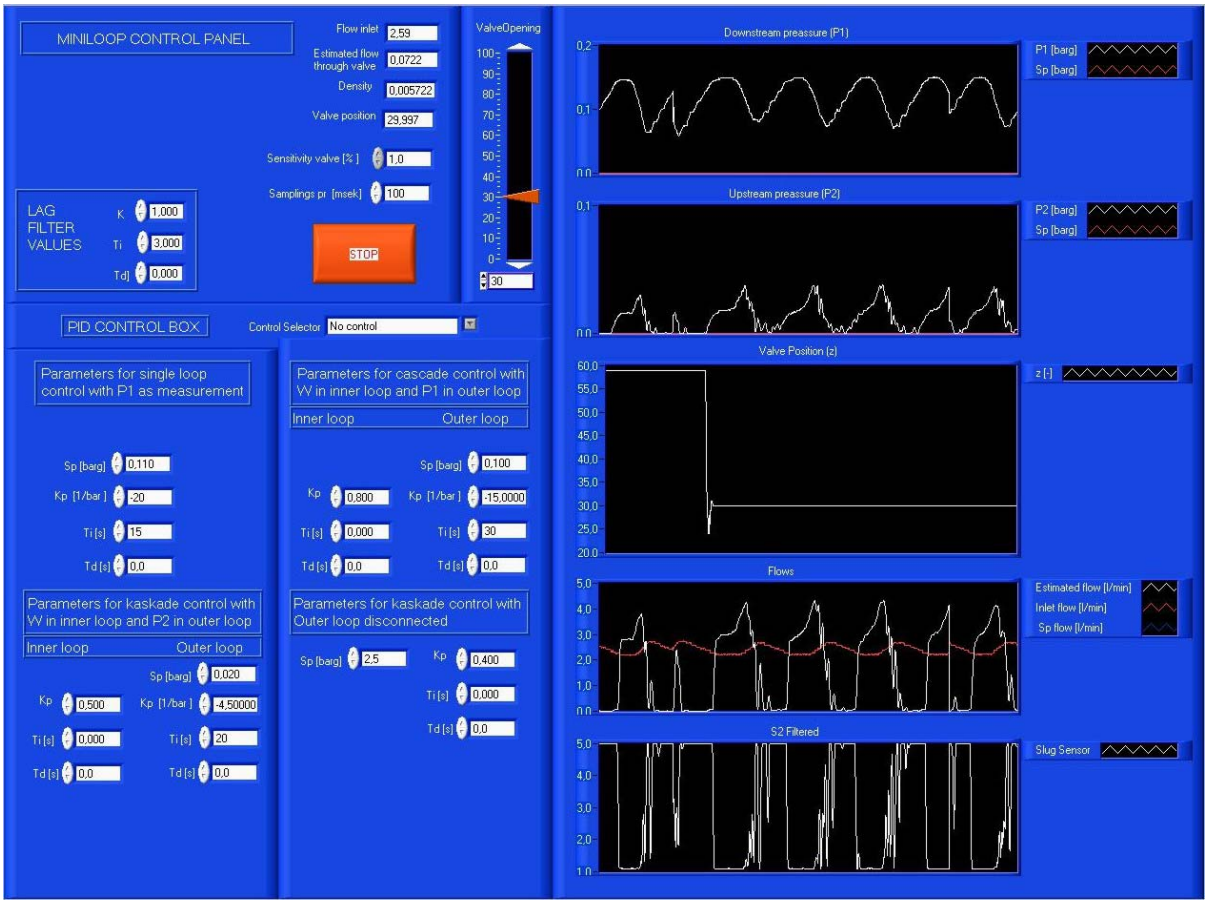

Figure 3.13 The front panel for the labview program miniloop.

The front panel has three main areas of interest. First you have the charts used to visualize the measurements, like pressure drop, valve opening, flow and hold up. The top chart displays the downstream pressure, while the second one displays the upstream pressure. If anti slug control is applied the mentioned charts will display the relevant set point. The third chart from the top plots the flow of water into the system and an estimate of the flow through the control valve. If a cascade controller is applied it will also show the relevant set point. The slug sensor results are plotted at the bottom. This measurement plots the filtered signal received from the optical sensors.

The PID control is located at the lower left corner of the screen. This is were the user chooses witch control structure to use. The loop is set to “no control” by default, but by clicking it you can choose the following control structures from the pull down menu:

- No control.
- PI control, with P1 as the controlled variable.
- Cascade control, with mass flow (W) as the main variable and P1 in outer loop
- Cascade control, with mass flow (W) as the main variable and P2 in outer loop.

The tuning parameters for the different controllers are also located here, witch means the user can change them by simply entering the new value.

In the upper left corner of the front panel the user will find some additional indicators that displays additional information about the system. These include density, actuator position and digital displays for the flow. When the system is running in open loop mode, “no control”, the valve opening can be set through the slide bar. Most measurements are already filtered to some degree, but since the estimated flow measurement is the one most prone to disturbances, an additional lag filter has been added. The parameters for this filter can be altered by changing the values in the filter box.

When the program is shut down it is recommended to use the big red stop button located on the front panel to ensure a controlled termination of the program, including the writing of data from memory to hard drive. The data will be stored in a text file with the following format

Table 3.2 Format of stored data.

t [msek]	S [V]	P_1 [Barg]	P_2 [Barg]	Q_{inlet} [l/min]	$W_{estimated}$ [kg/min]	Z [-]
…	…	…	…	…	…	…
…	…	…	…	…	…	…

All kinds of data can be written to the file, including other measurement, calculations etc. Adding another source of data to the stored file is a simple matter. All the user has to do is connect the measurement to be stored to a subVi in the block diagram. Consult the user manual in appendix B to learn how.

3.3.2 Miniloop block diagram.

As mentioned the block diagram contains the source code for the program. The diagram is too large to be displayed in its entirety, but figure 3.14 shows a simplified sketch of the dataflow inside the block diagram. A while loop encompass most of the program code.
The field point modules will provide the while loop with the data sampled from the measurement devices. Inside the loop the data is calibrated, filtered and modified to provide the measurement needed for control purposes. The box labelled “control structure” is a case structure that contains the different control structures mentioned in chapter 3.3.1. The code inside the while loop will provide the control structure with the measurements needed, and the actuator position will be send back to the field point modules through the while loop. If no control is active, the control structure will return the actuator position set by the sliding bar in the front panel.

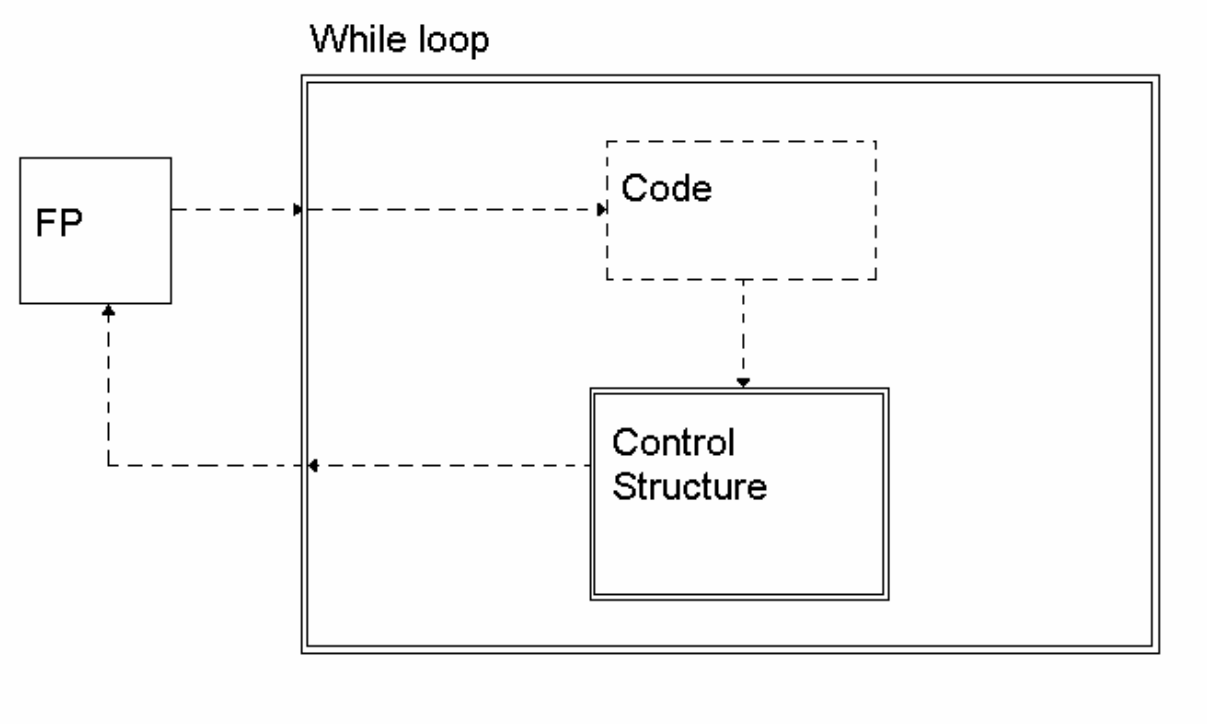

Figure 3.14 The data flow inside the block diagram.

Figure 3.15 shows about 1/4 of the block diagram associated with the miniloop program. To view the diagram in its entirety the reader should open the miniloop program on a computer with Labview installed and access the block diagram (ctrl+e). The program can be found on the cd that accompanied this thesis. The partial frame seen in the lower right corner is the control structure in figure 3.14.

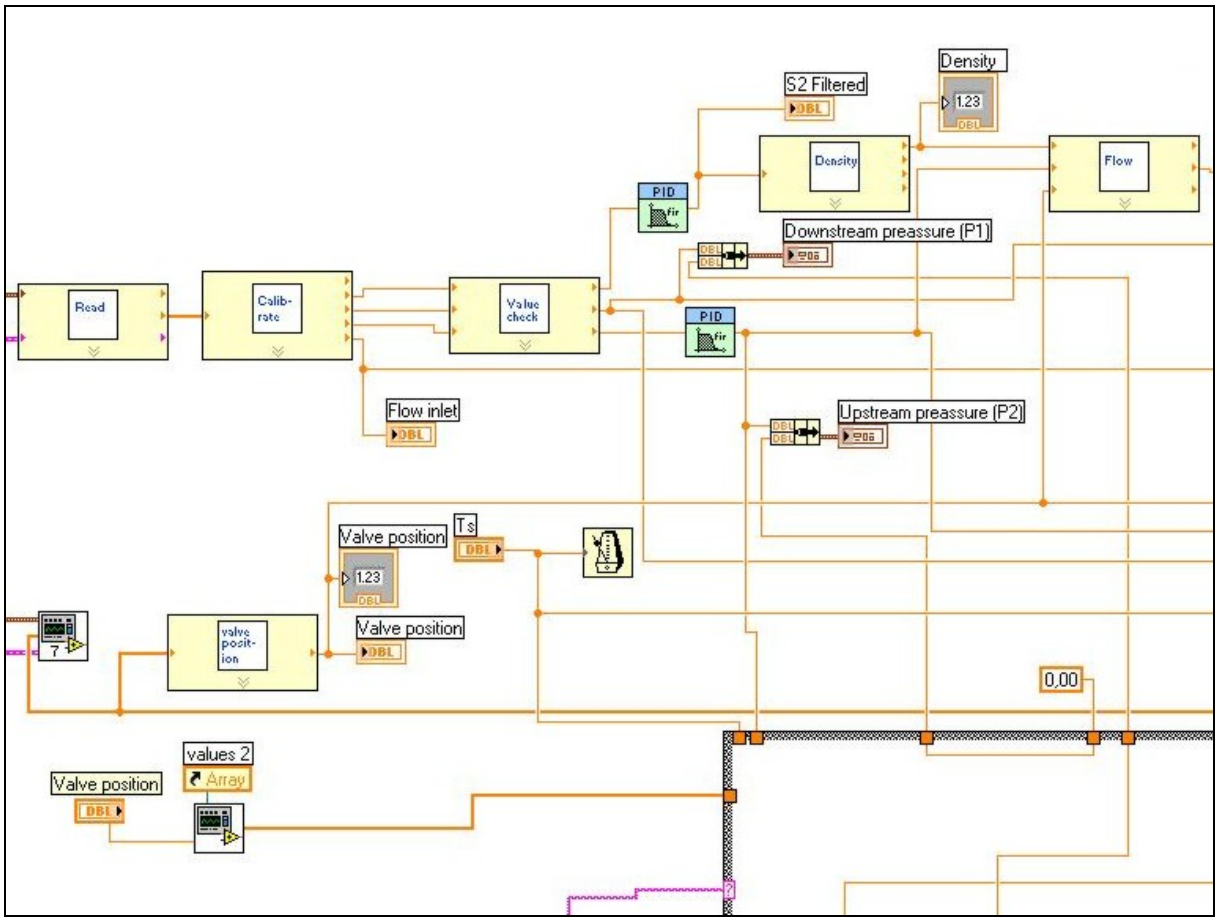

Figure 3.15 Section of the block diagram.

To make the programming environment in LabVIEW less messy, much of the code is grouped together to create different sub Vi`s. Figure 3.16 shows the content of the sub VI called “Calibrate”. In this sub Vi the different measurements are calibrated and converted from mA and V signals to engineering units. The hierarchy window (figure 3.17) shows the relationship between the different subVIs in the program.

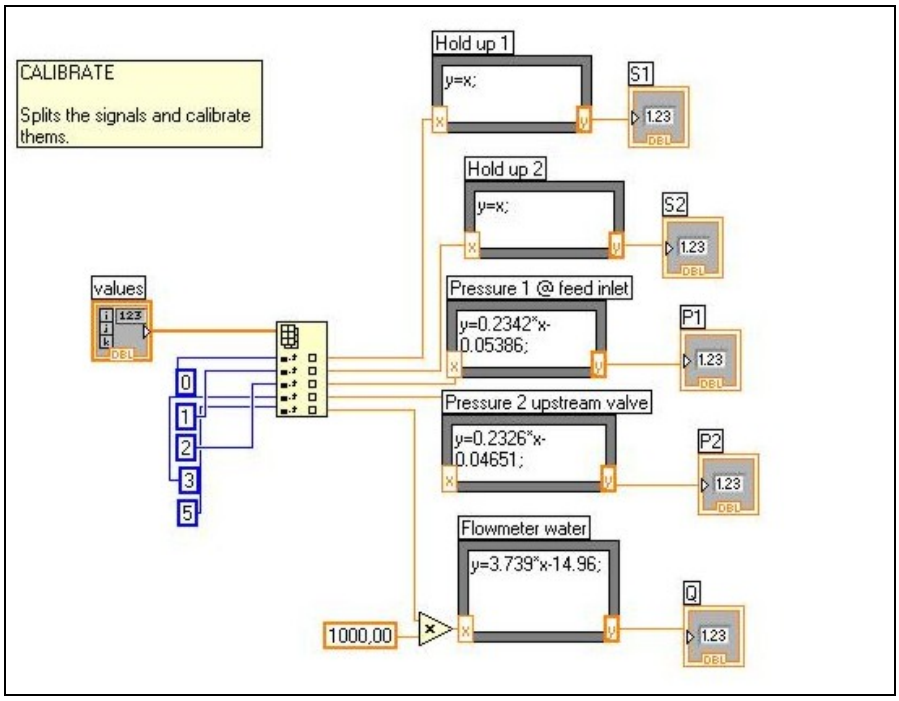

Figure 3.16 The content of the sub VI named "calibrate".

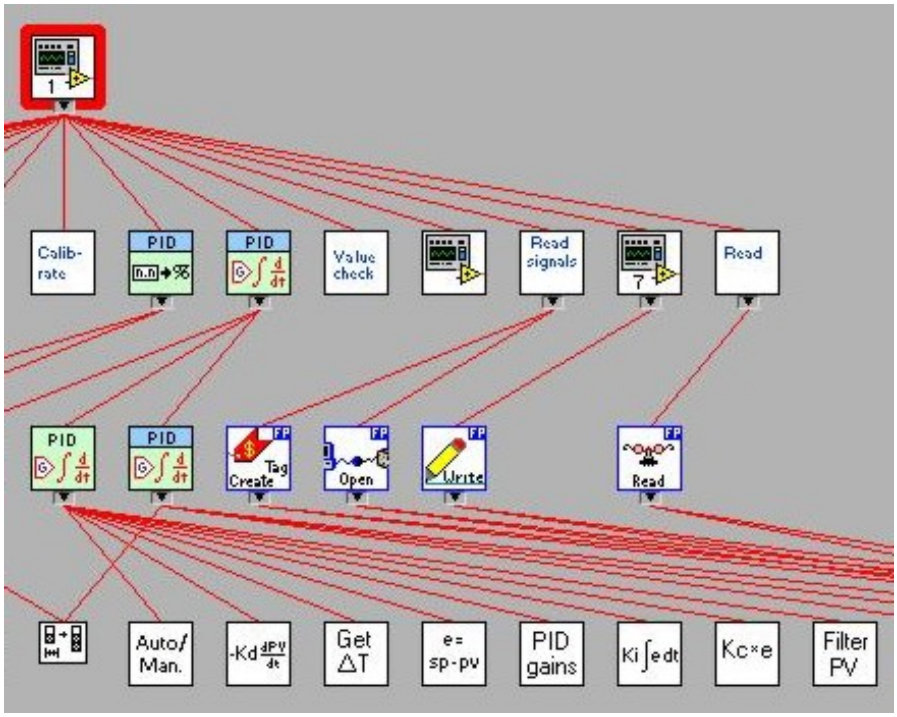

Figure 3.17 Section of the hierarchy window.

3.4 Data analyzing and filtering

Previous work on the Miniloop by Bårdsen included the implementation of a simple PI controller to stabilize the process. This controller used the downstream pressure (P1) as the controlling variable. This measurement however can be hard to obtain in practical problems like offshore installations. One of the goals of this thesis was therefore to expand the work done by bårdsen[3] by implementing a cascade controller. Previous work by Storkaas[4] suggested that a cascade controller using mass flow(W) or volume flow(Q) as the controlled variable could stabilize the process. A measurement of the mass or volume flow would have to be estimated from other available measurements like the slug sensor. Before such an estimate could be obtained the slug sensor had to be analyzed further.

3.4.1 Slug sensors

The slug sensors had been installed by Bårdsen when the loop was build, but no work had been done on analyzing the signals they produced. The original signals (figure 3.18) consisted mainly of a constant signal interrupted with spikes. The purpose of the slug sensors was to measure the hold-up, and it soon became apparent that the signals had to be treated further if any useful information were to be gained from them.

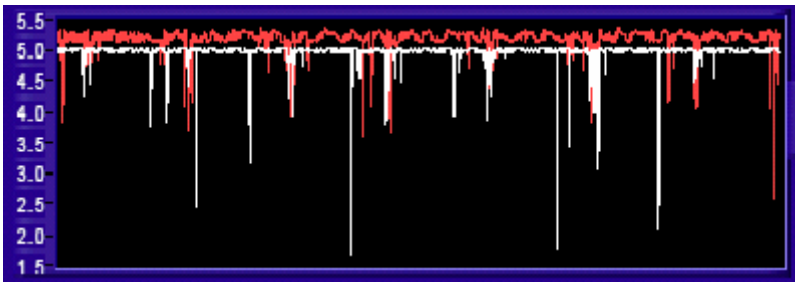

Figure 3.18 Initial readings from the slug sensors.

As mentioned earlier the slug sensors are based on fibre optical technology. Two separate optical cables are connected to a sensor. Light is emitted from the sensor and travels through one of the cables. As the light exits the first cable it will travel through the medium to be measured. The second cable is mounted on the other side of the medium, directly opposite the first cable. The light emitted from the first cable travels through the medium, and is returned to the sensor through the second cable. The sensor will produce a signal between 1 and 5 volts depending on the amount of light that returns. A signal of 1 volt means that no light has returned to the sensor, while 5 volts means all the light has returned.

The original range of application of the optical sensors is as a precision sensing device. The precise location of an object could be determined because the object would block part of the light beam, hence reducing the amount of light transferred between the cables. As long as only air was present in the pipe all the light would pass through the pipe and return to the sensor via the second cable. The goal was to estimate the hold up of liquid by measuring the amount of light absorbed by the liquid phase. Since the sensor was intended to be used on solid objects this turned out to be a big challenge.

As can be seen from figure 3.18 the optical sensors delivered a constant signal of 5 volt independent of whether it was liquid or air in the pipe. After further experimentation it was

discovered that the spiked were caused by a phase transition between air and liquid and vice versa. When the light hit such a transition the angle of the liquid surface would deflect the light away, resulting in the spikes witch indicated that no light returned to the sensor.

This still did not explain why the sensors showed the same value for both water and air. There were some speculations that the water didn't absorb enough light for the sensor to measure a difference. The solution proved to be as obvious as it was simple. The colouring matter used in the liquid was permanganate. This gives the liquid a red colour. However, the property of a red substance is that it will absorb all light from the colour spectrum except red. By taking the fact that the optical sensor used red light as its source into consideration, the solution was obvious. The water in the loop was changed and a blue colouring matter was added.

This gave the desired response on the sensors as can be seen from figure 3.19.

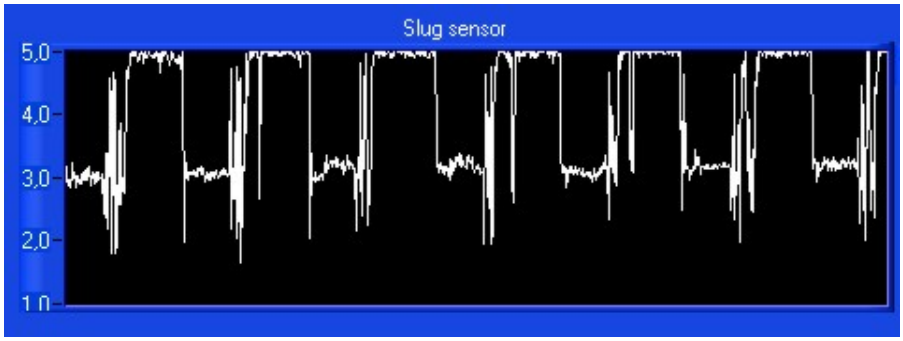

Figure 3.19 The slug sensor after the colouring matter was changed.

By adding more colouring matter, the amount of light absorbed by the liquid would increase, and the lower value corresponding to pure liquid was reduced from 3 Volt to 2 volt. The sensors digital display showed a value ranging from 0-4000, corresponding to 1-5 V, where the value 1500 represented pure liquid. The lower boundary for the sensor output was changed to 1700, making 1700 (pure water) correspond to 1 V and 4000 (pure air) to 5V. In effect this cuts off all values below 1700, including most of the spikes (figure 3.20).

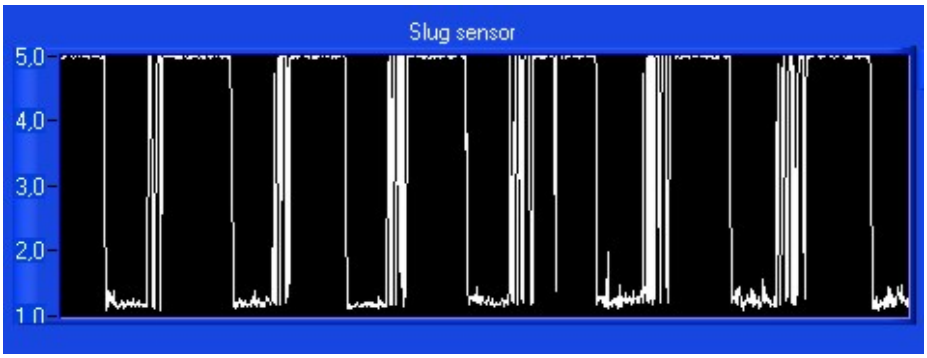

Figure 3.20 The slug sensor after signal scaling.

The slug sensor now gives a lot of information about the slug cycle. From figure 3.20 a value of 5 indicates that there is only air in the pipe. A slug is building up in the raiser, and when the downstream pressure gets high enough it will push the slug up through the raiser. This can be seen when the value drops from 5 to 1 volt. The air will eventually penetrate the liquid witch is represented by the oscillations between 1 and 5 volts. The liquid then falls back to the low point, causing the value to increase to 5 again before the cycle repeats itself.

The nature of the slug flow creates some restrictions and limitations witch reduces the effectiveness and accuracy of the slug sensor. In normal gravity induced slugging the gas would penetrate the liquid as bubbles in the liquid flow. This would allow the optical sensor to estimate the fraction of water passing the sensor giving us the hold up.**

However, conditions in the raiser produced a flow regime during closed loop where large volume of gas flowed as a separate phase in-between the liquid bulks (figure 3.21).

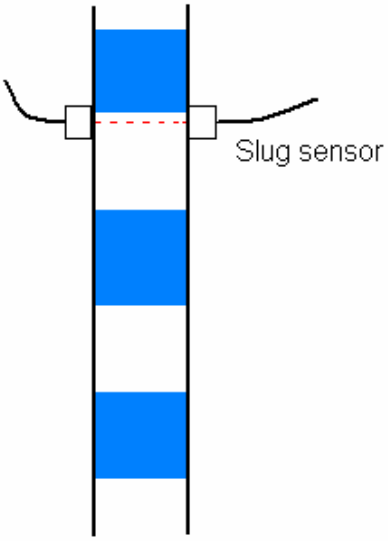

Figure 3.21 Slug flow pattern in the pipe

The slug sensor will therefore only be able to indicate the presence of water or air, not a mix of both. The oscillations (figure 3.20) are therefore a result of this flow pattern and the disturbances caused by the phase transitions. By adding a frequency filter in LabVIEW, the measurement was improved further (figure 3.22) by removing some of the disturbance and averaging the data.

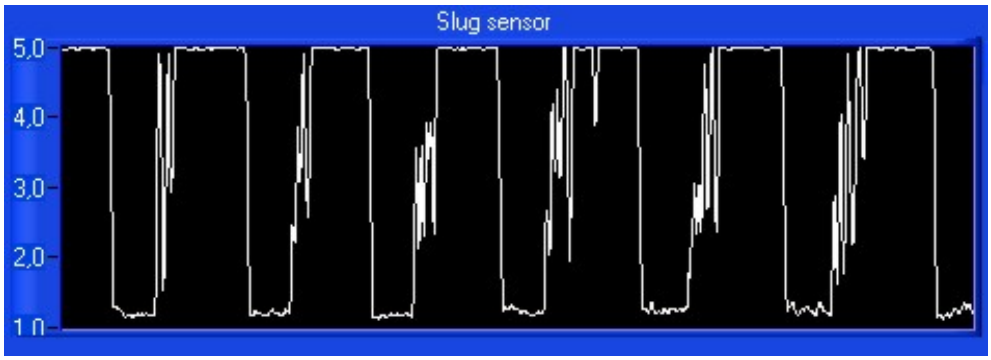

Figure 3.22 Final slug sensor readings.

To transform the volt signal in figure 3.22 to a hold-up measurement, some algebraic code were added to Labview. These take into account the geometry of the tube and scale the hold up to take values between 0 and 1.

** Had this been the case the slug sensor would probably not have been useable. The surface of the bubbles would have deflected the light away from the optical sensor, resulting in severe disturbances.

3.4.2 Estimating the flow through the choke valve

The mass and volume flow through the choke valve can be estimated by measuring the pressure drop over the choke and the mixture density. Multiphase flow through a choke valve is complex, but according to Skogestad there have been successful implementations of a cascade controller in the industry by using a simple valve equation for liquid flow. An attempt was therefore made to estimate the flow from equation 2-1.

The mixture density could be estimated from the hold up measurement, x_l, by the following equation :

$$\rho_m = x_l \cdot \rho_{water} + (1 - x_l) \cdot \rho_{air} \tag{3-1}$$

The biggest challenge lay in experimentally deciding the valve characteristics.
The only available measurements were the flow rates into the system. The slugging nature of the system also made it impossible to get any experimental stationary open loop values when using both gas and liquid. For that reason it was decided that the only viable option was to decide the valve characteristics using only liquid flow. When only water was pumped through the system, a simple conservation consideration meant that the flow meter at the inlet would show the liquid flow through the valve. Water was pumped through the system, the actuator position was altered, and the corresponding pressure drop over the choke valve and liquid flow into the system were recorded. For pure liquid flow the density in equation 2-1 could be dropped since ρ_m =1.

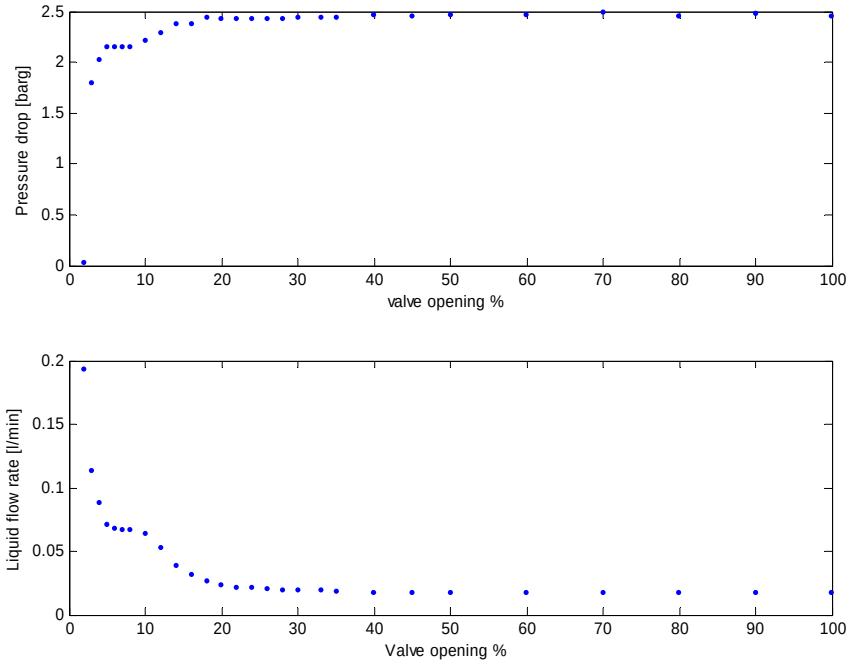

Figure 3.23 Pressure and flow vs. valve opening

As can be seen from figure 3.23 valve openings above 30% seems to have little or no effect on the pressure or flow rate. This suggested that the valve were oversized. If equation 2-1 were to be valid the relationship between Q and $z\sqrt{\Delta P}$ had to linear. However as can be seen from figure 3.24 this was not the case.

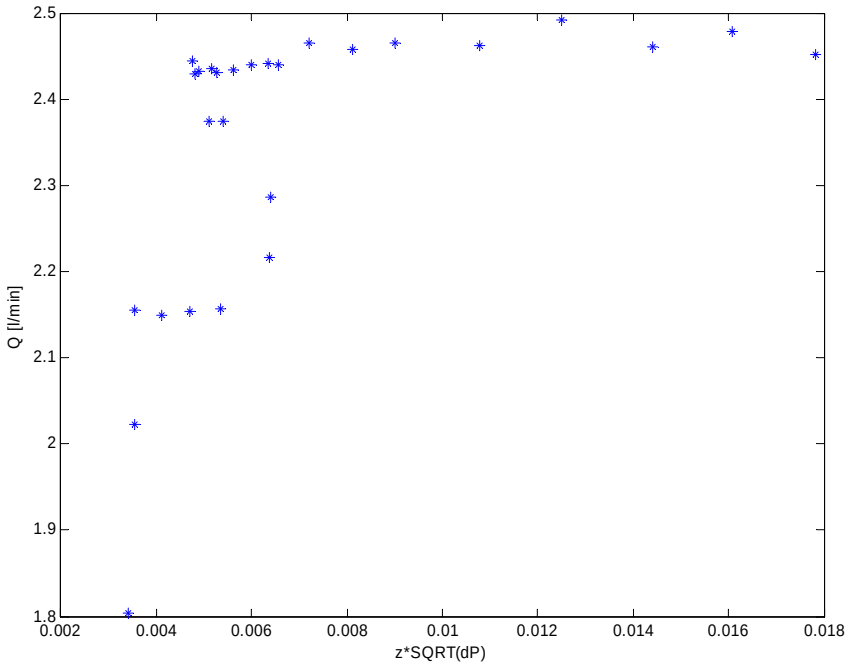

Figure 3.24 Q vs Z*SQRT(ΔP)

In an attempt to determine the valve characteristics two different approaches were tested. The first was to try and fit the experimental data to equation 3-2 by a linear parameter estimation(method a), and the second was to estimate f(z) from equation 3-3 by plotting $Q/\sqrt{\Delta P}$ against z(method b). Both methods are described in more detail in appendix A.4.

$$Q = k \cdot z^n \sqrt{\Delta P} \tag{3-2}$$

$$Q = f(z)\sqrt{\Delta P} \tag{3-3}$$

Both methods proved unsuccessful when trying to fit it to the entire data range. In order to get an estimate of the flow a purely mathematical approach had to be abandoned. For control purposes the priority had to be to obtain a satisfactory flow estimate in the area with small valve openings. As mentioned earlier valve openings above 30% seemed to have little or no effect on the flow rate. The two approaches mentioned above were therefore attempted on the data set below 30% valve opening. The best results were obtained by method b when a fifth order polynomial was used to describe f(z).

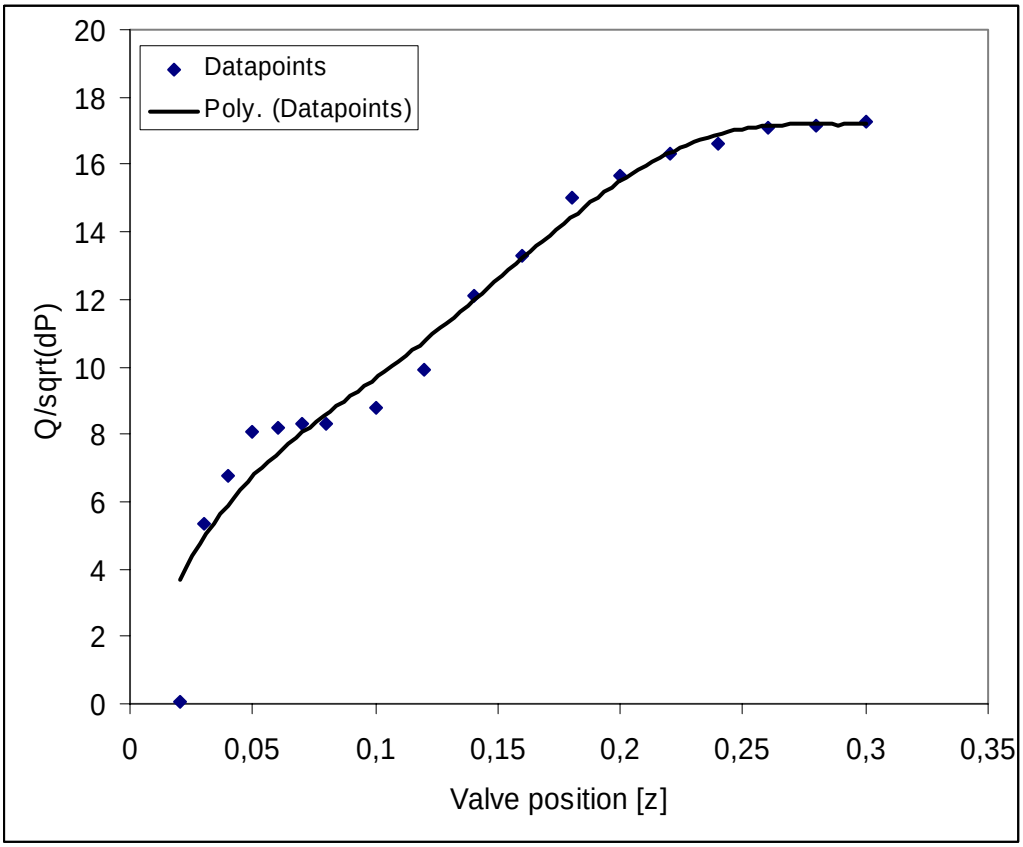

Figure 3.25 Fitting the f(z) to the datapoints.

The fifth order polynomial fitted to the data using the least squares method is

$$f(z) = 70223z^5 - 61350z^4 + 19191z^3 - 2705.4z^2 + 229.44z \tag{3-4}$$

Combined with equation 3-3 this estimated the flow through the valve for valve openings below 30%. To make the equation valid for valve positions above 30% a linear relationship were assumed between the flow rate and the pressure drop by setting f(z)=f(0.3) for all valve openings above 30%.

$$Q = \begin{cases} f(z)\cdot\sqrt{\Delta P} & for\ 0 \le 0.3 \\ f(0.3)\cdot\sqrt{\Delta P} & for\ z \succ 0.3 \end{cases} \tag{3-5}$$

Estimating the volume liquid flow through the choke was now possible. Unfortunately it proved impossible to get an estimate of the volume gas flow through the choke with the current measurement setup. This in turn made it impossible to estimate the total volume flow Q. The total mass flow W was still a viable option though. The mass flow of gas was assumed to be much smaller then the mass flow of the liquid. So setting the total mass flow W equal to the mass flow of liquid would not introduce to big an error. A simple rearrangement of equation 3-5 would therefore give an estimate of the total mass flow.

$$W = n \cdot \begin{cases} f(z) \cdot \sqrt{\Delta P \cdot \rho_m} & for\ 0 \le 0.3 \\ f(0.3) \cdot \sqrt{\Delta P \cdot \rho_m} & for\ z \succ 0.3 \end{cases} \tag{3-6}$$

Where n is a tuning parameter set to 1.3.

The system was forced into steady state by using active control. A simple mass balance consideration now implied that the total mass flow through the choke had to be the same as the mass flow into the system. The parameter n could then by tuned so that the estimated mass flow W would be the same as the measured liquid flow into the system.

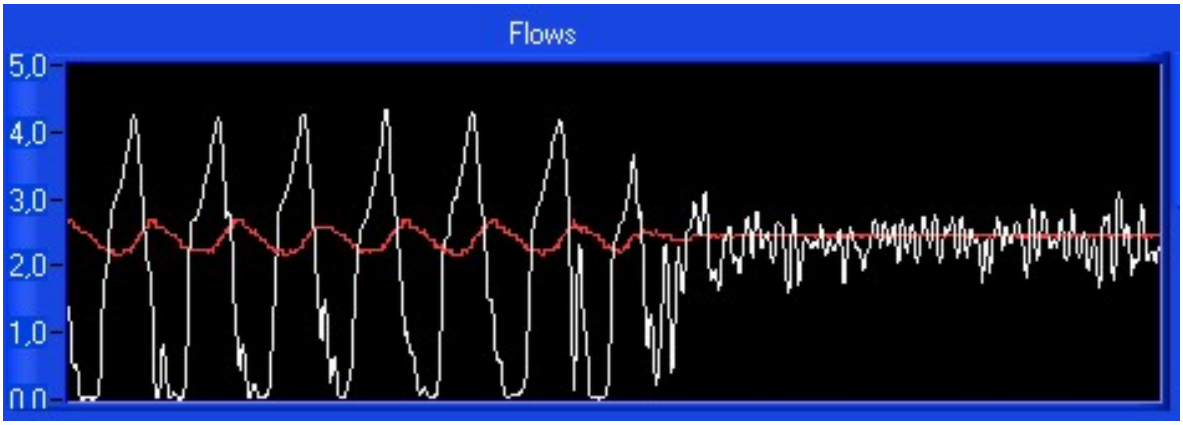

Figure 3.26 Snapshot of the chart showing displaying the measured mass flow.

Figure 3.26 shows a snapshot of the flow chart on the miniloop front panel. The red line is the measured flow into the system while the white line represents the estimated mass flow through the top side choke. The left side of the chart displays the Miniloop in open loop mode, while active control is used on the right side. The estimate of the mass flow could now be used for control purposes.

3.5 Open loop experimental data

The Miniloop was run in open loop and the valve opening was gradually changed from fully open till fully closed. The corresponding pressure drops were recorded and analyzed to create the bifurcation diagram(figure 3.27).

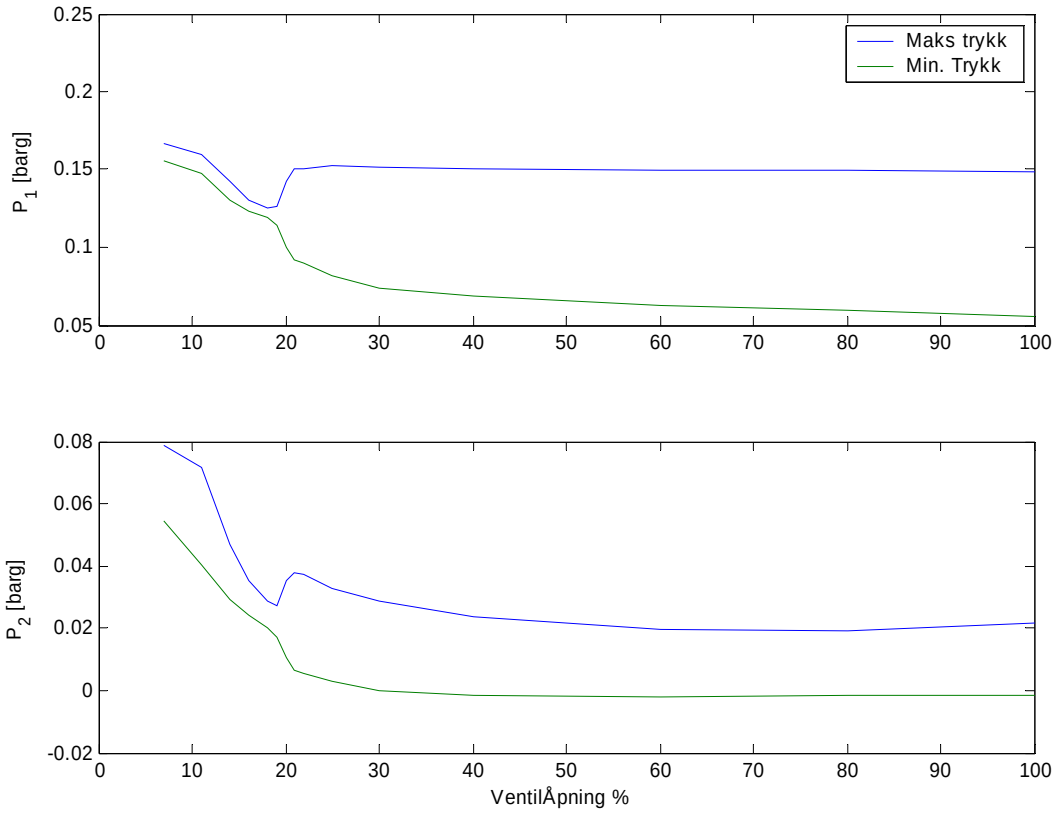

Figure 3.27 Bifurcation diagram for the experimental data.

As can be seen from figure 3.27 the system is stable up to a choke opening of 19 %. If the choke is opened further the system will enter the slug flow regime. The system becomes unstable and the pressure will start to oscillate. Early solutions to the slug problem in the oil industry utilized this property. By increasing the pressure drop over the top side production choke the slugging was successfully eliminated. However this solution also increased the total pressure drop in the well-pipeline system, resulting in lower oil recovery.

3.6 The simplified slug model

The model used to describe the riser slugging behaviour is not a partial differential equation system, but a simplified bulk model. The model has only three states, the mass of gas behind the slug, the mass of liquid in the slug and the mass of the gas in front of the slug. Riser slugging as described by the simplified model can be seen in figure 3.28.

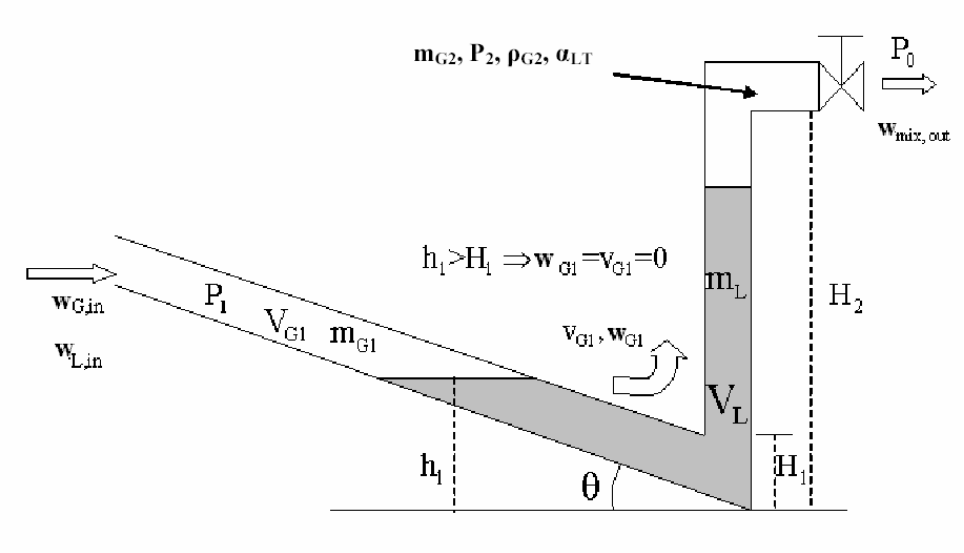

Figure 3.28 Model characteristics with important parameters.

The model was tuned to fit the experimental data as shown in figure 3.29. The red lines is the data from the simplified slug model while the blue dotted lines shows the experimental data- The red dashed line indicates the presence of an unstable stationary solution at the same choke valve openings as those corresponding to severe slugging.

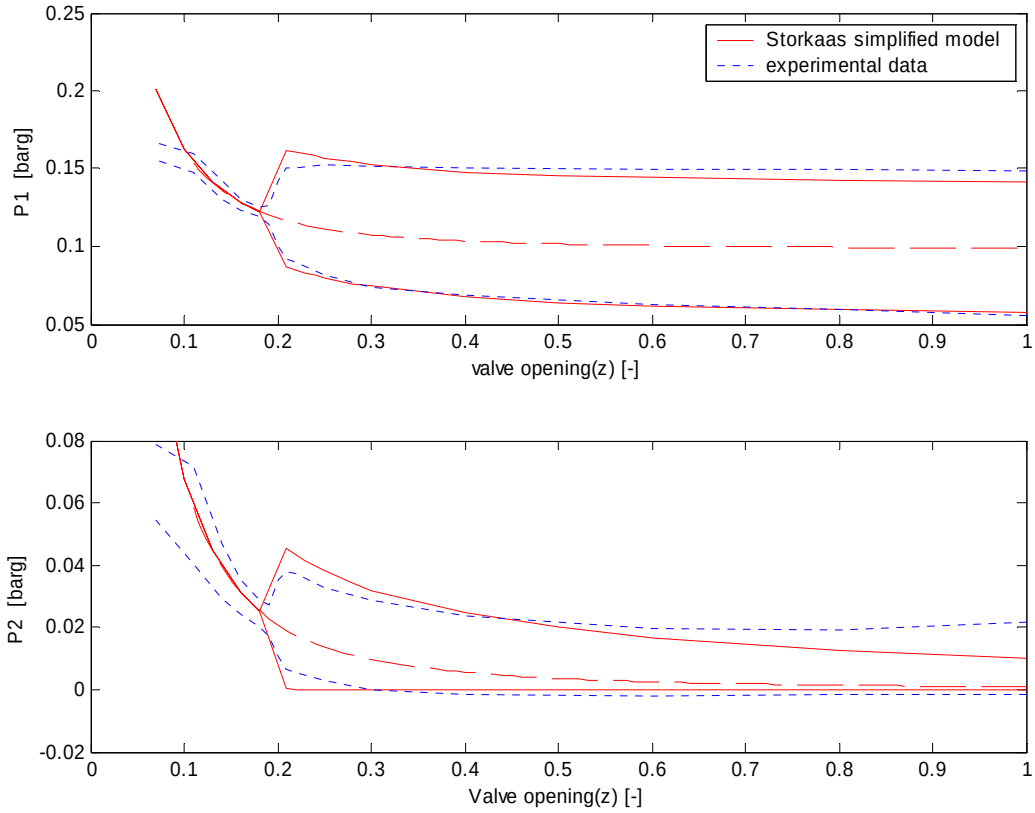

Figure 3.29 Bifurcation diagram for the simplfied slug modell.

It is unrealistic to achieve a good fit for both the slug regime and the stationary regime for the entire range of valve openings, so some priorities had to be made during the tuning of the model.

If the controller is to work properly the actuator has to have a significant impact on the process. For the high range valve openings, the pressure drop over the choke is too small for the effect of a small change in valve opening to be significant. This means that the only area of interest is that from medium to small valve openings. This can be seen from the bifurcation diagram because it shows little to no variations from medium to high valve openings.

Secondly, the unstable, stationary regime is more important then the stable oscillatory regime. The reason for this is that the goal is to achieve stationary flow with active control in the unstable area. By avoiding the slug regime and operating at the stationary regime, the focus is on where you want the process to be and not where you don't want it to be.

A good example of this was presented by Storkaas in [2].

"*If you are teaching someone to ride a bike, you are teaching them how the bike behaves when they have mastered the balancing act(the desired unstable operating point), not how it behaves when it lies on the ground (the undesired slug flow)"*

When taking these priorities into consideration the simplified model shows a good fit to the experimental data. The model fit to the experimental data for the upstream pressure (P1), is actually very good for the entire valve opening range. The fit for the downstream pressure is acceptable for the low to medium valve openings. The deviations in amplitude for higher valve openings are acceptable in light of the priorities given.

Part of the deviations for the downstream pressure fit may result from the disturbances associated with the downstream measurement. The downstream measurement is also located 15 cm below the valve, witch will cause the experimentally measured pressure drop to be a bit higher then it should. By examining the bifurcation diagram it can be seen that the experimental pressure drop over the choke is oscillating to a lesser degree in the stable regime. The mayor cause for this behaviour is caused by the flow behaviour as described by figure 3.21.

The frequencies of the oscillations are not included in the bifurcation diagram. Figure 3.30 and 3.31 shows the open loop behaviour for a valve opening of 30% for both the model and the lab scale Miniloop. The amplitude of oscillations for the upstream pressure P1 are almost the same for both the model and the Miniloop. The model calculates a bit lower amplitudes for the downstream pressure P2. By examining the frequency of oscillations it can be seen that the slug frequency is about 10% higher for the Miniloop compared to the simplified model. In this case the model was tuned to achieve a good fit for the amplitude. Since the upstream gas volume is fixed in the model it was impossible to fit both amplitude and frequency.

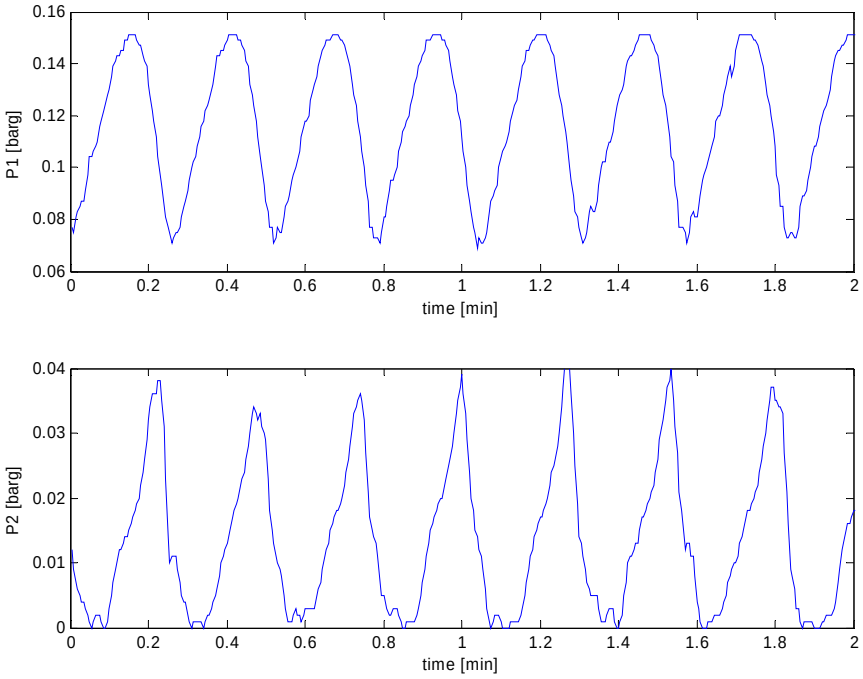

Figure 3.30 Open loop behavior for the miniloop (z=0.3)

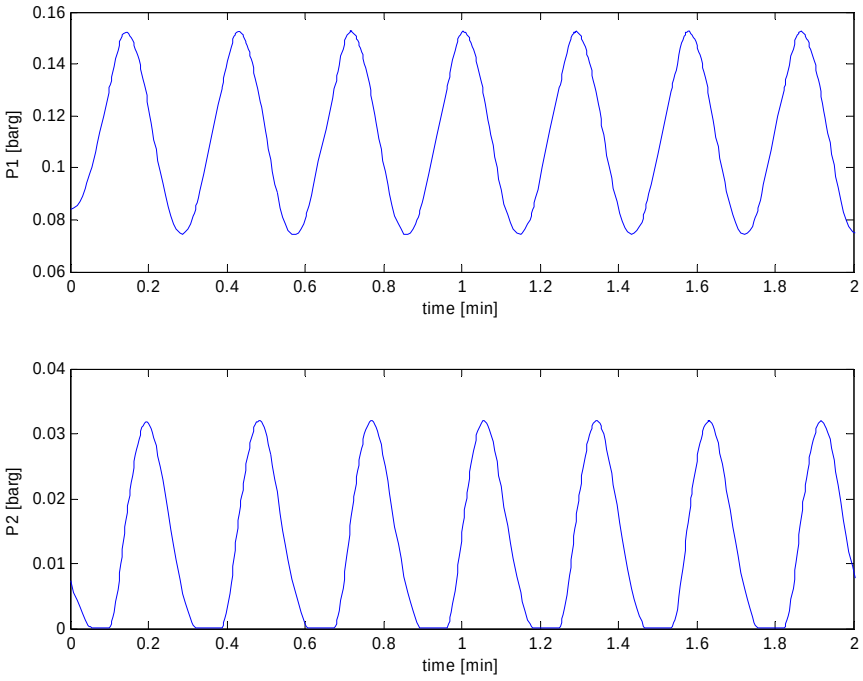

Figure 3.31 Open loop behaviour for the simplified model (z=0.3)

3.7 Controllability analysis

This analysis is based on a linearized model around a typical unstable operating point. The operating point chosen is z=0.3. The system is unstable for this valve opening in open loop since there is a complex pair of poles in the RHP (table 3.3). To compare it with an operating point that should be in the stable area according to the bifurcation diagram the poles for z=0.15 are also included in the table. As can be seen these poles are in the LHP, hence making the system stable. The poles and zeros for other operating points can be found in appendix A.3. The real part of the worst pole has been evaluated and plotted against the valve opening in figure. The poles start in the LHP and move over to the RHP when the valve opening is z=0.19. This corresponds with the bifurcation diagram where the system is unstable for $z \geq 0.19$.

RHP poler gives a lower limit on the bandwidth for the process. This means that the lower limit for the bandwidth will increase as the valve opening increases. The system can be stabilized by using feedback control to move the poles. RHP-zeros results in inverse response and imposes an upper limit on the bandwidth for the process. To obtain stability with a satisfactory performance the following is required

$$W_c > 1.15|p| \quad z_n > 2.3|p| \tag{3.6}$$

Table 3.3 System poles

Valve opening	λ_1	λ_2	λ_3	RHP-pole length
z=0.15	-9.5311	-0.0133 - 0.1862i	-0.0133 + 0.1862i	0.1867
z= 0.3	-10.4951	0.0522 - 0.3265i	0.0522 + 0.3265i	0.3306

The different measurements available are listed below.

Table 3.4 Available measurements.

Measurement	Unit	Description
P_1	[bar]	Upstream pressure(feed inlet)
P_2	[bar]	Downstream pressure
ρ_m	[Kg/m^3]	Density
W	[Kg/min]	Total mass flow
Q	[l/min]	Total volume flow

The only upstream (downside) measurement is the pressure P1. All the other measurements are upstream (topside) measurements. The zeros for the different measurements are given in table 3.3.

Table 3.5 Zeros for the different measurements at the operating point z=0.3.

P_1	P_2	ρ_m	W	Q
-0.1673	0.8720 + 0.6347i	0.0958	-13.027	-5.6430
	0.8720 - 0.6347i	0.0226	-0.0092 + 0.0614i	-0.1530
			-0.0092 - 0.0614i	-0.0401

The upstream pressure P_1 has one LHP-zero. Since LHP-zeros imposes no fundamental control problems P_1 would be the obvious choice of measurement. However, this measurement can in many cases be either unreliable or unavailable and other measurements have to be considered. From the bandwidth limitations imposed by equation 3.6 there cant be any RHP-zeros smaller then 0.7605. Of the alternatives in table 3.3 ρ_m have RHP-zeros close to the unstable poles. This makes it unsuitable as a measurement for a stabilizing controller due to the bandwidth limitations imposed. From table A.2 it can be seen that the zeros for P_2 increases as the valve opening increases. At the operating point of z=0.3 it is larger then 0.7605 and cant be directly dismissed as a possible measurement. The model in [4] gets lower zeros for P_2 conludes that it cant be used for a stabilizing controller. Both Volume flow Q and mass flow W appears to be better alternatives, but they both have LHP-zeros close to or at the imaginary axis. An attempt to stabilize the system with one of these measurements would result in an almost integrating closed loop system. According to Storkaas a cascade control could solve this problem by using a combination of a flow measurement and some other measurement, e.g pressure.

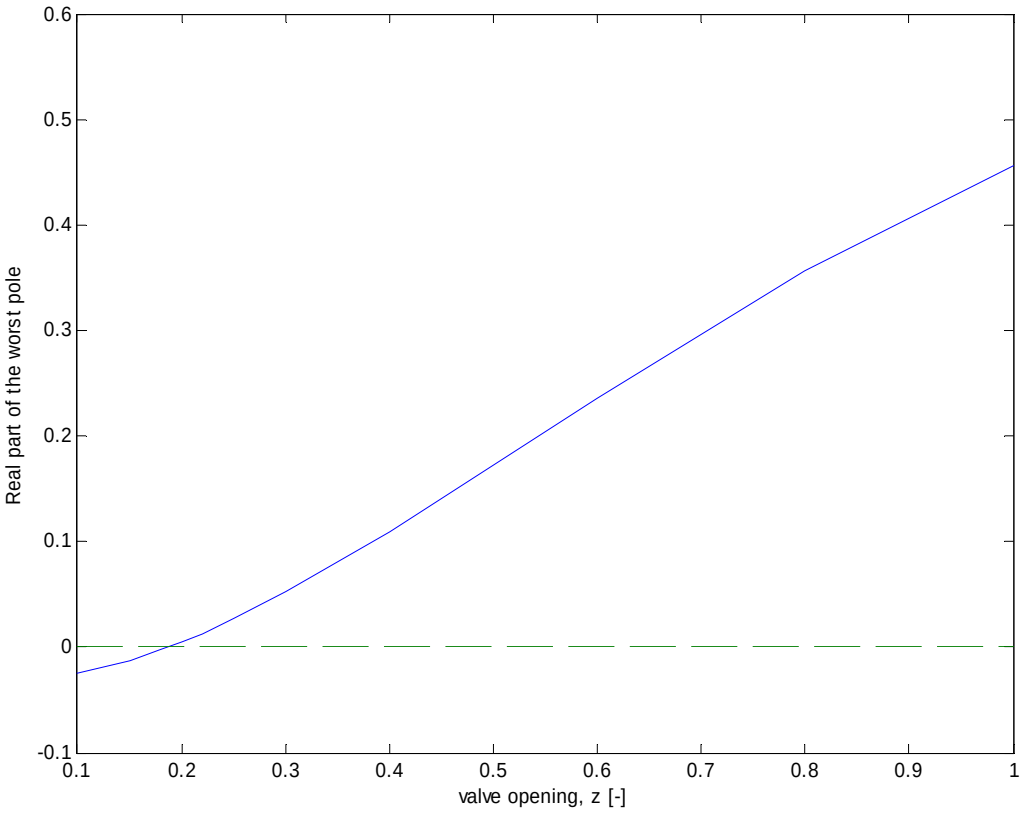

Figure 3.32 Real part of the worst pole.

3.8 Anti slug control

In this chapter different control structures will be tested on the Miniloop, and they will be compared to simulations performed on the simplified slug model. The criteria for satisfactory control is to stabilize the system at a valve opening that would normally result in severe slugging in open loop.

3.8.1 Control with upstream measurements

According to the controllability analysis the best choice of measurement would be the upstream pressure P1. A simple PI controller with gain K=22 bar^{-1} and integral time T_i=10s will stabilize the system as shown in figure 3.33. The system starts from a state of severe slugging, and the controller is turned on after two minutes. After an additional two minutes the controller is set to manual and the slugging reappears. The top chart in figure 3.33 shows the upstream pressure P1 vs. time. The blue line is the pressure and the red line is the set point for the pressure controller, witch was set to 0.115 barg. The controller stabilizes the system quickly if a bit aggressive. The stabilized system experiences small pressure oscillations, however these are small compared to the amplitude of the slugging, so the tracking performance of the controller is considered as good. The actuator use is acceptable. It's constantly making small adjustments to keep the system stable and at the stationary unstable solution. It is evident that the system is stabilized in the unstable region since the valve is operating at a valve opening that lies in the unstable are for open loop. This can be seen from the bifurcation diagram (figure 3.29). As excepted the slugging reappears quickly after the controller is turned off. In light of the control objective the pressure controller is performing very well.

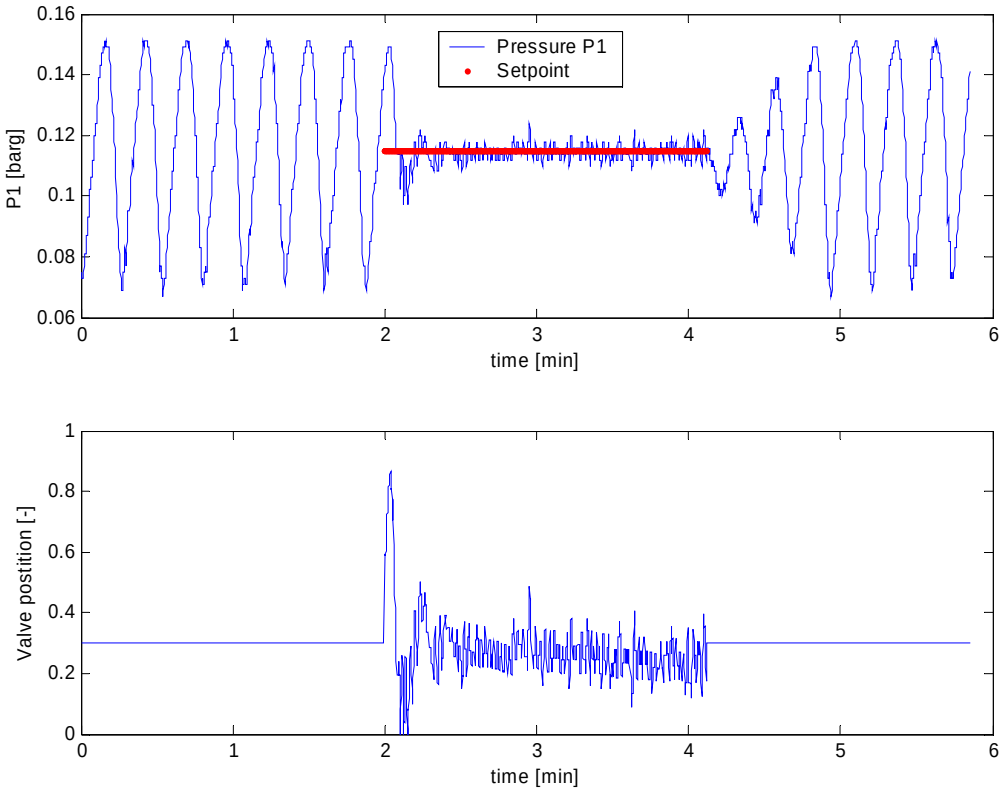

Figure 3.33 Performance of a pressure controller on the miniloop.

A simulation was also run on the simplified slug model (figure 3.34) using the same parameters for the gain and integral action as above. The set point for the controller was also the same (0.115 barg). As above the pressure is represented with the blue line and the red line indicates the set point. The simulation starts in open loop resulting in severe slugging. After 2 minutes the controller is turned on. After an additional 3 minutes the controller is returned to manual mode. The controller quickly stabilizes the system and the tracking performance is very good. The actuator use is minimal as it moves towards the valve opening corresponding to the set point of 0.115 barg. It seems to stay stable at this value, however if one had zoomed in on the graph one would have seen that the actuator is continuously making small corrections to hold the system stable.

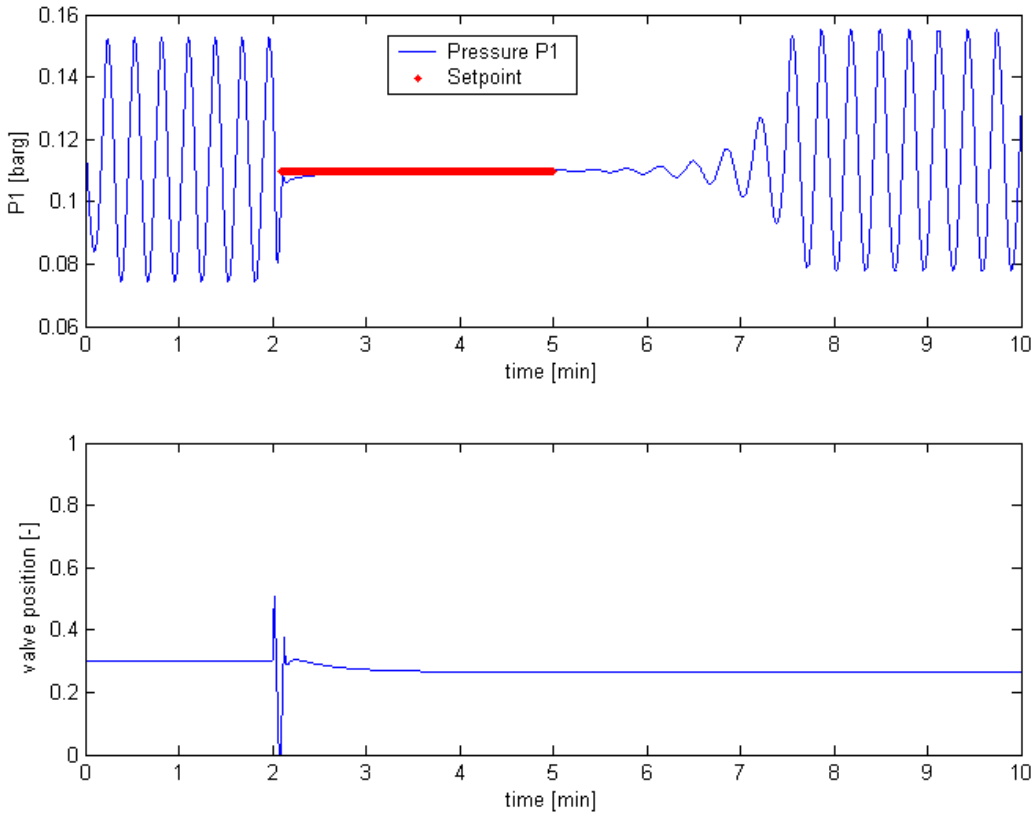

Figure 3.34 Performance of a pressure controller on the simplified model.

By comparing the simulation to the experimental data(figure 3.33) it is obvious that the simplified model is in accordance with the experimental data.
The simplified model simulates the results obtained experimentally very accurately. More importantly, the controller in the simulation reproduced the stability results obtained experimentally from the lab scale Miniloop. The biggest difference between the model and the Miniloop is the time it takes for severe slugging to reappear after the controller is turned off. While this takes less then a minute for the Miniloop, the model requires almost three minutes. The reason for this is that the simplified model contains little noise causing the pressure to stay close to the reference value for a longer time.

3.8.2 Control with downstream measurements

In the previous chapter it was shown that a simple PI controller could stabilize the system using one upstream measurement (P1). As mentioned earlier this measurement is in many cases not even installed. In other cases it will often prove unreliable or unusable for control. The controllability analysis in chapter 3.7 provided the basis for exploring other possibilities.

P2 as measurement.
The controllability analysis could not dismiss the pressure drop as possible measurement. For this reason an attempt was made to stabilize the Miniloop by using a pressure controller with P2 as the measurement. All attempts to stabilize the system proved unsuccessful and P2 was dismissed as a possible measurement for a stabilizing controller. Since the controllability analysis in [4] had excluded P2 as a measurement it will not be treated any further here.

3.8.3 Cascade control

According to the controllability analysis both the total mass flow W and total volume flow Q were better suited for a stabilizing controller. However stabilizing the system with one of these measurements would lead to an (almost) integrating closed loop system, but a cascade configuration with a pressure measurement in the outer loop could solve this problem.

Because of the problems with obtaining an estimate of the volume flow rate (chapter 3.4.2) the mass flow W was chosen as the measurement. Two different cascade configurations were tested where the downstream- and upstream pressure were used for feedback purposes.

3.8.4 Mass flow W and upstream pressure P1

Figure 3.35 shows that a cascade controller using mass flow W in the inner loop and upstream pressure P1 in the outer loop will stabilize the system. The system is started in open loop with severe slugging and the controller is turned on after 2 minutes. After an additional 3.2 minutes the controller is switched back to manual. The inner loop uses a pure proportional controller while the outer loop uses both proportional and integral action. The parameters for the gain and integral action are listed in table 3.6.

Table 3.6 Tuning parameters

	Inner loop	Outer loop
K	0.8 [bar^{-1}]	15 [min/kg]
T_i	-	30 [s]

The two upper charts show the pressure vs. time and the mass flow vs. time. The red line indicates when the controller is active and represents the set point of 0.115 barg for the outer loop. The set point for the inner loop is provided by the outer loop. The actuator use is displayed in the bottom chart.

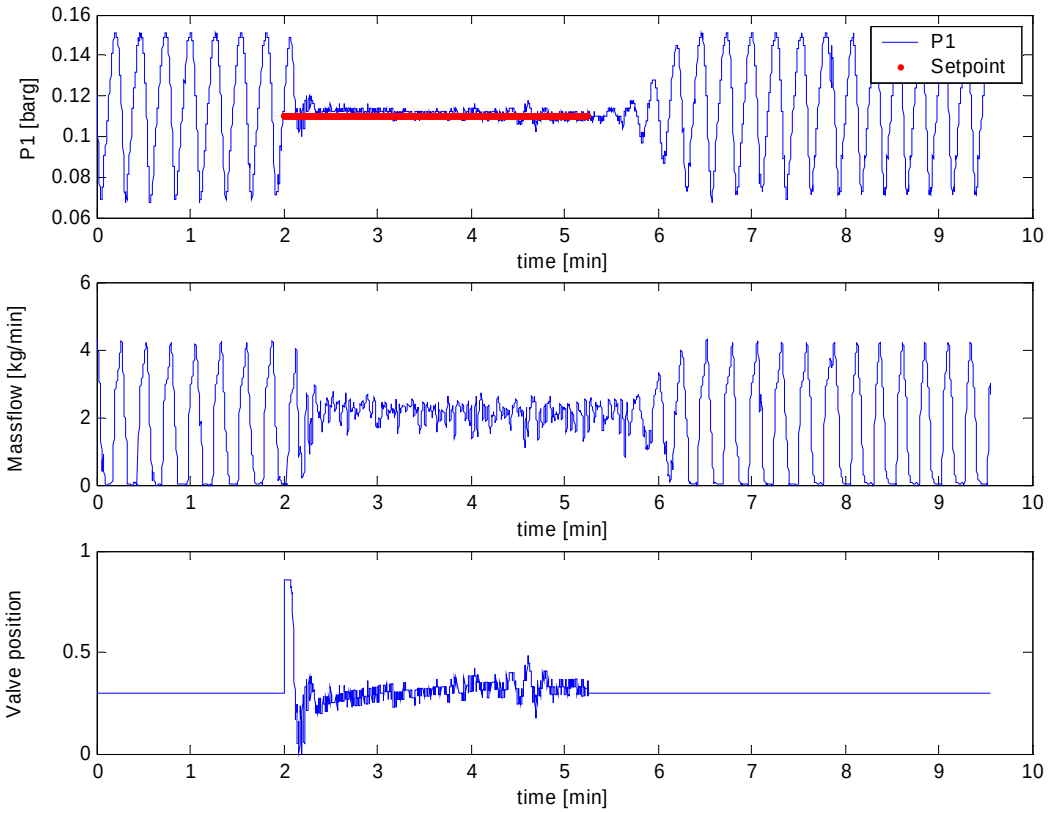

Figure 3.35 Cascade control with W in inner loop and P1 in outer loop (miniloop)

By examining the actuator usage one can see that the system is stabilized at a valve opening in the unstable region for open loop.
When the controller is turned on the slugging is quickly eliminated, but the cascade controller uses a bit more time to reach the reference value compared to the pure PI controller in chapter 3.8.1. This is outweighed by the better tracking performance exhibited by the cascade controller. The amplitude of the pressure oscillations during active control is small, meaning that the controller successfully keeps the pressure tighter around the reference value compared to the PI controller. This didn't come as a surprise. Because of the low gain in the inner loop the actual stabilizing is done by the outer loop. In the case above the inner loop merely serves as a filter for the outer loop.

Tuning the controllers turned out to be a difficult and time-consuming task of trial and error. An attempt was made at disconnecting the outer loop and tuning the inner loop first. When this proved unsuccessful the outer loop was reconnected and both loops were tuned simultaneously. The overall strategy of the tuning was as follows. By operating at a higher set point the corresponding valve opening would be in the stable area of the bifurcation diagram(figure 3.29). At this valve opening the system would already be stable in open loop. When the controller was turned on the actuator would operate in the stable area and the process would stabilize regardless of the parameters used. The nest step was to tune the controller so that the pressure was brought to its reference value, still in the stable region. Then by slowly lowering the set point the process was forced towards the unstable area. When the set point was low enough the valve opening would start to operate in the unstable area above $z = 0.19$. In the start the process would start to oscillate at this point, but by tuning the parameters the process was slowly brought into the unstable area. The biggest challenge lay in the inner loop gain. It was evident that the gain had to be increased further if the inner loop were to take over the stabilizing task. All attempts to increase the gain further resulted in an oscillating behaviour where the actuator and the flow estimate would oscillate between min and max values. The problem lay in the noise and disturbance in the flow measurement. Different filters were tested as the tuning progressed but combined with the flow pattern described in chapter 3.4.1 the noise picture made it impossible to stabilize the system with the inner loop.

The current parameters used in table 3.6 allowed the process to operate at a higher valve opening then what was possible for the PI controller before the system would go unstable. By lowering the set point even more to 0.1 barg the process would operate at valve openings over 30 %. This would allow even better oil recovery in real life applications in the oil industry.

Figure 3.36 show the same case simulated using the simplified slug model. The parameters are the same as those given in table 3.6. The simulation starts in open loop and the controller is switched on after 2 minutes. After an additional 5 minutes the controller is returned to manual. The controller in the simulation also reproduced the stability results shown experimentally above. The pressure is effectively stabilized even though the model takes a bit longer to reach the reference value. Like the previous case it takes more time before the slugging reappears in the model compared to the Miniloop. All in all the simulated response is in accordance with the experimental data.

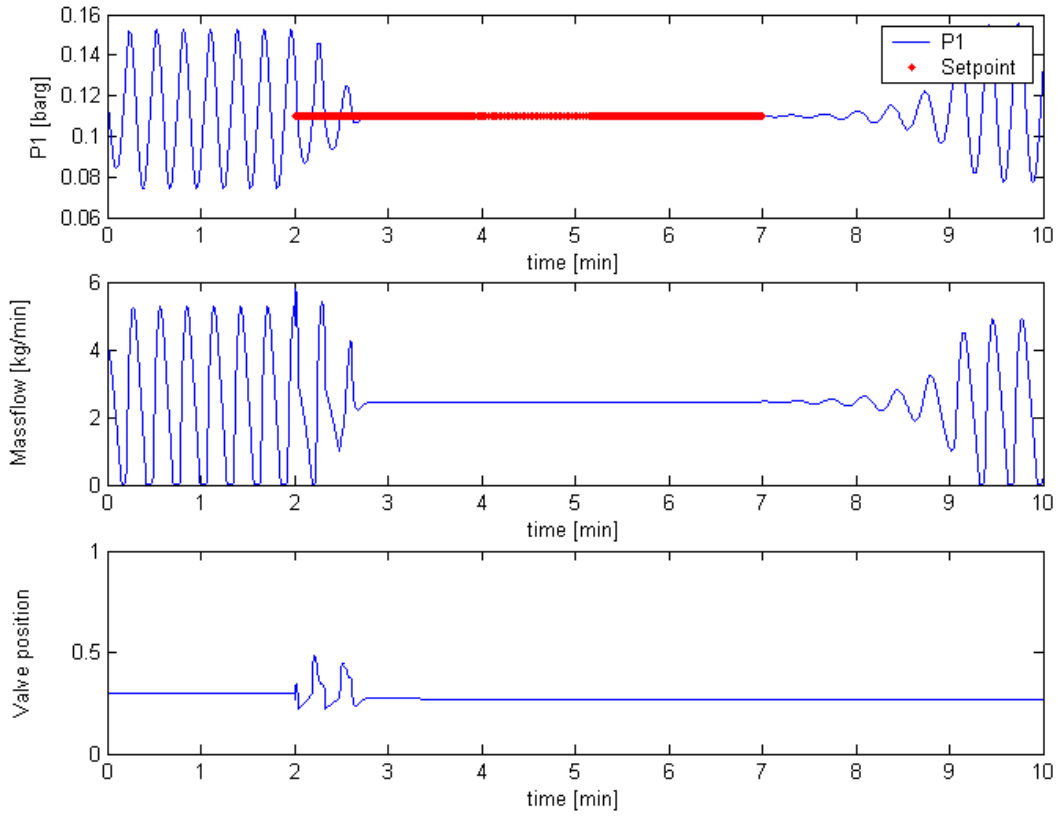

Figure 3.36 Cascade control with W in inner loop and P1 in outer loop (Model)

3.8.5 Mass flow W and downstream pressure P2

In light of the results obtained in the previous chapter the prospect of achieving satisfactory control of the system using only downstream measurements were grim. The noise picture and nature of the slug flow prevented the inner loop from stabilizing the system when the mass flow was used. The reason it was possible to stabilize the system lay in the stabilizing property of the outer loop. In this case, the pressure drop over the choke valve (P2) is unsuitable for a stabilizing controller according to the controllability analysis. The same noise picture that created the problems for the previous case would still be present for this control configuration. However an attempt was made using the same tuning strategy as for the case in chapter 3.8.4.

The system was brought to steady state in the stable region and gradually forced towards the unstable area by changing the set point and tuning the parameters. Figure 3.37 shows the response obtained with the tuning parameters in table 3.7. The process starts in open loop with sever slugging and the controller is turned on after 70 s with a set point of 0.02 barg. The controller first stabilizes the system by bringing it into the stable area. The straight line in the bottom chart is the valve opening (z = 0.19) corresponding to the bifurcation point in figure 3.29. Valve openings below this value are in the stable area and visa versa. As can be seen from the chart the pressure is slowly brought to its reference value as the valve approach the valve opening (z=0.19) corresponding to the set point.

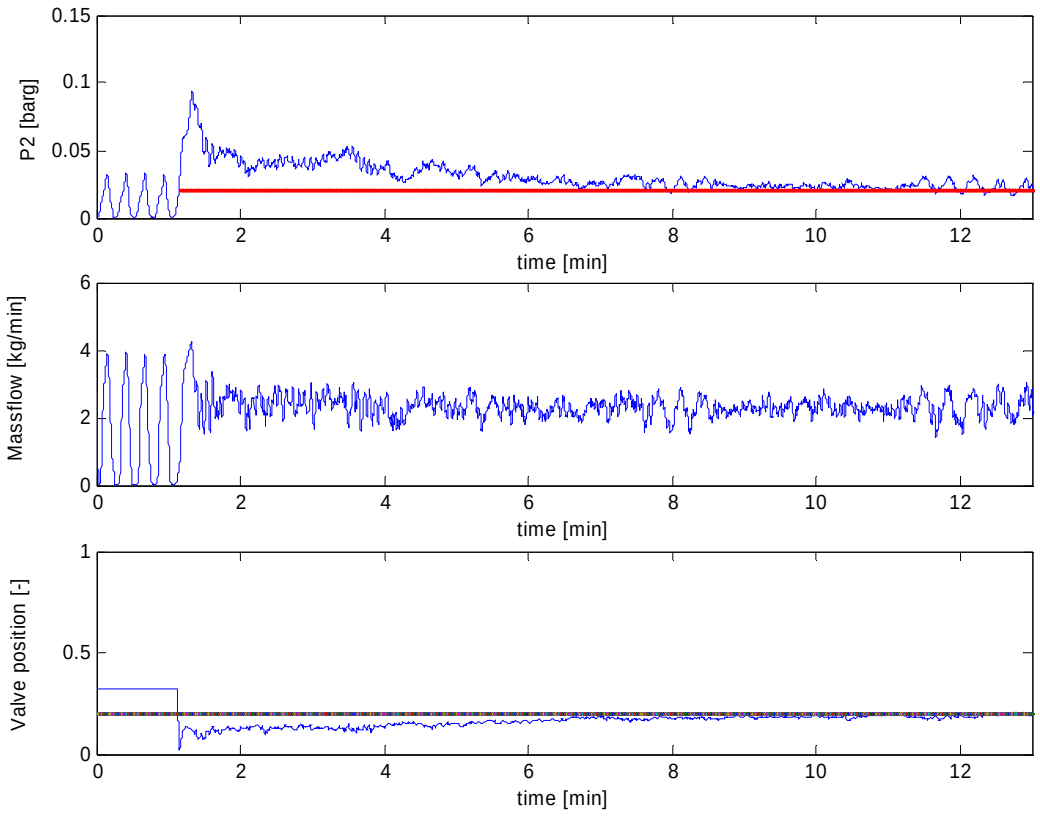

Figure 3.37 Cascade control with W in the inner loop and P2 in the outer loop (Miniloop).

However the valve opening is still not in the unstable area. Further attempts to force the process into the unstable area only resulted in the reappearance of the pressure oscillations associated with slugging.

Table 3.7 Control parameters.

	Inner loop	Outer loop
K	0.28 bar^{-1}	1.5 min/l
T_i	-	20 s

Like in the previous case the low gain in the inner loop means that the stabilizing task is left to the outer loop. All attempts to increase the gain led to severe oscillations for the actuator and the flow measurement due to the disturbances and noise picture as described in the previous chapter.

According to storkaas[2] the cascade configuration with mass flow in the inner loop and pressure drop over the choke valve should stabilize the process. To prove this a simulation was done using the simplified slug model. Attempts to tune the controllers manually were not successful, but by using the model storkaas was able to produce tuning parameters that would stabilize the given system.

Figure 3.38 show that the cascade controller with the tuning parameters given in table 3.8, stabilizes the system. The set point for the pressure was 0.010 barg.

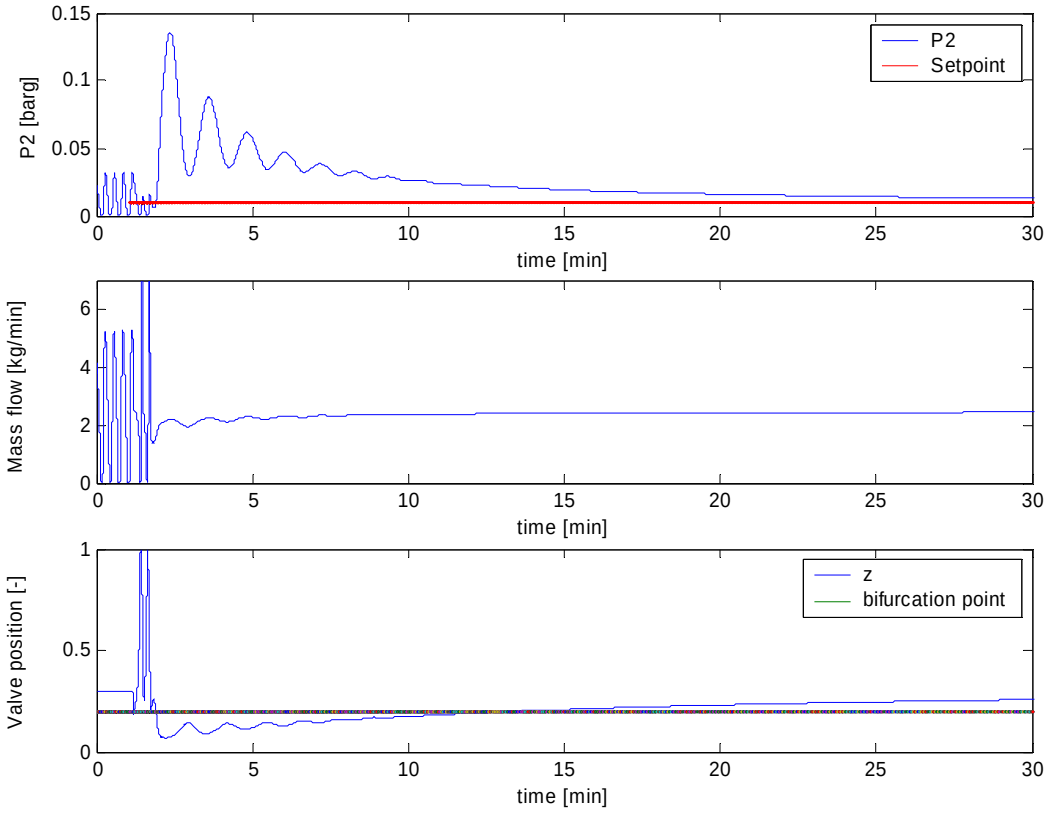

Figure 3.38 Cascade control with W in inner loop and P2 in outer loop (model).

The system start in open loop with severe slugging and the controller is turned on after 70 s. The controller forces the pressure up by closing the valve to an opening lying within the stable area. Then the pressure is slowly driven towards the reference value as the system enters the unstable are. After 30 minutes of simulation the pressure reaches its reference value. As can be seen from the actuator usage the system is stabilized in the unstable area because the valve opening is at a value corresponding to slugging for open loop.

Table 3.8 Control parameters.

	Inner loop	Outer loop
K	10 bar^{-1}	-0.02 min/l
T_i	-	30 s

The higher value for the gain in the inner loop proves that the stabilizing work is performed by the inner loop.

The tuning parameters in table 3.8 were also tested on the Miniloop. The controller acted by closing the valve resulting in an increase in pressure. The pressure eventually became so high that the experiment had to be aborted for safety reasons. The simplified slug model continues to show its similarity to the experimental data. Even though the cascade controller failed to stabilize the slugging in the unstable area the response is similar. In both cases the controller brought the system into the stable area before it attempted to bring the pressure to its reference value by bringing the system into the unstable area.

3.9 User manual

As a stage in documenting the work done on the Miniloop during this thesis a user manual has been written. The manual is considered as a part of this thesis and it can be found in appendix B. However it is written as a separate report so it can be used independently. Because of this the user manual contains some of the information reported in chapter 3.

4 Future work

- The noise picture and disturbances associated with the flow measurement made it impossible to stabilize the process with mass flow in the stabilizing loop. If a more accurate measurement of the flow could be estimated the cascade configuration in chapter 3.8.5 might have worked.
    - The flow pattern when the system is stable (figure 3.21) contained large Tailor shaped bubbles. The large gas volume in between the liquid bulks caused the data registered by the slug sensor to vary between liquid and air. This in turn caused the flow estimate to oscillate. Changing the piping to one with a bigger diameter may change the flow pattern during stable flow. If this could be achieved the slug sensor would be able to estimate a more stable and continuous flow rate.
    - The simplest solution would be to replace the slug sensors with a measuring device more suited for the task. A capacitance meter has been implemented with great success by Kaasa [5]. The capacitance meter gives an accurate value off the hold-up, and if used in series the delay can give the slug velocity.
- The cascade configuration with mass flow in the inner loop and the pressure drop over the choke valve failed to stabilize the process even though it should be possible according to the theory. Perhaps a more advanced MISO controller would prevail where the cascade configuration failed. In [6] an advanced multivariable H_∞ design were developed and tested and compared with a cascade configuration. It concluded that the MISO H_∞ controller outperformed the cascade configuration. The H_∞ controller could handle large uncertainties, up to 80 %. Perhaps this would allow it to stabilize the process even with the current measurement setup.

5 Conclusion

By fitting the simplified model to the experimental data gathered from the Miniloop, it has been shown that the model is a good representation of the process. This can be seen from the good fit of the bifurcation diagram.

The controllability analysis shows that the best measurement alternative for a stabilizing controller is the upstream pressure P1. Both the downstream pressure P2 and ρ_m are badly suited as a stabilizing controller. The controllability analysis show that the total mass flow or total volume flow are better alternatives. Stabilizing the system with one of these two measurements will result in an almost integrating process. But a cascade configuration with flow in the inner loop and pressure in the outer loop could solve this problem.

A simple PI controller using the upstream pressure P1 as measurement stabilized the system. Two different cascade configurations were also tested. One used the upstream pressure P_1 in the outer loop, while the other one used the downstream pressure P_2 in the outer loop. Both cascade configurations used the mass flow W in the inner loop.

The cascade configuration with P_1 in the outer loop managed to stabilize the process around a valve opening that would result in severe slugging during open loop. The low gain in the inner loop means that the actual stabilizing task is done by the outer loop. The inner loop merely acts as a filter.

The cascade configuration with P_2 in the outer loop also stabilized the system, but around a valve opening within the stable region. Attempts to force the process into the unstable region resulted in the reappearance of slugging. Simulations on the simplified slug model however managed to stabilize the system in the unstable area. The reason the cascade controller failed to stabilize the Miniloop is because of the disturbances and the noise picture associated with the mass flow measurement.

In light of the control objective given in chapter 1 this cascade configuration did not achieve acceptable control, but both the simple PI controller and cascade controller using the upstream pressure P1 did.

The simulations done with the simplified model are in good accordance with the results obtained experimentally. The response and behaviour of the simulations described the real process very well. This thesis therefore adds to the growing list of papers that verifies the simplified slug model as a useful tool for control purposes.

References

[1] Golan, M., ”Internal Notes on Orfice Valve Equation (Thornhill Carver Equation,” NTNU, 2003.
[2] Storkaas, E., Skogestad, S., “A low-dimensional dynamic model of sever slugging for control design and analysis,” NTNU, June 2003.
[3] Bårdsen, I., “Anti-slug control for two phase flow. Experimental verification (In Norwegian),” NTNU, autumn 2003.
[4] Storkaas, E., Skogestad, S., “Stabilization of sever slugging based on a low-dimensional nonlinear model,” NTNU, 2002.
[5] Kaasa, L., “Demonstration and control of multiphase production wells,” NTNU, July 2003.
[6] Haukelidsæter, B., “advanced control – Robust control of pipeline-riser slugging,” NTNU, june 2004.
[7] Skogestad, S., Postlethwaite, I., *Multivariable Feedback Control- Analysis and Design.* John Wiley & Sons Ltd., second ed., 2001.
[8] Havre, K., Stornes, K., and Stray, H., “Taming slug flow in pipelines,” ABB review 4, 2000, pp. 55-63.
[9] Matlab model “simplified slug model” aviable at : http://www.nt.ntnu.no/users/espensto/SlugModel/
[10] Seborg, D. E., Edgar, T. F., and Mmellichamp, D. A., *Process dynamics and control*, John Wiley & Sons Ltd., 1989.
[11] Sinnott, R. K., *Coulsons & Richardson’s Chemical Engineering*, Volume 6, Butterworth-Heinemann, Third edition, 1999.
[12] National instruments: http://www.ni.com/aap/

Appendix A

A.1 *Miniloop – Experimental data*

The experimental data used to create the bifurcation diagram for the Miniloop were stored and are shown in figure A.1-A.13. The figures show the upstream pressure P1 and the downstream pressure P2 vs. time. To create a "cleaner" visualization of the pressures a Savitzky-Golay filter was added.

A.2 *Savitzky-Golay filters*

The data used to create figures A.1 to A.13 are stored as the miniloop program received them i.e. without additional filtering. The filter applied to the data in A.1 had a frame size f=21 and a polynomial order k = 3.

> Savitzky-Golay filters are optimal in the sense that they minimize the least-squares error in fitting a polynomial to frames of noisy data.
>
> ***y = sgolayfilt (x,k,f) applies a savitzky-Golay FIR smoothing filter to the data in vector x. If x is a matrix, sgolayfilt operates on each column. The polynomial order k must be less then the frame size, f, witch must be odd. If k = f-1, the filter produces no smoothing.***

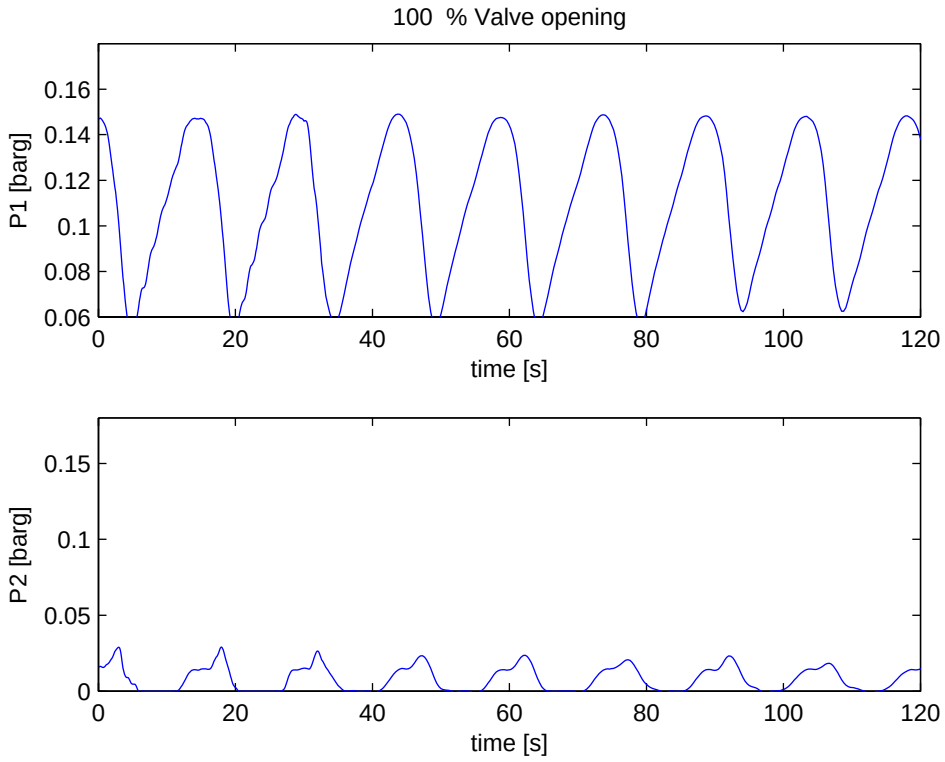

Figure A.1 Open loop data for z = 1

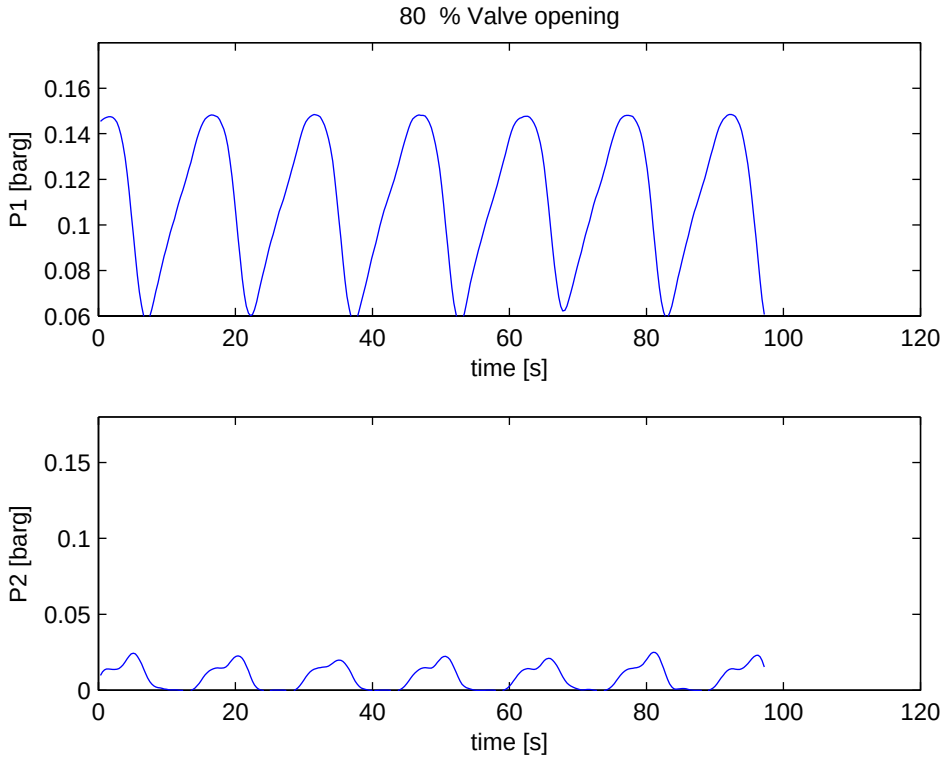

Figure A.2 Open loop data for z = 0.8

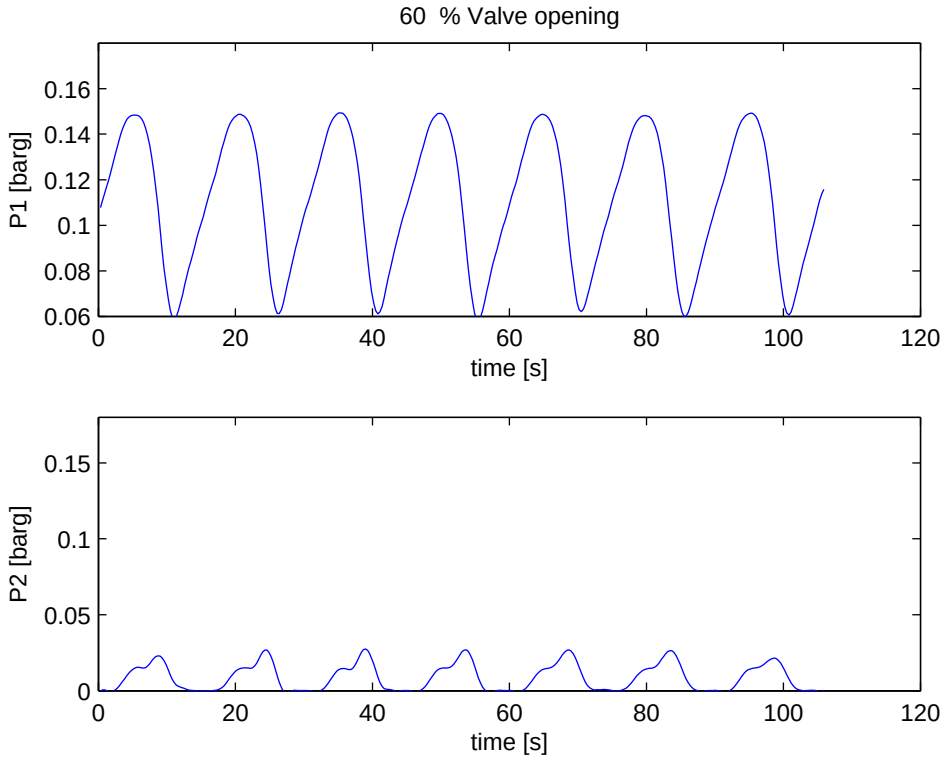

Figure A.3 Open loop data for z = 0.6

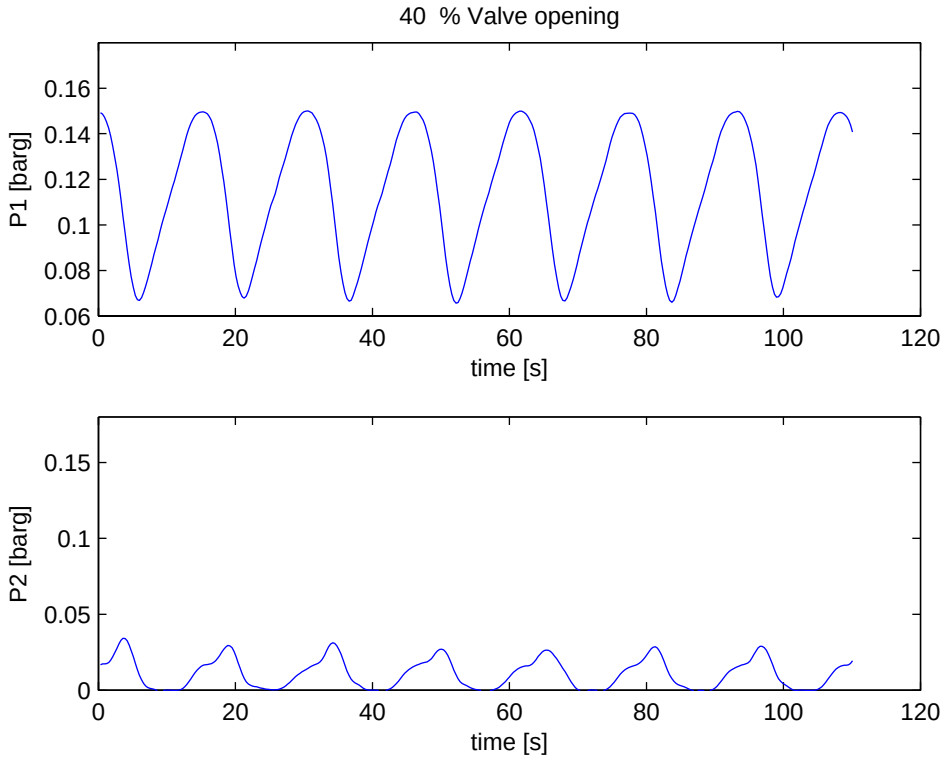

Figure A.4 Open loop data for z = 0.4

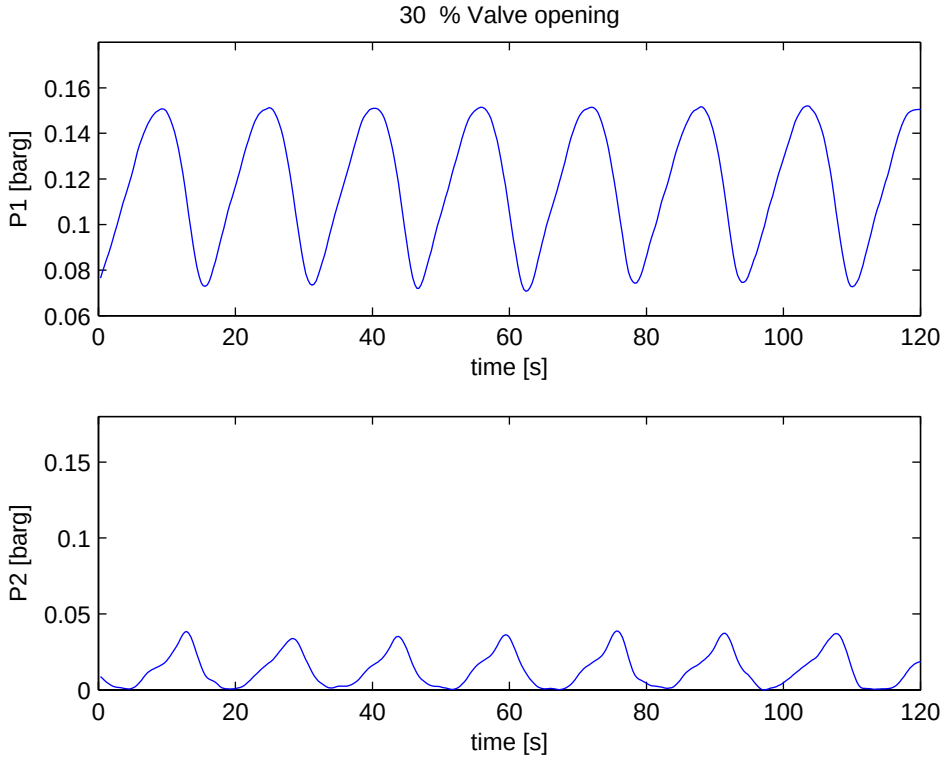

Figure A.5 Open loop data for z = 0.3

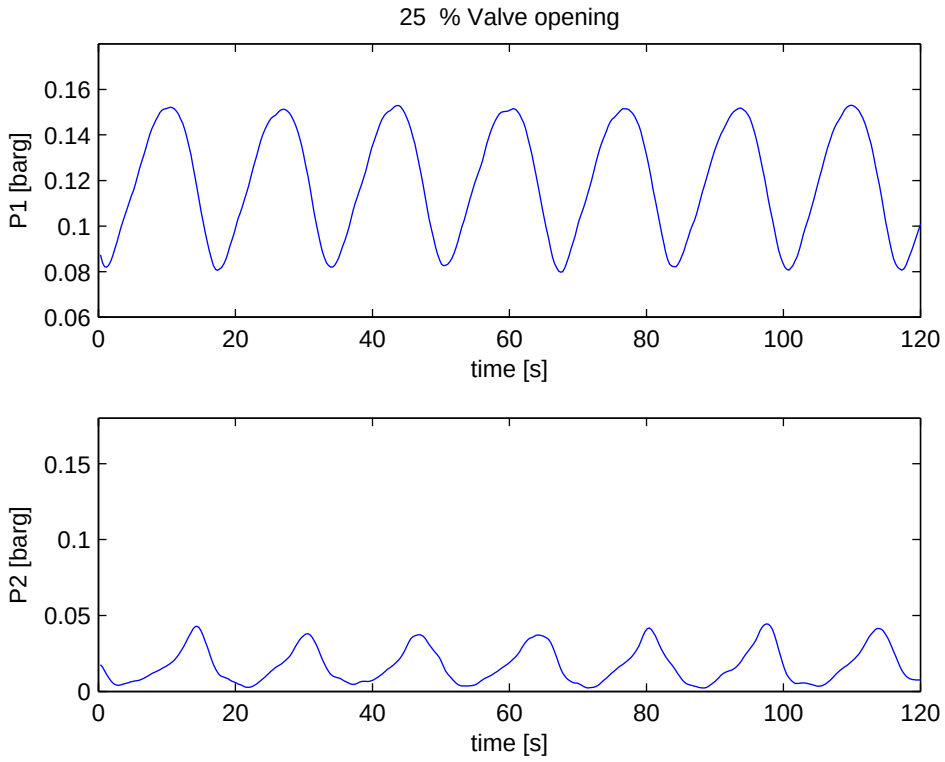

Figure A.6 Open loop data for z = 0.25

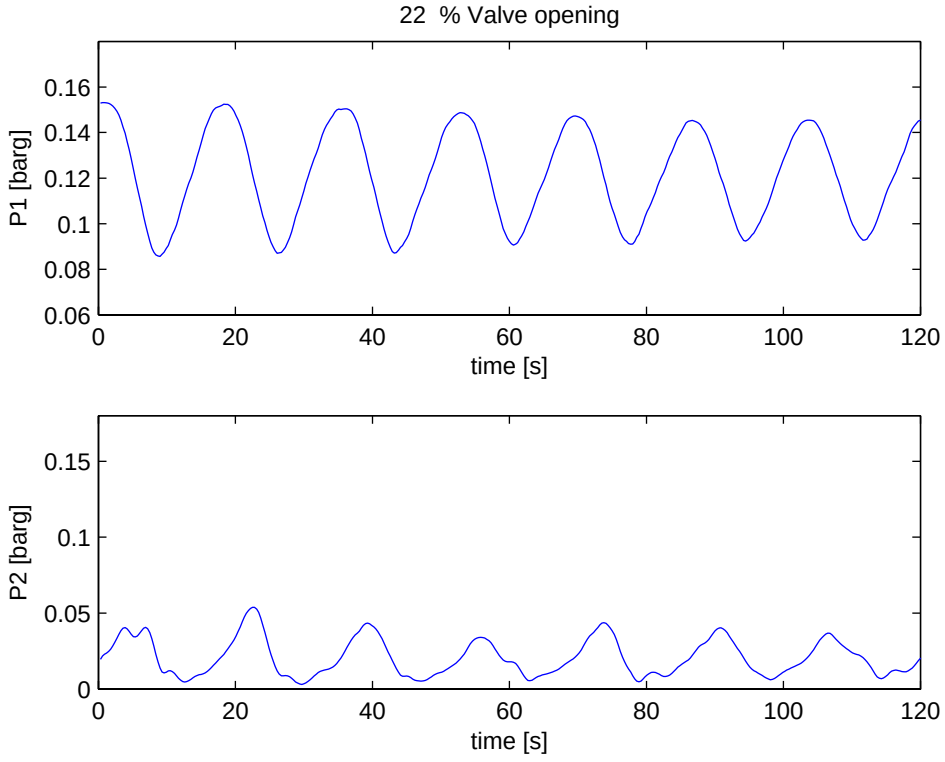

Figure A.7 Open loop data for z = 0.22

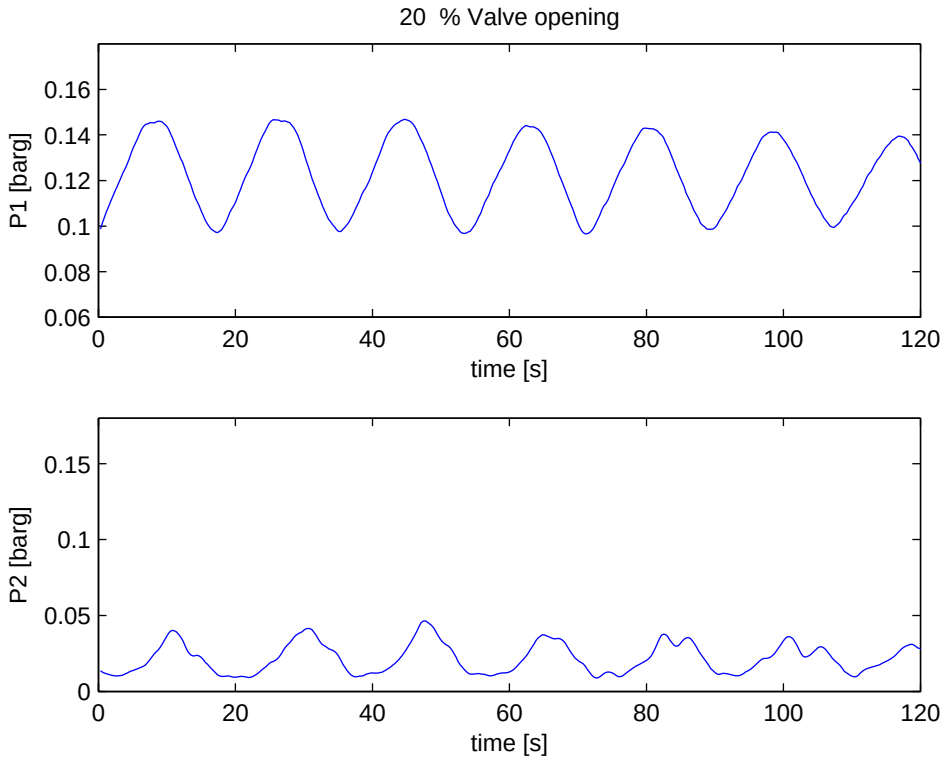

Figure A.8 Open loop data for z = 0.2

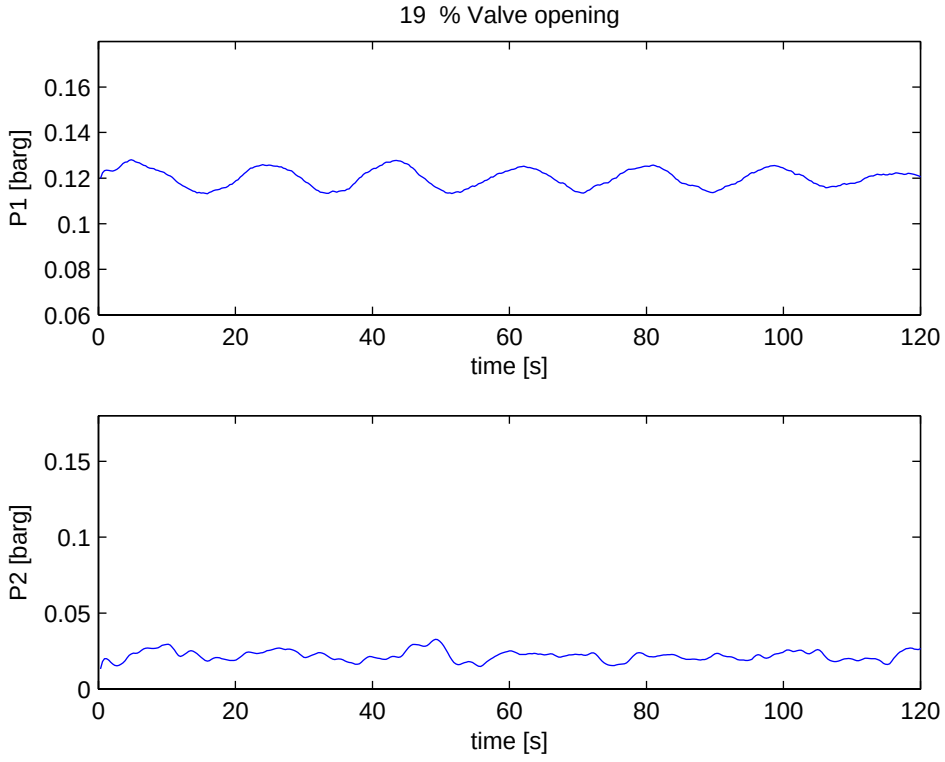

Figure A.9 Open loop data for z = 0.19

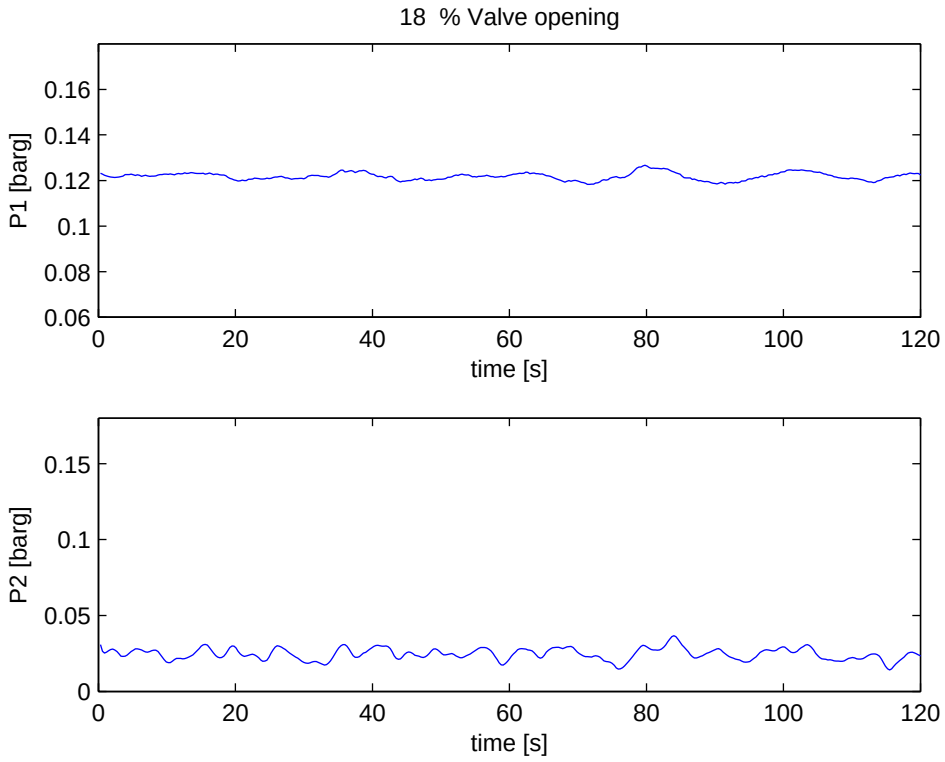

Figure A.10 Open loop data for z = 0.19

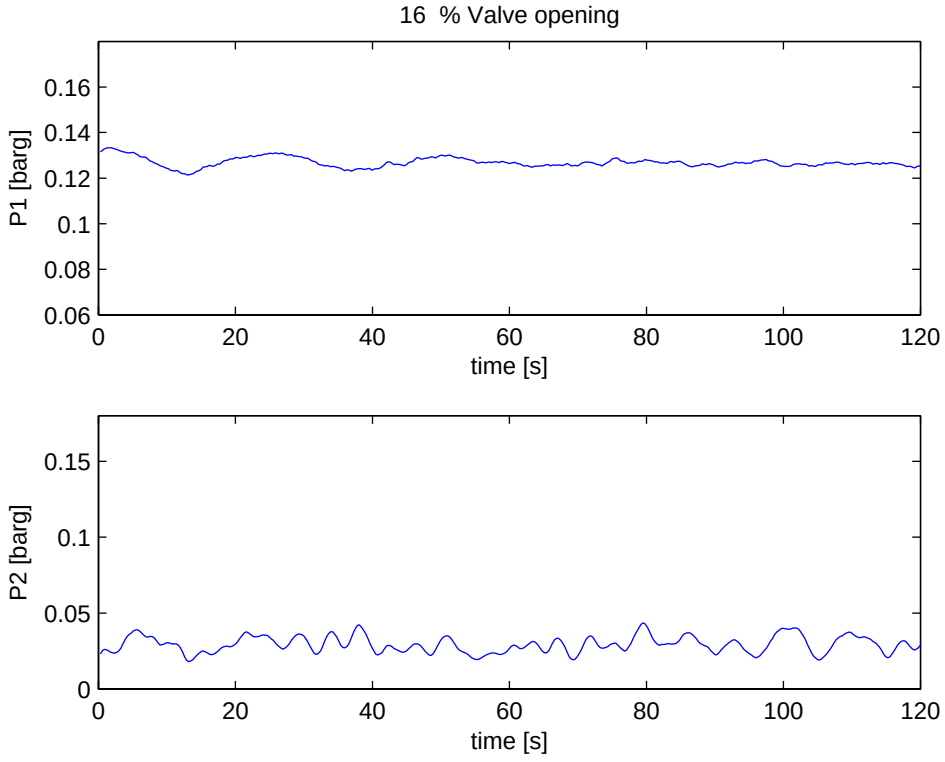

Figure A.11 Open loop data for z = 0.18

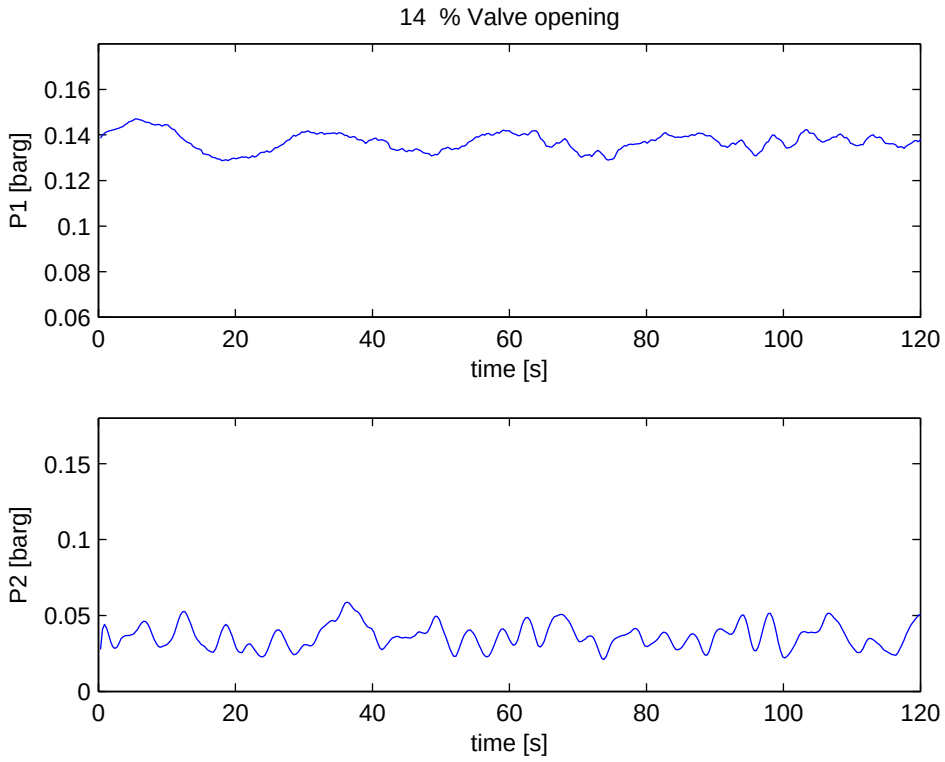

Figure A.12 **Open loop data for z = 0.14**

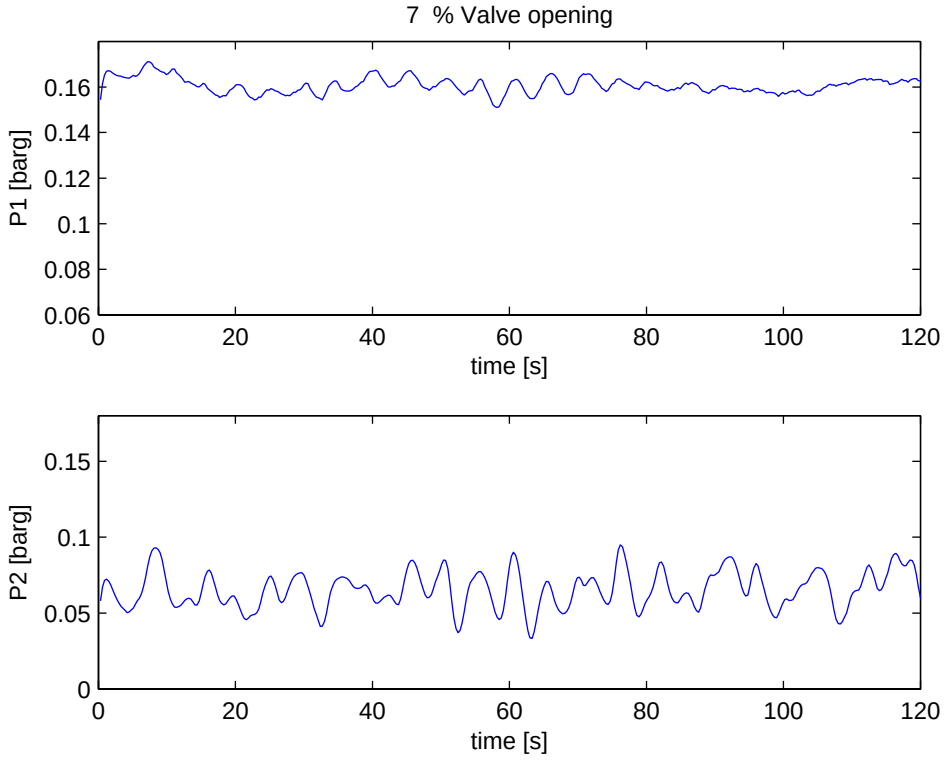

Figure A.13 **Open loop data for z = 0.07**

A.3 Generated data from the simplified slug model.

Table A.1 shows the different zeros for the measurement alternatives at different valve openings. The corresponding system poles at the same valve openings are located in table A.2.

Table A.1 Zeros for the different measurements at different valve openings.

Z	P1	P2	ρ_m	W	Q
0,1	-0.1520	0.5239 + 0.8920i 0.5239 - 0.8920i	0.0532 + 0.0107i 0.0532 - 0.0107i	-12.670 -0.0100 + 0.0650i -0.0100 - 0.0650i	-5.4594 -0.1379 -0.0453
0,15	-0.1597	0.7002 + 0.7915i 0.7002 - 0.7915i	0.0812 0.0312	-12.843 -0.0096 + 0.0631i -0.0096 - 0.0631i	-5.5478 -0.1456 -0.0424
0,18	-0.1626	0.7668 + 0.7394i 0.7668 - 0.7394i	0.0874 0.0273	-12.913 -0.0094 + 0.0624i -0.0094 - 0.0624i	-5.5836 -0.1484 -0.0415
0,20	-0.1640	0.7969 + 0.7125i 0.7969 - 0.7125i	0.0899 0.0259	-12.945 -0.0094 + 0.0621i -0.0094 - 0.0621i	-5.6002 -0.1498 -0.0411
0,22	-0.1650	0.8197 + 0.6907i 0.8197 - 0.6907i	0.0918 0.0248	-12.969 -0.0093 + 0.0619i -0.0093 - 0.0619i	-5.6131 -0.1507 -0.0407
0,25	-0.1661	0.8449 + 0.6648i 0.8449 - 0.6648i	0.0937 0.0237	-12.997 -0.0093 + 0.0616i -0.0093 - 0.0616i	-5.6274 -0.1518 -0.0404
0,3	-0.1673	0.8720 + 0.6347i 0.8720 - 0.6347i	0.0958 0.0226	-13.027 -0.0092 + 0.0614i -0.0092 - 0.0614i	-5.6430 -0.1530 -0.0401
0,4	-0.1686	0.8996 + 0.6012i 0.8996 - 0.6012i	0.0979 0.0216	-13.058 -0.0092 + 0.0611i -0.0092 - 0.0611i	-5.6593 -0.1542 -0.0397
0,6	-0.1695	0.9198 + 0.5745i 0.9198 - 0.5745i	0.0993 0.0209	-13.081 -0.0091 + 0.0609i -0.0091 - 0.0609i	-5.6713 -0.1551 -0.0394
0,8	-0.1700	0.9269 + 0.5658i 0.9269 - 0.5658i	0.0996 0.0207	-13.090 -0.0091 + 0.0609i -0.0091 - 0.0609i	-5.6756 -0.1556 -0.0394
1	-0.1718	0.9301 + 0.5706i 0.9301 - 0.5706i	0.0979 0.0209	-13.097 -0.0091 + 0.0612i -0.0091 - 0.0612i	-5.6776 -0.1574 -0.0392

Table A.2 Poles for the system at different valve openings.

Valve opening z	poles
0,1	-9.2653
	-0.0246 + 0.1459i
	-0.0246 - 0.1459i
0,15	-9.5311
	-0.0133 + 0.1862i
	-0.0133 - 0.1862i
0,18	-9.7067
	-0.0030 + 0.2157i
	-0.0030 - 0.2157i
0,20	-9.8250
	0.0047 + 0.2351i
	0.0047 - 0.2351i
0,22	-9.9468
	0.0131 + 0.2543i
	0.0131 - 0.2543i
0,25	-10.1399
	0.0268 + 0.2823i
	0.0268 - 0.2823i
0,3	-10.4951
	0.0522 + 0.3265i
	0.0522 - 0.3265i
0,4	-11.3499
	0.1100 + 0.4042i
	0.1100 - 0.4042i
0,6	-13.6612
	0.2365 + 0.5159i
	0.2365 - 0.5159i
0,8	-16.7605
	0.3561 + 0.5807i
	0.3561 - 0.5807i
1	-20.6258
	0.4565 + 0.6196i
	0.4565 - 0.6196i

A.4 Hold-up measurement

The hold-up measurement is calculated from the optical sensor (slug sensor).
The slug sensor provides a signal between 1 and 5 volt, where 1 volt means that the tube is filled with water and 5 volt means the tube is filled with air.

The following calculations are added into the LabVIEW code, and represents how the program calculates the hold-up based on the signal received from the optical sensor. The calculations is carried out within the subVi called density.

A linear relation is assumed between the amount of light absorbed by the liquid and the amount of liquid the light from the sensor has to pass through. Equation A-1 calculates the height of the liquid (h) in the pipe based on the sensor signal (S).

$$h = 1.9 - ((1.9/3.9) \cdot S - (1.9 \cdot 1.1/3.9)) \tag{A-1}$$

Equation A-1 is merely a scaling of the signal from 1-5 volts to 0-1.9 cm. 1.9 cm is the diameter of the pipe.
Equation A-2 will calculate the area of the segment of pipe covered with water.

> *Consider a circle of radius a (cross section of pipe) and imagine that the liquid has reached height h, measured from the lowest point on the circle. Note that 0 <= h <= 2a. The area A_w of the segment of the circle covered by the liquid is then given by (a=0.95):*

$$A_w = \frac{\pi \cdot 0.95^2}{2} - 0.95^2 \cdot \arcsin\left(\frac{1-h}{0.95}\right) - (0.95 - h) \cdot \sqrt{(h * (2 * 0.95 - h))} \tag{A-2}$$

By dividing the area of the segment of pipe covered with water with the total area of the cross section we get the hold up.

$$x_w = \frac{A_w}{\pi \cdot 0.95^2} \tag{A-3}$$

A.4 Parameter estimation

The liquid flow estimate [l/min] is based on the two following equations

$$Q = k \cdot z^n \sqrt{\Delta P / \rho_m} \quad \text{(A-4)}$$

$$Q = f(z)\sqrt{\Delta P / \rho_m} \quad \text{(A-5)}$$

Method a) *Linear parameter estimation*

This method uses equation A-1. There are two parameters, k and n, and three variables Q, z and ΔP . The idea is to rearrange equation A-1 so that the two parameters can be estimated. Since only water is present in the system ρ_m = 1, reducing A-4 to

$$Q = k \cdot z^n \sqrt{\Delta P} \quad \text{(A-6)}$$

By taking the natural logarithm on both sides the equation can be rearranged to

$$\ln(Q) = \ln(k) \cdot + n \ln(z) + \frac{1}{2}\ln(\Delta P) \quad \text{(A-7)}$$

Further rearrangement gives

$$\ln(Q) - \frac{1}{2}\ln(\Delta P) = \ln(k) \cdot + n \ln(z) \quad \text{(A-8)}$$

This is a normal first order equation with two variables and two parameters

$$x_1 = p_1 + p_2 \cdot x_2 \quad \text{(A-9)}$$

Where

$$x_1 = \ln(Q) - \frac{1}{2}\ln(\Delta P)$$
$$x_2 = \ln(z)$$
$$p_1 = \ln(k)$$
$$p_2 = n$$

By plotting x_1 vs. x_2 the two unknown parameters can be estimated. p_1 will be the intersection with the y-axis and p_2 will be the slope.

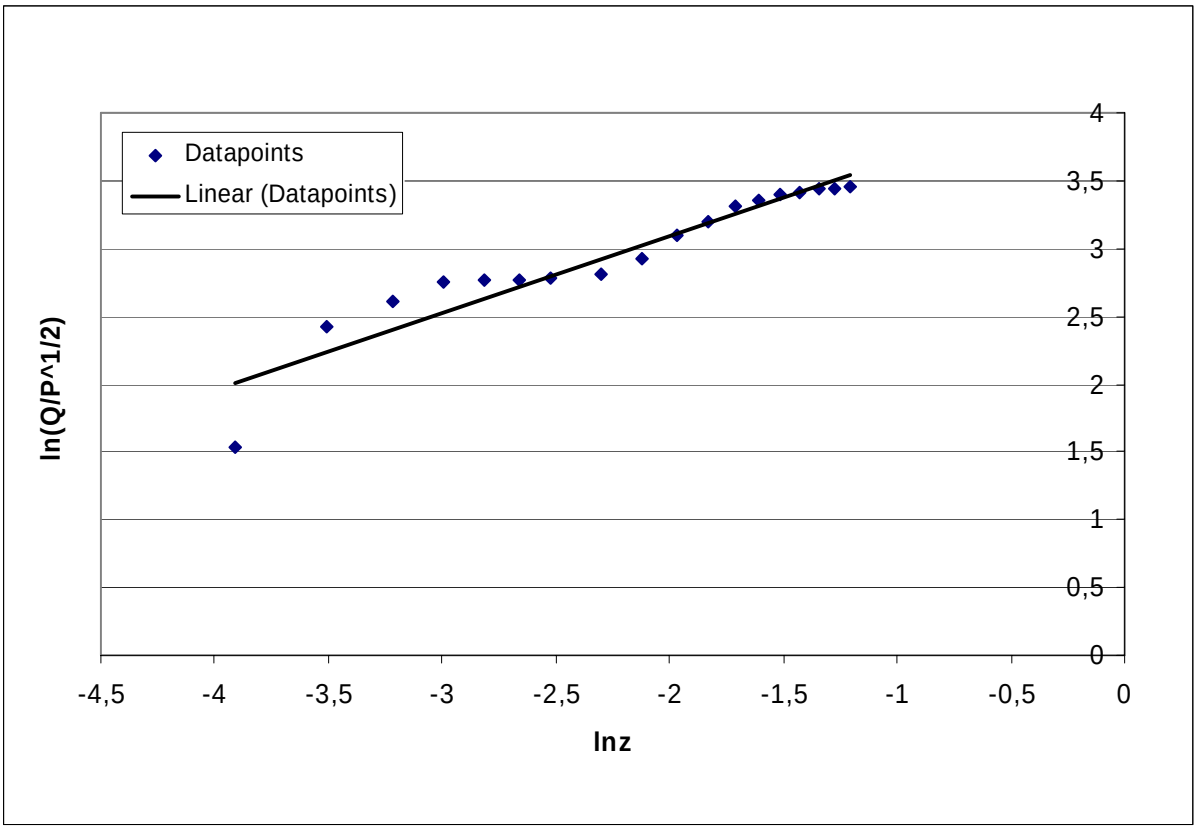

Figure A.14 Linear parameter estimation plot.

The first order equation fitted to the data points is y = 0,5665x + 4,2264.

This gives

$k = e^{p_1} = 68.4$
$n = p_2 = 0.56$

Resulting in the following valve equation

$$Q = 68.4 \cdot z^{0.56} \sqrt{\Delta P} \qquad \text{(A-10)}$$

Method b) *Fitting the function f(z)*

This method is based on equation A-5. The density term is removed since its 1 for water.

$$Q = f(z)\sqrt{\Delta P} \qquad \text{(A-11)}$$

A simple rearrangement gives

$$Q / \sqrt{\Delta P} = f(z) \qquad \text{(A-12)}$$

By plotting $Q/\sqrt{\Delta P}$ vs. Z in figure A.14 and fitting a 5th order polynomial (forced through origo) to the data points gives the following estimate of f(z)

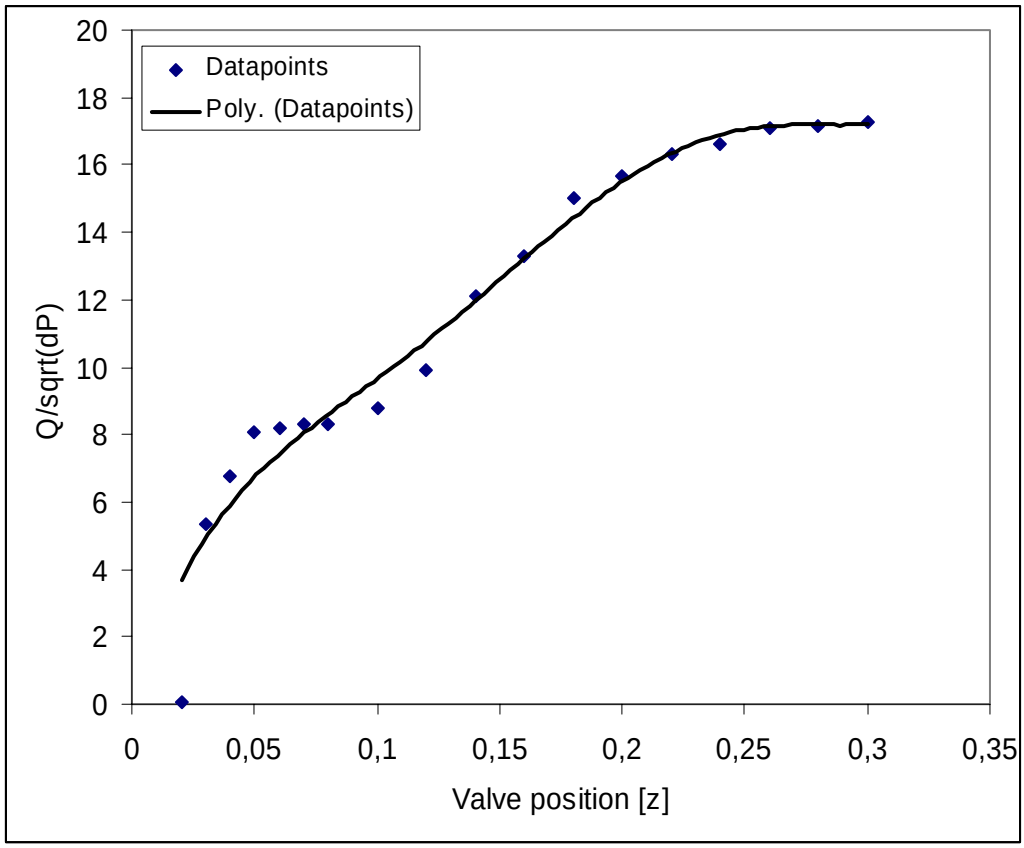

Figure A.15 Estimation of f(z).

The fifth order polynomial fitted to the data using the least squares method is

$$f(z) = 70223z^5 - 61350z^4 + 19191z^3 - 2705.4z^2 + 229.44z \qquad \text{(A-13)}$$

Exponential and logarithmic fits were also attempted, but A-13 gave the best results. Equation A-13 inserted in A-5 gives the valve equation used to estimate the liquid flow.

Appendix B

USER MANUAL

USER MANUAL

For the lab scale

MINILOOP

Table of content

1 Introduction

The Miniloop was originally constructed by Bårdsen [1] as a part of his fifth grade project with the Department of Chemical Engineering at NTNU. Since then some work has been done on the Miniloop by Søndrol[2] as a part of his thesis. New measurements have been added and analyzed. A new user interface has been constructed to obtain the new measurements and to allow different control structures.

This user manual was written as a part of the thesis [2], however it is meant to be a stand alone user manual. This means that some of the things presented in this manual can also be found in the Diploma thesis [2].

The Miniloop is essentially very easy to use. However there are some issues the user should be aware of. It is therefore recommended to read this user manual before performing any experiments on the Miniloop.

2 Miniloop and equipment

Figure 2.1 shows an overview of the lab scale Miniloop. The different components are listed in table 2.1.

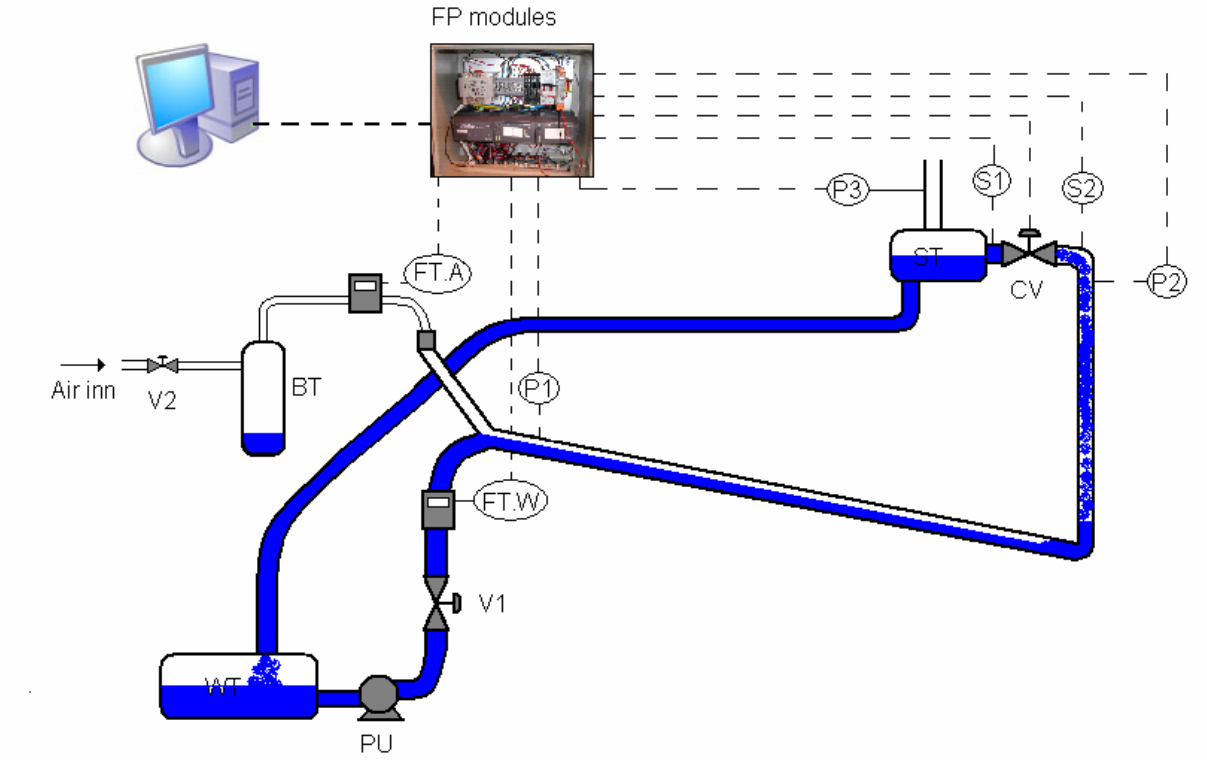

Figure 2.1 Flow sheet for the Miniloop.

As can be seen from the figure the Miniloop has a water (WT) sorce and an air source. The water is pumped from the reservoir into the system, while the air is let into the system from a pressurized air outlet in the wall. The flow rate of water and air is controlled by manually adjusting valves V1 and V2. The pipeline system is constructed of several connecting sections of transparent plastic tubes. The pipeline is meant to imitate the pipeline topography where gravity induced slugging occurs, which is a low point connected to an inclined section of the pipe. At the top of the riser the multiphase flow passes the control valve before it enters the separator. At this point the air is released out of the system through an open hole in the separator, while the water is returned to the reservoir. To monitor the behaviour of the system a combination of pressure measurements and slug sensors are used. The measured signals are transmitted to a computer through the FieldPoint (FP) modules, where they can be analyzed, stored and manipulated.

Table 2.1 List of equipment.

Denote	Equipment
FT.W	Rate meter for water(Gemu 3021)
FT.A	Rate meter for Air
P1	Pressure sensor (MPX5100DP) Feed inlet
P2	Pressure sensor (MPX5100DP) Valve
P3	Pressure sensor (MPX5100DP) Separator air outlet
S1	Slug sensor (E3X-DA-N)
S2	Slug sensor (E3X-DA-N)
PU	Pump (Eheim 1060)
WT	Reservoir
BT	Buffer tank
ST	Separator
CV	Control valve

Consult table A.1 for more info about the distributors and prises. More detailed information about the different equipment can be found in appendix B. The different equipment will be briefly discussed below.

The rate meter for water (figure 2.1) is placed in front of the mixing point of water and air. The digital display shows the rate of water in l/min. It provides a signal between 4-20mA, depending on the rate of flow, which is send to the computer.

The rate meter for air (figure 2.2) is placed in front of the mixing point of water and air. It has a digital display that shows the rate of air in percent of its operating area, witch is 0-2.2 l/min. The rate meter also provides a signal between 0-5 V which is send to the computer.

The pressure sensors (figure 2.3) are one of Motorola's differential pressure sensors that delivers a signal between 0.2-4.5 V. The relationship between voltage and pressure is linear and its operating area is between 0-100kPa.

The slug sensors (figure 2.4) are fibre optical sensors. Each slug sensor is made up of two fibre optical cables connected to a sensor. The light emitted from the senor will travel out through one of the cables and back through the other. The device will provide a signal between 1-5 V depending on how much light is transmitted between the two cables.

The pump (figure 2.5) used is a standard aquarium pump. It can deliver up to 38 l/min and work against a head of 3.1 m. Special care must be taken to make sure it doesn't pump air as this can damage the pump.

The reservoir (figure 2.6) is a cylindrical container made of transparent glass. It serves as the water source for the Miniloop, and the water is returned to the tank from the separator.

The separator (figure 2.7) is also a cylindrical glass container with one inlet and two outlets. The air is released to the surroundings through an open hole in the top, while the water is returned to the reservoir.

The buffer tank (figure 2.8) is a cylindrical container made of transparent glass. For slugs to appear the system needs a sufficiently large air volume. The air volume in the tank can be altered by adding water to the tank.

The control valve (figure 2.9) is located at the top of the riser before the separator inlet. The valve requires a 24V power supply and is controlled by a signal to the actuator between 4-20 mA. The relationship between the valve's actuator and the valve opening is linear. To operate the actuator an external pressurized air source of 4-8 bar is required to counteract the spring power. The lab has its own pressurized air source, which was used for this purpose.

Figure 2.1 Flow meter

Figure 2.1 Flow meter

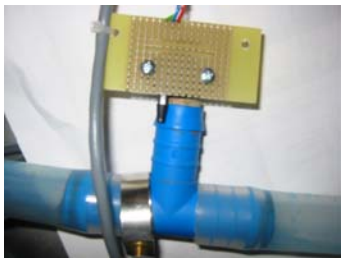

Figure 2.3 Pressure sensor

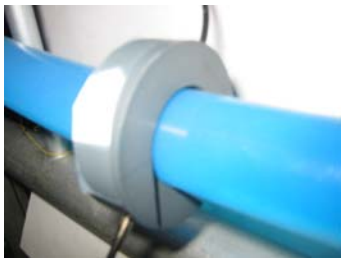

Figure 2.4 Slug sensor

Figure 2.5 Pump

Figure 2.6 Reservoir

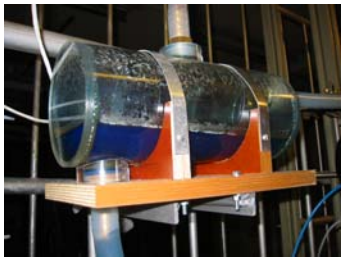

Figure 2.7 Separator

Figure 2.8 Buffer tank

Figure 2.9 control valve

3 Operating the Miniloop

3.1 Start up and shut down procedures.

Start up

1. Start the computer and open the LabVIEW program miniloop.
2. Make sure valve V1 and V2 are closed.
3. Connect the power to the field point modules.
4. Turn the field point modules on by using the switch.
5. Connect the power to the pump.
6. Put the miniloop program into run mode.
7. Turn valve V2 until the desired air flow is reached.
8. Turn valve V1 until the desired water flow is reached.

Shut down

1. Shut of the water supply first(valve V1 first), then the air supply (valve V2).
2. Disconnect the power supply to the pump
3. Turn of the field point modules with the switch.
4. Disconnect the power source to the field point modules.
5. Close LabView and shut down the computer.

Comments

- The air supply must always be turned on first and shut down last. The reason is to obtain a certain pressure inside the hose to prevent backflow of water into the buffer tank(BT).
- The pump will start to work as soon as the power supply is connected. So make sure there is no air in the pipe leading from the water reservoir to the pump. Also make sure that the water level in the reservoir tank is higher then the outlet leading to the pump.
- The valve will always close itself when the field point modules are turned off. The miniloop program therefore has to be put in run mode to open the valve before air or water is introduced to the system. Failure to do this will result in a quick pressure build up in the pipe and a blow out of the pressure sensors.

Adjusting flow rates

During system start up it is recommended to adjust the air flow to the desired flow rate before introducing water into the system. Once the air flow is adjusted the water flow rate can be adjusted to the desired rate. Take note that the water flow rate will vary depending on the upstream pressure. The water flow will normally vary around 10%. To maintain consistency it’s recommended to use the max flow rate during these variations as the reference.
The air flow measurement is dependent on the temperature inside the measuring device. This means that the measured flow rate of air will drop during the first minutes after start up as the temperature inside the device stabilize it self. Because of this its not recommended to initiate any experiments until the measurement is stable (approx. : 5-10 mins.)

3.2 User interface

The Miniloop is controlled by a computer through the user interface.

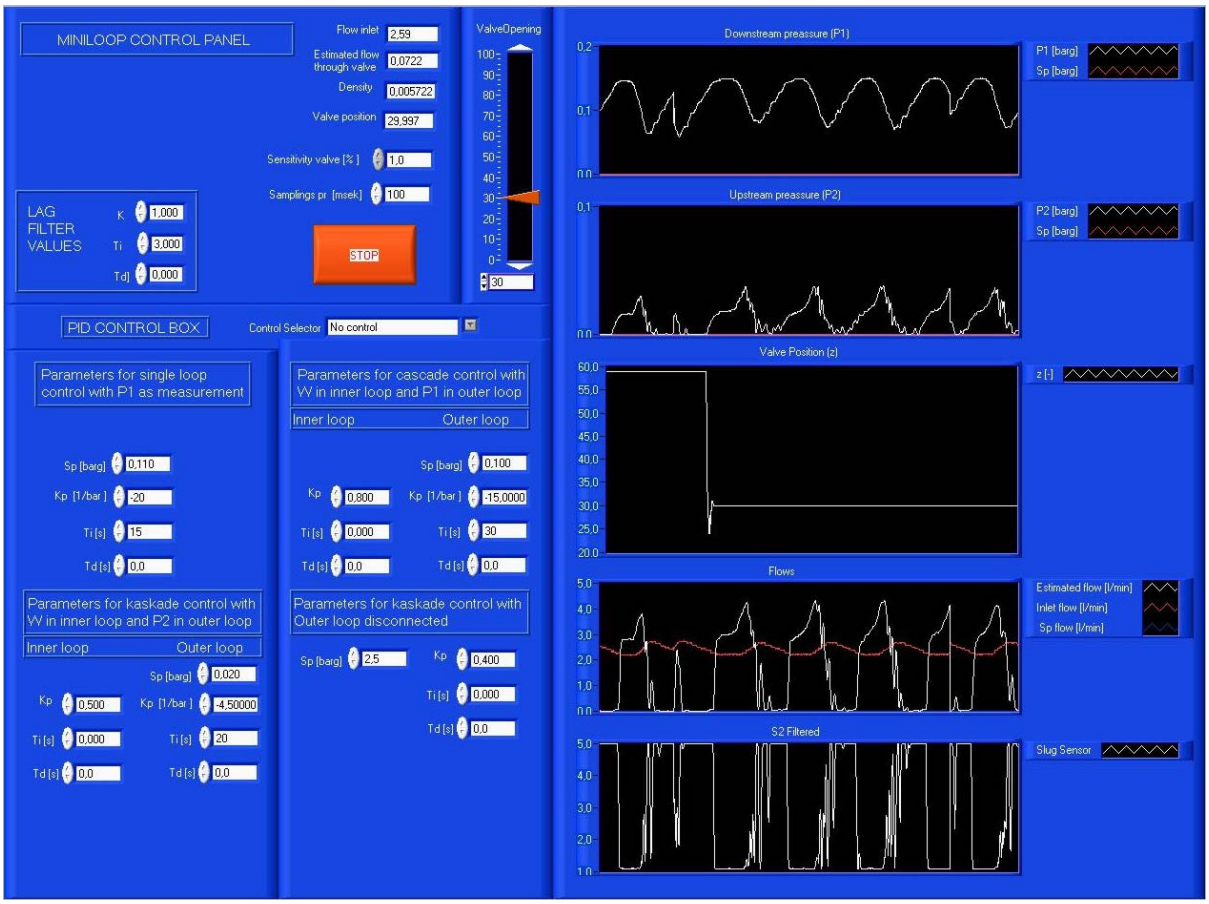

Figure 3.1 User interface for the Miniloop.

The front panel has three main areas of interest. First of you have the charts used to visualize the measurements, like pressure drop, valve opening, flow and hold up. The top chart displays the downstream pressure, while the second one displays the upstream pressure. If anti slug control is applied the mentioned charts will display the relevant set point. The third chart from the top plots the flow of water into the system and an estimate of the flow through the control valve. If a cascade controller is applied it will also show the relevant set point. The slug sensor results are plotted at the bottom. This measurement plots the filtered signal received from the optical sensors.

The PID control is located at the lower left corner of the screen. This is where the user chooses witch control structure to use. The loop is set to “no control” by default, but by clicking it you can choose from the available control configurations from a pull down menu : The tuning parameters for the different controllers are also located here, witch means the user can change them by simply entering the new value.

In the upper left corner of the front panel the user will find some additional indicators that displays additional information about the system. Most measurements are already filtered to some degree, but since the estimated flow measurement is the one most prone to disturbances, an additional lag filter has been added. The parameters for this filter can be altered by changing the values in the filter box.

3.3 Active control

To apply active control the user have to open the pull down menu in the PID control box and choose witch control configuration to use. The control selector is set to “No control” by default. Choosing a different control structure then this will immediately switch the system from open loop (manual control) to closed loop (active control). The chosen controller will use the relevant tuning parameters given in the PID control box. The default parameters will stabilize the system at the given set point. Both parameters and set points can be altered during active control. However one must pay close attention to the system if these values are changed. Wrong parameters during active control can make the valve close it self, leading to a pressure build up and a blow out of the pressure sensor. If this happens the user must switch the control selector back to “no control” to reset the valve position and prevent the build up of pressure.

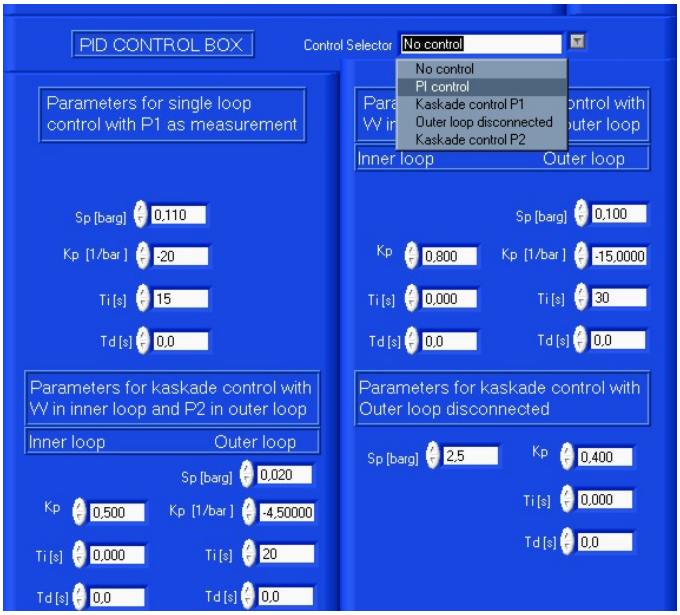

Figure 3.2 PID control box.

3.4 Manual control

When the control selector is set to “No control” in the PID control box the process will run in open loop mode. The user can adjust the valve opening by adjusting the slide bar or by entering the new value for the valve opening in the small box below.

Figure 3.3 Manual valve control.

4 The Miniloop block diagram.

In this chapter the most important components or subVi's in the block diagram will be briefly explained. Understanding of the block diagram is essential if the user wish to add more code or alter the existing code. More information about the detailed tasks of each component can be learned by reading the text boxes inside each subVi or by using the help function in LabVIEW.

4.1 The subVi's

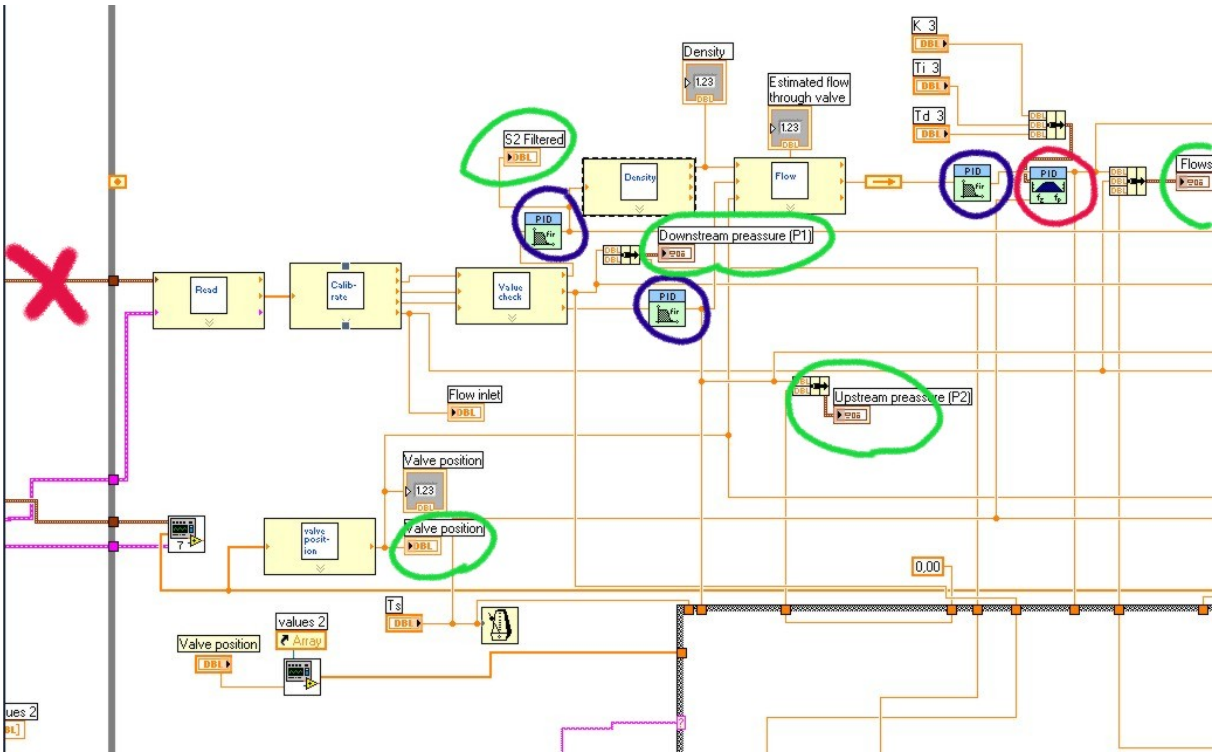

Figure 4.1 The block diagram.

Figure 4.1 shows a section of the block diagram. The yellow boxes with name tags in the middle are different SubVi's. Each of them contains additional code that can be accessed by double clicking the block in the actual program. The programming follows the flow of data. A while loop encompasses most of the code and the measurements will enter the while loop in the wire marked with a big red X. Once it is inside the while loop it will pass from box to box by following the different wiring.

The different subVI's and their purpose are listed below.

Read: Here the data is indexed and tagged.
Calibrate: The data is split into separate data streams and calibrated.
Value check: Here the different measurements are checked to ensure they don't take inconsistent values. Disturbance and noise may cause a measurement to take illegal values i.e. a pressure becoming negative. This subVi will remove these values and force the measurement to take values within a given limit.

Density: The slug sensor signal is send to this SubVi, and the density is calculated based on the equations inside the SubVi.

Flow: This subVi needs the density calculated in the previous subVi, the pressure drop across the valve and the valve opening. It will then estimate the total mass flow through the valve.

Valve position: This subVi will calculate the valve opening from the actuator position.

4.2 Filters and charts.

The block diagram in figure 4.1 are marked with green, blue and red circles. They are there so the user can quickly identify the following components.

Green circles: The componets inside the green circle are indicators. They plot the corresponding data in the charts located in the front panel. The different measurements being plotted are downstream pressure P1, upstream pressure P2, valve position z, flow Q and W, and the slug sensor S2.

Blue circles: The blue circles encompass the PID Control Input Filters. These filters apply a fifth-order low-pass FIR filter to the input value. Filter cut-off frequency is designed to be 1/10 of the sample frequency of the input value. Use this function to filter measured values (such as process variable) in control applications.

Red circle: The red circle encompasses a lag filter. This filter has been added to the estimated mass flow measurement. The filter parameters can be adjusted in the filter box on the front panel.

4.3 CASE structure and the controllers.

The different control structures are located inside within the case structure. New control configurations can be included in the program by adding a new case and filling in the relevant code. Below is an example of case 3. This is a cascade configuration that uses mass flow W in the inner loop and upstream pressure P1 in the outer loop. The measurements and set point is passed from the while loop to the case. The controllers then calculate the valve position and sends it back to the while loop.

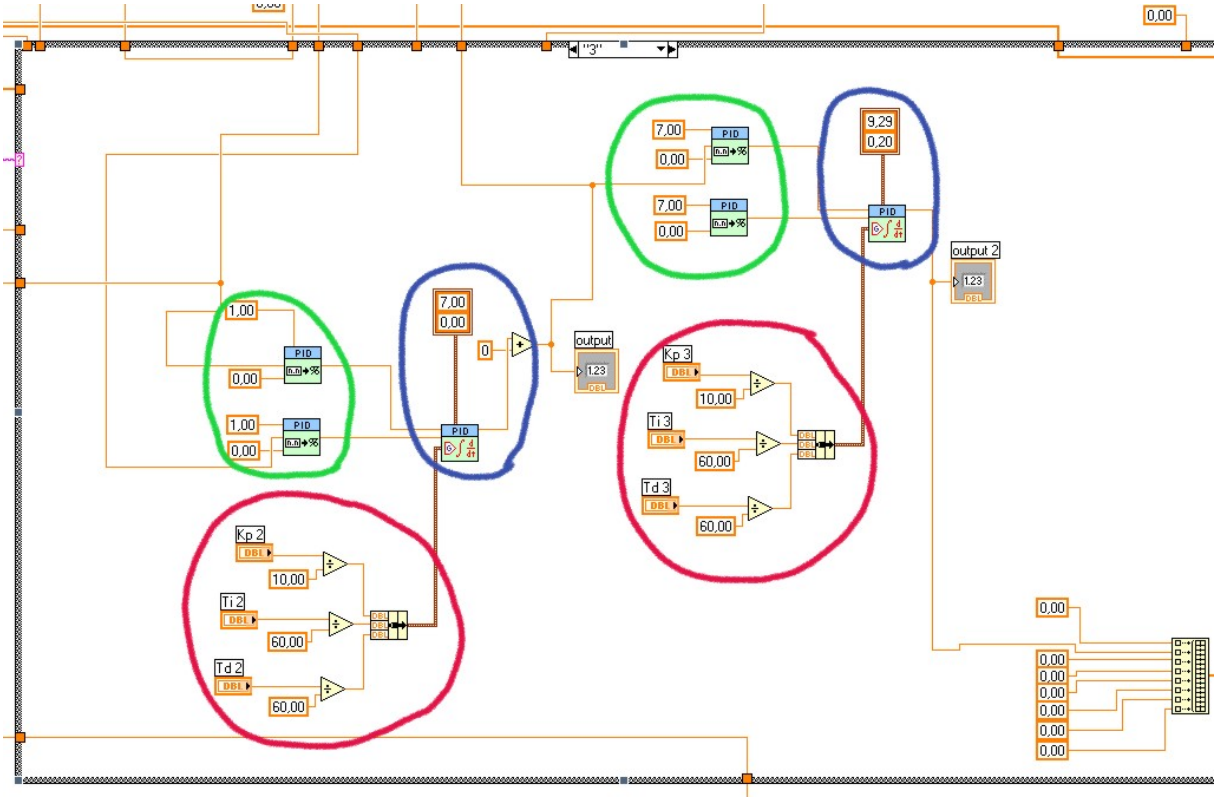

Figure 4.2 Case structure, the controller.

The PID controllers: The actual PID controllers are located within the ***blue*** circles. The parameters associated with the PID controller are the min-max output signals the controller can take. In case of the outer loop, these parameters represent the values that the set point in the inner loop may take

The tuning parameters: These are located within the ***red*** circles. They actual values are set in the front panel.

Set point and variable: The set points and measurements have to be converted from engineering units to percent of operating area, this is done in the ***green*** circles**.** The parameters set here correspond to the min and max values that the set point and variables can take.

4.4 Writing the data to a file.

The miniloop program will automatically write the selected data to a .txt file when the program is stopped using the large stop button. The data will be stored in the following format.

Table 4.1 Format of stored data.

t [msek]	S [V]	P_1 [Barg]	P_2 [Barg]	Q_{inlet} [l/min]	$W_{estimated}$ [kg/min]	Z [-]
…	…	…	…	…	…	…
…	…	…	…	…	…	…

To store additional data to file use the following procedure.

1. Open the block diagram and locate the “write to file” function in the right most section of the diagram. All the data will be collected in the yellow block, and collected in one array. Its then send the the little white block and written to file upon termination of the program.

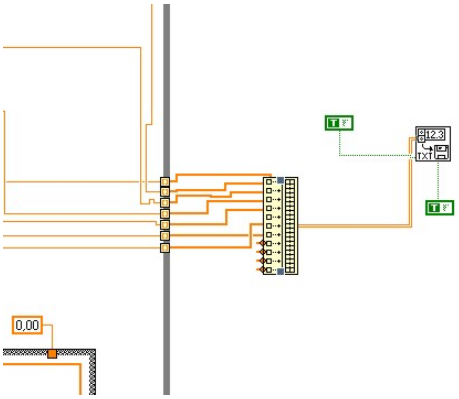

Figure 4.3 Create a free node.

2. By clicking the yellow box and holding you can increase the length of it, allowing more data stream to be added to it. The box in figure 4.3 has been increased to allow 4 more data streams.

3. The next stage is to locate the data you wish to store to the file. Then simply wire it to an available node on the yellow box(figure 4.4). The additional data stream will now be stored to the same file.

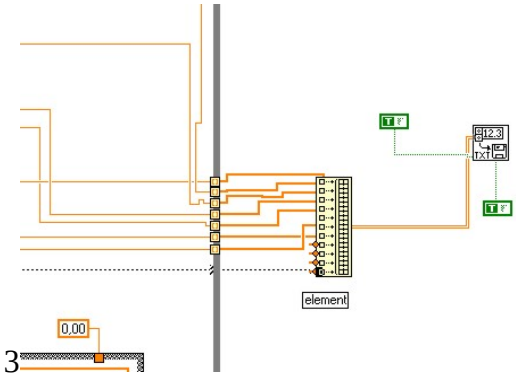

Figure 4.4 Wire the data.

5 Maintenance.

The Miniloop do not require much maintenance. However the user should be aware of a few things.

5.1 Reservoir tank.

The user has to make sure the liquid level in the reservoir tank doesn't get to low. From figure 5.1. one can see that there are two tubes connected to the tank. The top tube is connected to the separator, and the water will return to the reservoir through this tube. The second tube is connected on the flat end side of the tank. This is connected to the pump witch pumps the water into the Miniloop. Before the pump is turned on the user has to make sure the liquid level is higher then this outlet, if not air may enter the tube. This can damage the pump, and in the worst case damage it. The water level should at least be 3 cm higher then the outlet. Additional water can be added to the tank through the open hole on the flat side, above the outlet. There is a water source available with a long enough hose in close proximity to the loop. To empty the tank the user can remove both tubes and pour the liquid into the sink.
If the user wish to clean the tank with water make sure it is not to hot. Using only hot water to clean the tank may cause the glass to crack.

Figure 5.1 Reservoir tank.

5.2 Buffer tank.

The buffer tank is used to create enough upstream volume for the gas. This is a prerequisite for slugging to occur. The volume available for the gas will influence the amplitude of the pressure oscillations. The volume can be altered by adjusting the liquid volume inside the tank. To add more water the user has to disconnect both tubes leading to it. As for the reservoir tank the buffer tank mustn't be cleaned with to hot water as this may result in cracks.

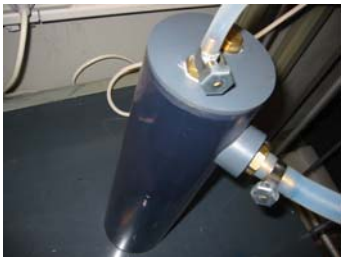

Figure 5.2 Buffer tank.

5.3 The slug sensor

There are quite a few things that can cause the slug sensor to fail. The slug sensor should always be checked to make sure it is operating as intended before an experiment is started. The easiest way to check the sensor is to make sure the slug sensor chart in the user interface (miniloop program front panel, figure 3.1) is taking values between 1 and 5. It should be 1 when measuring pure water and 5 when measuring only air. If this is not the case, something is causing the sensor to malfunction. Take note that the problem may not be with the sensor itself, but with the Miniloop. This chapter will show the user how to reconfigure the sensor from start. However, if the sensor is malfunctioning consult the trouble shooting in chapter 5.3.2. Figure 5.3 shows the actual sensor and the different settings on it.

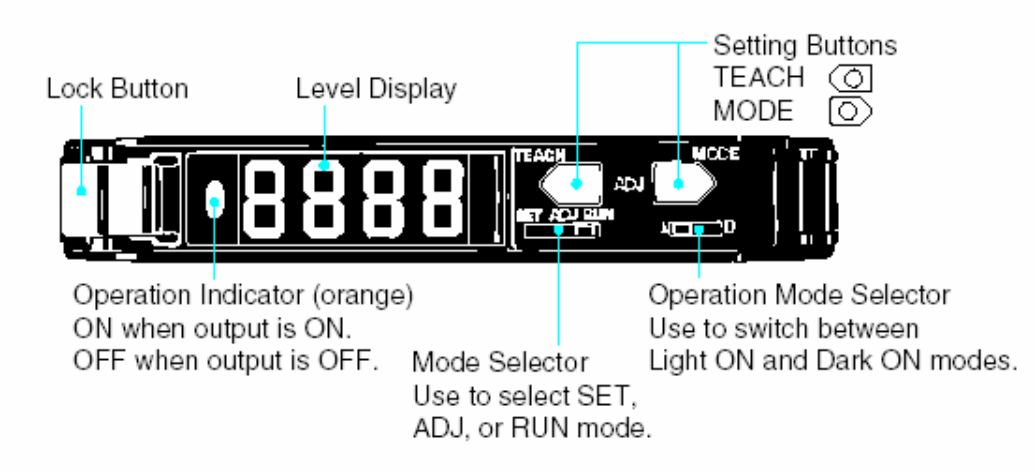

Figure 5.3 The sensor settings.

5.3.1 Calibrating the slug sensor.

Step 1) Reset the sensor to default settings as shown in figure 5.4.

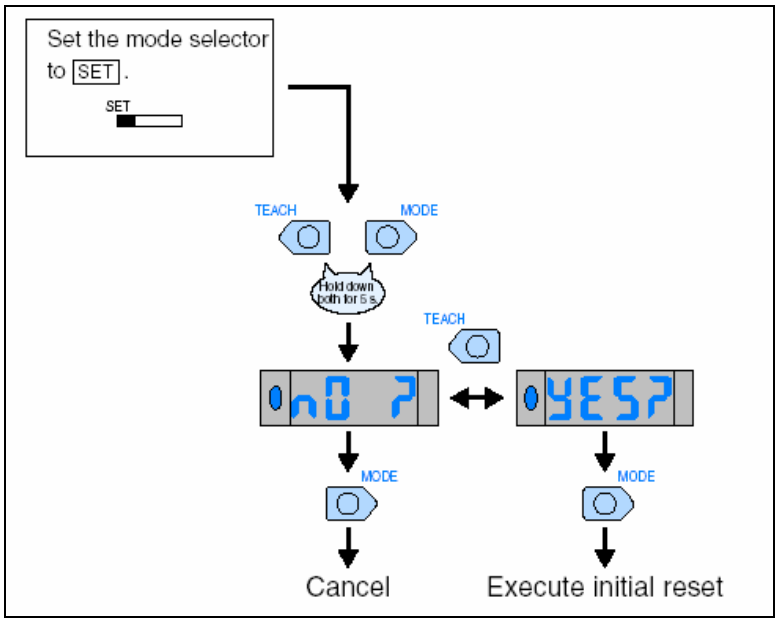

Figure 5.4 Resetting the slug sensor to default setting.

Step 2) Recording the sensor value corresponding to pure water..

Record the value showing in the sensors digital display when measuring pure water. The display will vary between 0 and 4000. The value will depend on the amount of light being returned to the sensor. 4000 means all the light has returned(as for air). When measuring water the display should take a value between 500 and 1500. If the value is higher then 1500 the water is absorbing to little light. Add more colouring matter as described in chapter 5.4 until the value is within the given bounds.

Step 3)Setting the lower limit for monitoring.

The user must then set the lower limit for monitoring a bit higher then the value recorded for pure water. This is done to remove the unwanted spikes caused by the surface of the phase transitions. If the digital display is showing a value of 1000 for pure water the user should set the lower limit for monitoring at 1200.

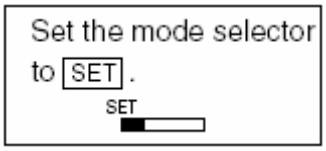

Press and hold the mode button

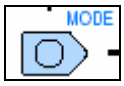

until the display shows :

Then press and hold the teach button until the display show the desired value for the lower limit as shown in figure 5.5. The lower limit will increase in increments of 100. When the desired value is reached release the teach button and switch the mode selector back to run mode.

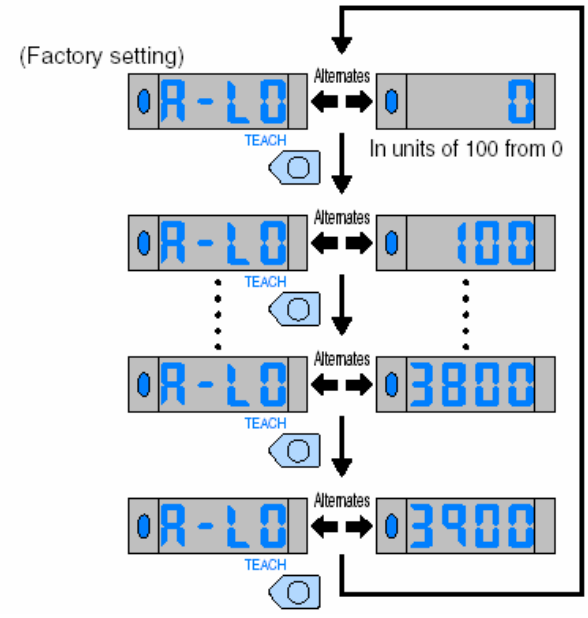

Figure 5.5 Setting the lower limit for monitoring.

5.3.2 Troubleshooting the slug sensor.

This chapter should solve the most common problems with the slug sensor.

Problem: The slug sensor chart in the user interface is not taking values between 1 and 5.

The slug sensor chart is showing values below 5 for pure air when it should show 5.

Solution: When there is only air in the tube no light should be absorbed, and the sensor should show its max value. Check the digital display on the sensor. The display should show 4000 when only air is present. If it shows less something is interfering with the light beam. Make sure the sensor is not placed on a stained part of the pipe as stains may block some of the light, moving it to a different location or changing the stained section of pipe will most likely solve the problem. The cables may also be bent resulting in a failure within the cable. Make sure the cable is running loosely and smoothly from the sensor to the bracket without to large angels.

The slug sensor chart is showing values higher then 1 for pure water when it should show 1.

Solution: Most likely the lower limit for monitoring is set to high, or there is too little colouring matter in the water. Check step 2 in chapter 5.3.1.

5.4 Colouring matter

The colouring matter used to give the water a blue colour is called Vulcanosol-Blau 684. More colouring matter can be obtained from Engineer Arne Fossum at his office in K3-019. Very little substance is needed to dye the water. It's recommended to gradually add small amounts of substance until the desired slug sensor value has been achieved. The system should be set to pump water through the system to disperse to substance properly.
One spatula is enough to dye all the water in the system if the reservoir tank is half full.

6 References

[1] Bårdsen, I., “Anti-slug control for two phase flow. Experimental verification (In Norwegian),” NTNU, autumn 2003.
[2] Søndrol, M., “Anti-slug control. Experimental testing and verification,” NTNU, spring 2005

Appendix A Equipment suppliers and prises

Table A.1 lists the suppliers and prises for the different components in the Miniloop.

Table A.1 List of equipment, suppliers and prises.

Equipment	Type	Delivered by	Prise [NOK]
Rate meter for water Control Valve	Gemu 3021 Gemu 554	J.S. Cock 3991 P.O.BOX 68 Stovner N-0913 OSLO Phone:+47 22 21 51 00	3991 4502
Rate meter for air	D-5110-HAB	Flow-Teknikk as Olav Brunborgsv.27 P.O.BOX 244 1377 Billingstad Phone : +47 66 77 54 00	9914
A1-Module AO-Module Termination base Communication module	FP-AI-100 FP-AO-210 FP-TB-2 FP-1000	National Instruments 2745 P.O.BOX 177 N-1386 Asker Phone:+47 66 90 76 60	2745 3555 1512 3105
Signal transducer for the control valve	MICROANALOG DC/DC Select	JF.Knudtzen AS P.O.BOX 160 N-1378 Nesbru Phone:+47 66 98 33 50	1550
3 x Pressure sensors	MPX5100DP	Silica/Avnet Nortec AS P.O.BOX 63 N-1371 Asker Phone:+47 66 77 36 00	796
Pumpe	Eheim 1060	Petshop at city syd	1566
3x Optic sensors	E3X-DA-N	Omron P.O.BOX 109 Bryn N-0611 OSLO Phone:+47 22 65 75 00	2825
3x Tanks	Transparent glass	Produced by NTNU	9000
Tubes	Silicone		4000

Appendix B Equipment manuals

The equipment manuals are large and comprehensive. Because of this not all of them will be appended to this user manual. However the table below will list where they can be found.

The manuals for the equipment listed in table B.1 can be found in appendix B in [1], while the manuals listed in table B.2 can be found in this appendix.

Table B.1 Reference to equipment manuals.

Equipment	Page
Pressure sensor	43
Signal transducer (control valve)	51
FieldPoint A1-Module	55
FieldPoint AO-Module	69
FieldPoint Terminal base	81

Table B.2 Reference to equipment manuals.

Equipment	Appendix
Rate meter for liquid	B1
Rate meter for gas	B2
Optic sensor (In Danish)	B3

GEMÜ®

Flow transmitter

Construction

An intelligent flow transmitter which can be used for measuring liquid inert and corrosive aqueous media. The keypad at the front of the unit enables simple setting of measurement units, required display values etc.

Features

- High-resolution turbine flow measurement
- Medium wetted parts in plastic and ceramics
- Can be used as totalizer (flow counting) or batch controller (dosing function)
- Extremely low pressure loss

Advantages

- Easy operation via keypad
- Process adaptable
- Short inlet and outlet distances
- Freely scalable measurement range
- Integrated flow rectifier

Dimensional drawing GEMÜ 3021 (mm)

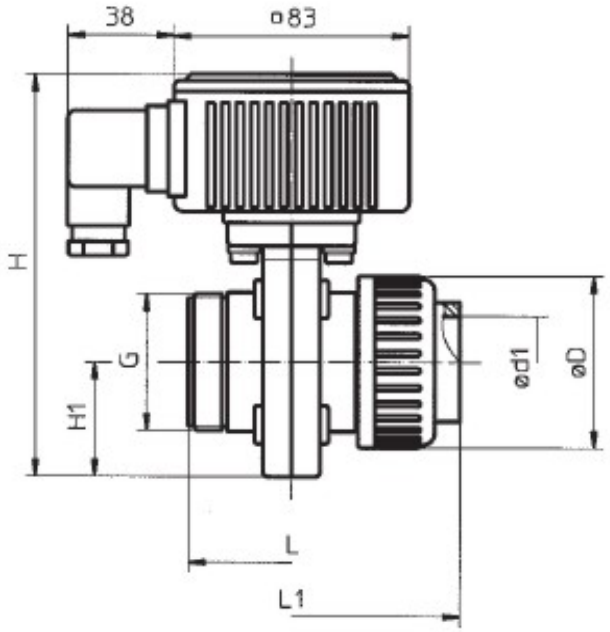

DN	L	L1	H1	ød1	øD	G	H
25	73	123	40	32	60	G 1 1/2	140
50	105	187	63	63	103	G 2 3/4	189

GEMÜ® 3021

Technical specifications

Working medium

Any liquid inert or corrosive aqueous media subject to the correct choice of body and seal materials.

Max. perm. temperature of working medium: see datasheet "Technical Information on Plastic Materials"

Electrical specifications

Power supply U:	18-30 V DC
Power consumption P:	typ. 1 W
Current consumption I:	typ. 40 mA (for current output = 0 mA)
Output signals:	
Pulse output, PNP	$U-U_{Drop}$
typ. U_{Drop}	1.7 V at 24 V / 5 mA 2.5 V at 24 V / 10 mA 5.0 V at 24 V / 20 mA
Pulse rate	≤ K-factor/2 (adjustable, K-factor see measuring certificate)
Current	0/4-20 mA
Resolution	≤ 23 µA (10 bit)
Accuracy	±1,5 bit
Load impedance ≤ 500 Ohm, load control 0.25 %	
Relay	(resistive load)
Voltage	250 V AC / 220 V DC
Current	2 A AC / 2 A DC
Power	≤ 60 W
Electrical connection:	Plug according to DIN 43650-A
Cross section of cable:	8-10 mm

Measuring ranges:	DN 25	DN 50
Measuring span	120-7200 l/h	500-25000 l/h
Start-up	≤ 80 l/h	≤ 500 l/h
Medium	aqueous liquids	

Accuracy:	±1 % FS
Repeatability:	±0,5 % FS
(FS = full scale)	
Optical display:	LC-Display 2 x 16 characters digit height 5.55 mm

Working conditions

Ambient temperature:	-10 ... +60° C
Storage temperature:	-20 ... +60° C
Type of medium:	liquid
	≤ 120 $\frac{mm^2}{s}$ (120 cSt)
Medium temperature:	
Ref. no. 1 PVC-U	-10° ... +60° C
Ref. no. 20 PVDF	-10° ... +80° C
Working pressure:	≤ 10 bar (20° C)
Characteristic see "Technical Information on Plastic Materials".	

General information

Housing protection class to EN 60529:	IP 65
Weight: DN 25:	600 g
DN 50:	1500 g
Dimensions L x W x H:	see dimensional drawing
Mounting position:	optional
Mounting note:	Inlet/outlet distances 5 x DN

Note:
We recommend installation of a dirt filter for filtering particles contained in the medium
Mesh width 100 µm

Directives:	EC Machine directive 98/37/EC EMC 89/336/EEC
Measuring certificate:	Calibration data for water 20°C are included

Materials

Medium wetted parts
- Inner turbine components: PVDF
- Body: PVC-U or PVDF
- Bearing / shaft: Glass / ceramics (Al2O3)
- Seals: FPM

Flow transducer:
- Housing: ABS
- Housing cover of measuring instrument, size B: PMMA
- Housing seal: NBR
- Housing bolt: 1.4303

Plug:
- Plug housing: PA 6
- Plug bolt: VQSt 36-2-4,8
- Profile packing: Nitrile rubber

Further housing materials upon request

Order specifications

Nominal size	Ref. no.
DN 25	25
DN 50	50

Seal material		Ref. no.
FPM	Viton®	4

Body configuration	Ref. no.
Straight through	D

Display position	Ref. no.
See diagrams on last page	

Connection	Ref. no.
Unions (metric)	7
Unions (imperial)	33

Functional profile	Ref. no.
Totalizer (0/4-20 mA + pulse output)	T41
Batch controller (2x Relay outputs)	BR2

Body material	Ref. no.
PVC-U	1
PVDF	20

Supply voltage	Ref. no.
24 V DC	C1

Order example	3021	25	D	7	1	4	A	T41	C1
Type	3021								
Nominal size (ref. no.)		25							
Body configuration (ref. no.)			D						
Connection (ref. no.)				7					
Body material (ref. no.)					1				
Seal material (ref. no.)						4			
Display position (ref. no.)							A		
Functional profile (ref. no.)								T41	
Supply voltage (ref. no.)									C1

Display position with regard to flow direction

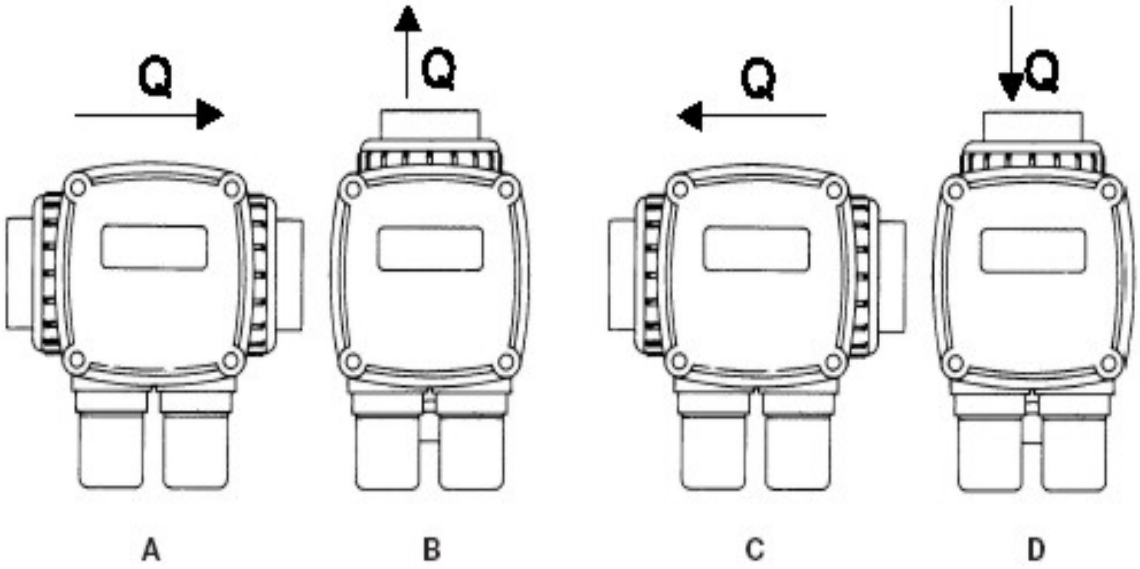

Electrical connection diagram

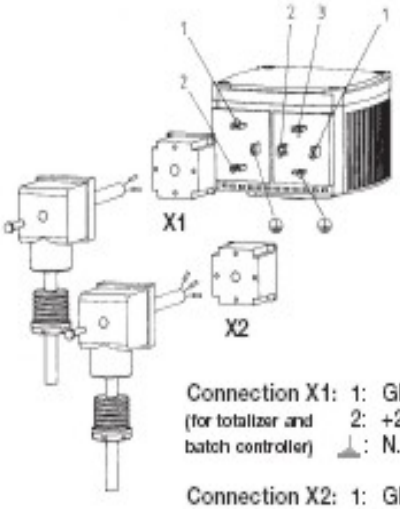

Connection X1: 1: GND
(for totalizer and batch controller) 2: +24V
⊥: N.C.

Connection X2: 1: GND
(for totalizer) 2: Current output (0 / 4 - 20 mA)
3: Impulse output (PNP)
⊥: N.C

Connection X2: 1: Common
(for batch controller) 2: Relay output BQty
3: Relay output BFast
⊥: N.C.

Flow-Teknikk as

Mass Flow Meters and Controllers for Gases

MASS-STREAM®

M+W Instruments
Your partner

Key Facts

M+W Instruments was founded in 1988 and has always specialised in mass flow meters and controlers.

In 1995, M+W Instruments was the first company to introduce the direct measuring principle for thermal mass flow meters with the sensor following the constant temperature anemometer principle.

In 1997 M+W Instruments joined the Bronkhorst Group.

Today we are working along side more than 20 distributors worldwide. You will find your personal contact on the back page of this brochure or under www.mw-instruments.com.

Our intruments are suitable for the use in the pharmaceutical, chemical and semiconductor industries as well as in the gas and food industry. Of course we are your competent address for special solutions.

Content

Principle of Operation

Basically the instruments consits of a metal block with a straight bore. Two stainless steel probes protrude inside the bore; a heater probe and a temperature probe. A constant difference in temperature (ΔT) is created between the two and the energy required to maintain this ΔT is dependent of the mass flow rate.

Generally speaking we can say that the higher the flow the more energy is required to maintain the chosen ΔT, which is usually approx. 38° C. Overall we can state that King's law applies to the relationship between heater energy and mass flow, and the following formula can be derived.

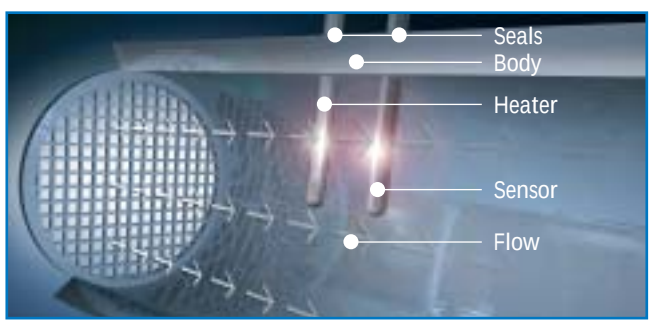

Basic structure of the Mass-Stream®-flow sensor

$$P = P_0 + C\emptyset_m^{\,n}$$

P = total heater power
P_0 = heater power offset at zero flow
C = constant
$\emptyset_m$ = mass flow
n = dimensionless number (typ. 0.5)

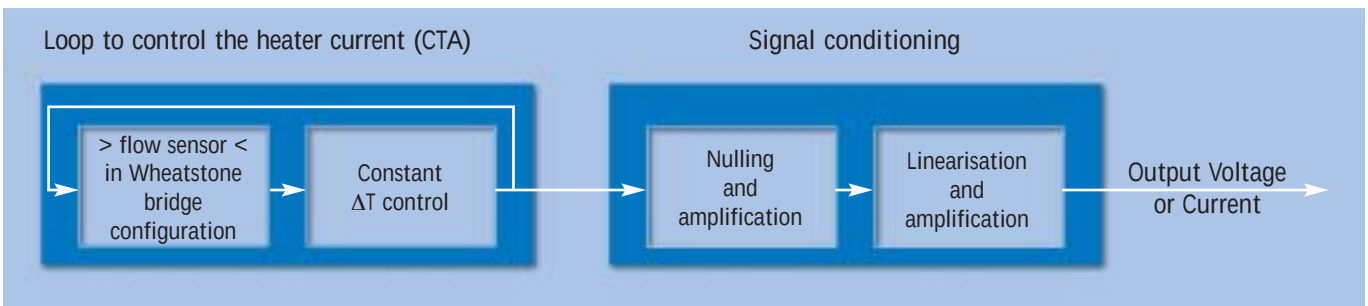

"MASS-STREAM®"
Features and Applications

Worth knowing

MASS-STREAM® is the synonym for a metering principle having the following advantages:

Smallest standard range
0,005...0,1 l_n/min (Air)

Highest standard range
100.0...7500.0 l_n/min (Air)

Lower and higher ranges available on request.

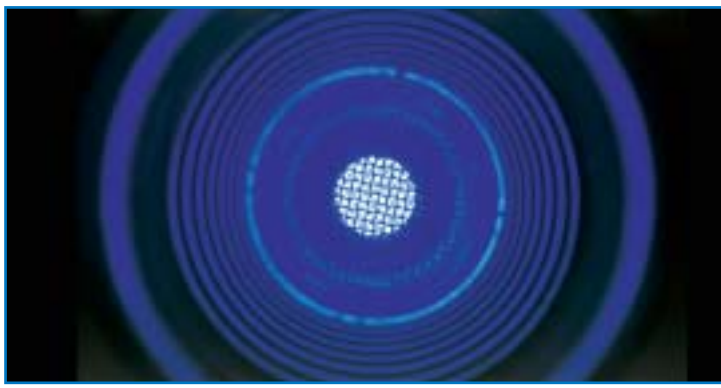

Features

- Low pressure drop
- Rugged design
- Lower sensivity concerning dirt and humidity
- Measuring independent of pressure and temperature changes
- Installable in virtually any position
- No moving parts
- Bodies in stainless steel or as a more economical aluminium version

Applications

- Gas consumption metering
- Exhaust gas metering
- Semiconductor industry
- Analytical intruments
- N_2/O_2-generators
- Fuel cells
- Mechanical engineering
- And much more

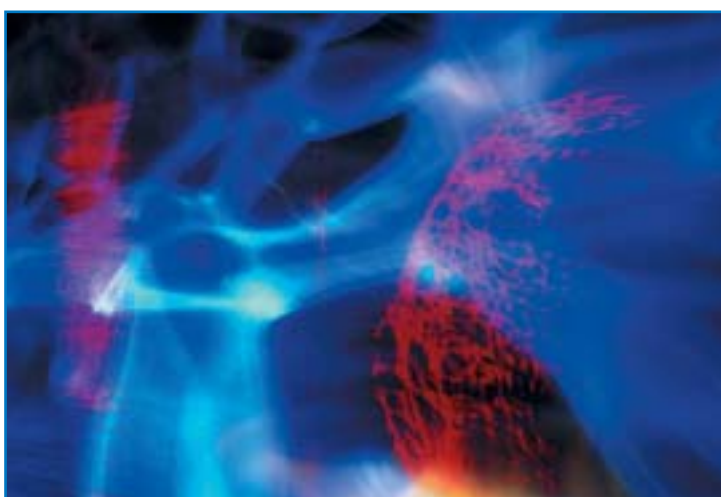

Options

- "Low ΔP" version
- Integrated totalisation
- Integrated actual display
- Integrated setpoint potmeter
- Readout systems

Mass Flow Meters

Principle of Operation

Flowmeters of M+W Instruments are suitable for all kinds of applications in industrial, chemical, medical and laboratory environments.

- Usuable for virtually every kind of gases
- No moving parts
- Very low pressure drop
- Unique all stainless steel sensor
- Pressure and temperature independent metering system

Main advantages of these instruments are:

- Installable in virtually every position
- No inlet pipes needed (62xx series)
- Optional with integrated flow display
- Optional with totalisation
- No maintance needed
- Two body materials on stock (others on request)

The 62xx series working principle is shown on page 2.

For lower flow values the by-pass measurement principle is applied.

Standard Flow Capacities

Mass Flow Meters Model			Flow capacitiy (Air) (intermediate ranges available)	
D-5110	- AAA - BB - AA -	12 - A - A - A	0.005...0.1	l_n/min Air
		22	0.010...0.2	l_n/min Air
		52	0.025...0.5	l_n/min Air
		13	0.05...1.0	l_n/min Air
		23	0.1...2.0	l_n/min Air
		53	0.25...5.0	l_n/min Air
		14	0.5...10.0	l_n/min Air
D-6210	- HAB - BB - AA -	53 - A - A - A	0.25...5.0	l_n/min Air
		14	0.5...10.0	l_n/min Air
		24	1.0...20.0	l_n/min Air
D-6230	- HAB - BB - AA -	24 - A - A - A	1.0...20.0	l_n/min Air
		54	2.5...50.0	l_n/min Air
		15	5.0...100.0	l_n/min Air
D-6250	- HAB - CC - AA -	15 - A - A - A	5.0...100.0	l_n/min Air
		25	10.0...200.0	l_n/min Air
		45	20.0...400.0	l_n/min Air
D-6270	- HAB - CC - AA -	55 - A - A - A	25.0...500.0	l_n/min Air
		16	50.0...1000.0	l_n/min Air
		26	100.0...2000.0	l_n/min Air
D-6280	- HAB - DD - AA -	36 - A - A - A	150.0...3000.0	l_n/min Air
		46	200.0...4000.0	l_n/min Air
		56	250.0...5000.0	l_n/min Air
D-6290	- HAB - DD - AA -	66 - A - A - A	300.0...6000.0	l_n/min Air
		76	375.0...7500.0	l_n/min Air

Higher flows and other current junctions on application.

Model D-6210 MFM

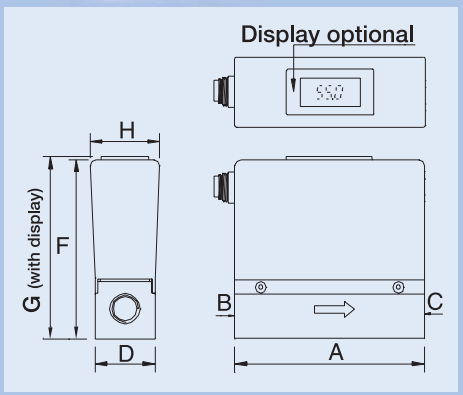

Model	A	B	C	D	F	G	H
D-5110	95	G1/4"	G1/4"	30	90	92	35
D-6210	95	G1/4"	G1/4"	30	90	92	35
D-6230	95	G1/4"	G1/4"	30	90	92	35
D-6250	95	G1/2"	G1/2"	30	90	92	35

Model D-6270

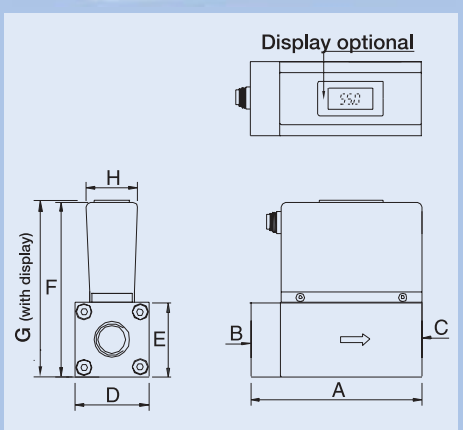

Model	A	B	C	D	F	G	H
D-6270	116	G1"	G1"	50	123	125	35
D-6280	116	G1"	G1"	70	141	143	35
D-6290	143	G1"	G1"	110	171	173	35

All specifications subject to change without notice.

Mass Flow Controllers (MFC)

Principle of Operation

Based on the concepts of our flow meters; compact flow controllers are also available.

The modular construction solenoid valve is integrated to the base when flows are up to approx. 500l/min. N_2 equivalent.

When higher flows are needed an external valve is employed.

The following kv_s-values are available: 6,6E-2, 0,35; 1,0;
(for higher values please contact factory)

Features

- Suitable for almost all gases and mixtures
- No moving parts in the sensor
- Good response times
- PI-control loop
- No inlet pipe necessary (D-62xx series)
- Optional: integrated actual flow display
- Optional: integrated totalisation display
- No maintainance required
- Almost independent to attitude

Standard Flow Capacities

Mass Flow Controllers Model			Flow capacitiy (Air) (intermediate ranges available)	
D-5111	- AAA - BB - AA -	12 - A - A - A	0.005...0.1	l_n/min Air
		22	0.010...0.2	l_n/min Air
		52	0.025...0.5	l_n/min Air
		13	0.05...1.0	l_n/min Air
		23	0.1...2.0	l_n/min Air
		53	0.25...5.0	l_n/min Air
		14	0.5...10.0	l_n/min Air
D-5121	- AAA - BC - AA -	14 - A - A - A	0.5...10.0	l_n/min Air
		24	1.0...20.0	l_n/min Air
		54	2.5...50.0	l_n/min Air
D-6211	- AAA - BB - AA -	53 - A - A - A	0.25...5.0	l_n/min Air
		14	0.5...10.0	l_n/min Air
		24	1.0...20.0	l_n/min Air
D-6231	- AAA - BB - AA -	24 - A - A - A	1.0...20.0	l_n/min Air
		54	2.5...50.0	l_n/min Air
		15	5.0...100.0	l_n/min Air
D-6251	- AAA - CC - AA -	15 - A - A - A	5.0...100.0	l_n/min Air
		25	10.0...200.0	l_n/min Air
		55	20.0...400.0	l_n/min Air
D-6271/004	- AAA - CC - AA -	55 - A - A - A	20.0...500.0	l_n/min Air
		16	50.0...1000.0	l_n/min Air

Higher flows and other current junctions on application.

Model D-5121 MFC with LCD display

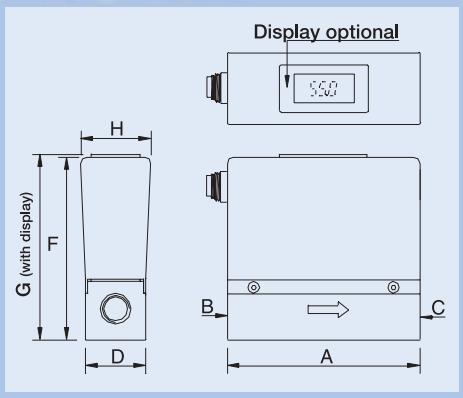

Model	A	B	C	D	F	G	H
D-5111	95	G1/4"	G1/4"	30	90	92	35
D-5121	95	G1/2"	G1/4"	30	94	96	35
D-6211	95	G1/4"	G1/4"	30	90	92	35
D-6231	95	G1/4"	G1/4"	30	90	92	35

Model D-6251

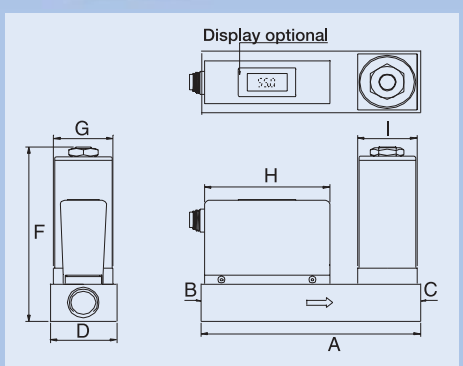

Model	A	B	C	D	F	G	H	I
D-6251	145	G1/2"	G1/2"	50	132	45	95	45
D-6271	Dimensions please on application							

All specifications subject
o change without notice.

Conversion factors

The MASS-STREAM®-Series flow meters are normally calibrated on air. For use on other gases than air a conversion factor must be applied. This factor is determined by applying a complex formula.
However, for a number of common gases you will find the values below:

Conversion factor table

(L_n: 1013mbar und 0°C air temperature)

Series / Gas	D-62xx	D-51xx
Air	1.00	1.00
Ar	2.01	1.40
CH_4	0.67	0.76
C_2H_2	0.75	0.61
C_2H_4	0.89	0.60
C_2H_6	0.89	0.60
C_3H_8	0.63	0.34
C_4H_{10}	0.42	0.25
C_5H_{12}	0.25	0.21
CO	1.04	1.00
CO_2	1.20	0.74

Series / Gas	D-62xx	D-51xx
H_2	0.15	1.01
He	0.24	1.41
HCL	1.58	0.99
N_2	1.00	1.00
NH_3	0.80	0.77
NO	1.02	0.97
N_2O	1.15	0.71
N_2O_2	1.00	1.00
O_2	0.98	0.98
Xe	6.08	1.38

Factors for further gases available on request.

Best accuracy is reached by calibrating the instruments und actual process conditions. The conversation factor introduces an additional error in abolute accuracy in order of:

CF ≥ 1 : 2xCF in % FS
CF ≤ 1 : 2/CF in % FS

When using our D-62xx serie with balloon gases like helium and hydrogene it is always recommended to make use of the optional gas calibration.

Flow profile sensivity

Normally mass flow measurement principles are sensitive to variations in the shape of the flow profile.

The MASS-STREAM®-Flow meters has been designed in such a way that there is always a fully developed flow profile in the metering section ans is thus virtually insensitive to changes upstream piping conditions.

Pressure drop

The pressure drop of the instruments (serie D-62xx) is almost comparable to a straight run of pipe of the diameter ans is thus negible.

However, to make the instruments insensitive to upstream piping configurations, a number of mesh screens are required to condition the flow profile. These meshes create a certain pressure drop as can be seen from the table set out below.

For further informations please contact factory.

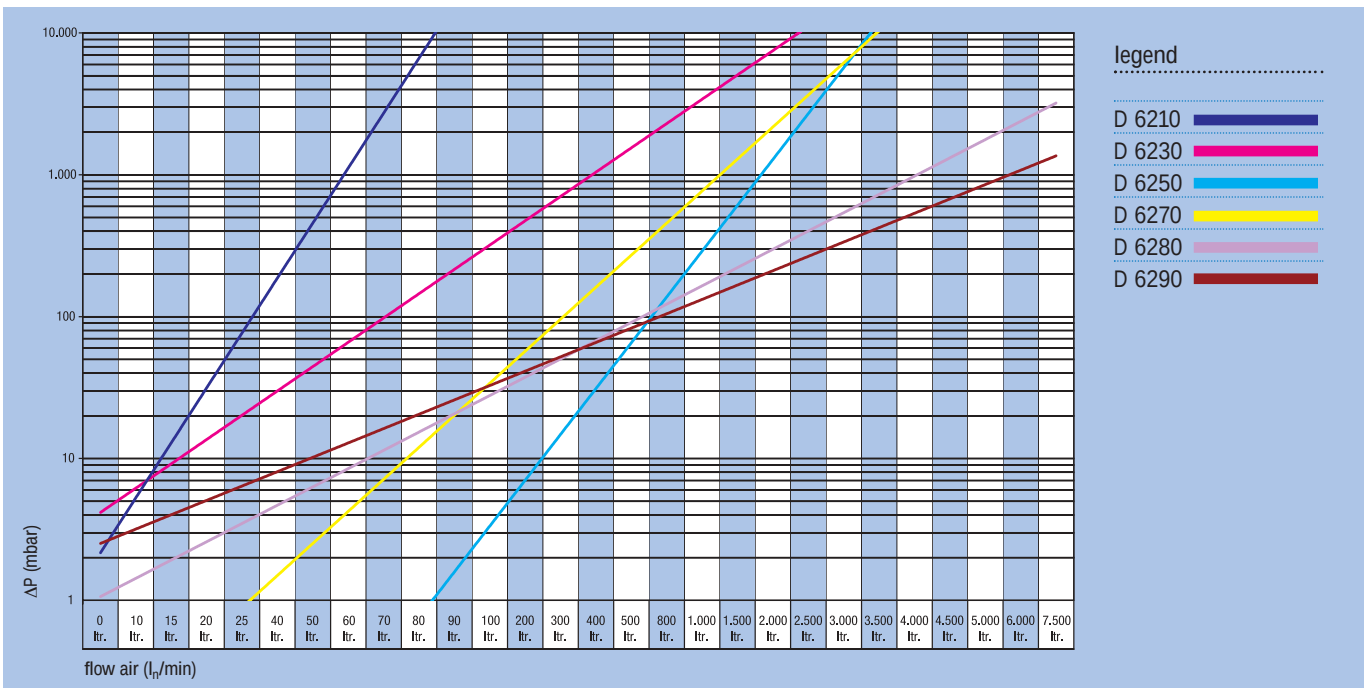

In some applications a very low pressure drop is required. To fulfil these inquires we are able to build a special version of our instruments where the pressure drop is extremely low.

For further information please refer to the second table set out below.

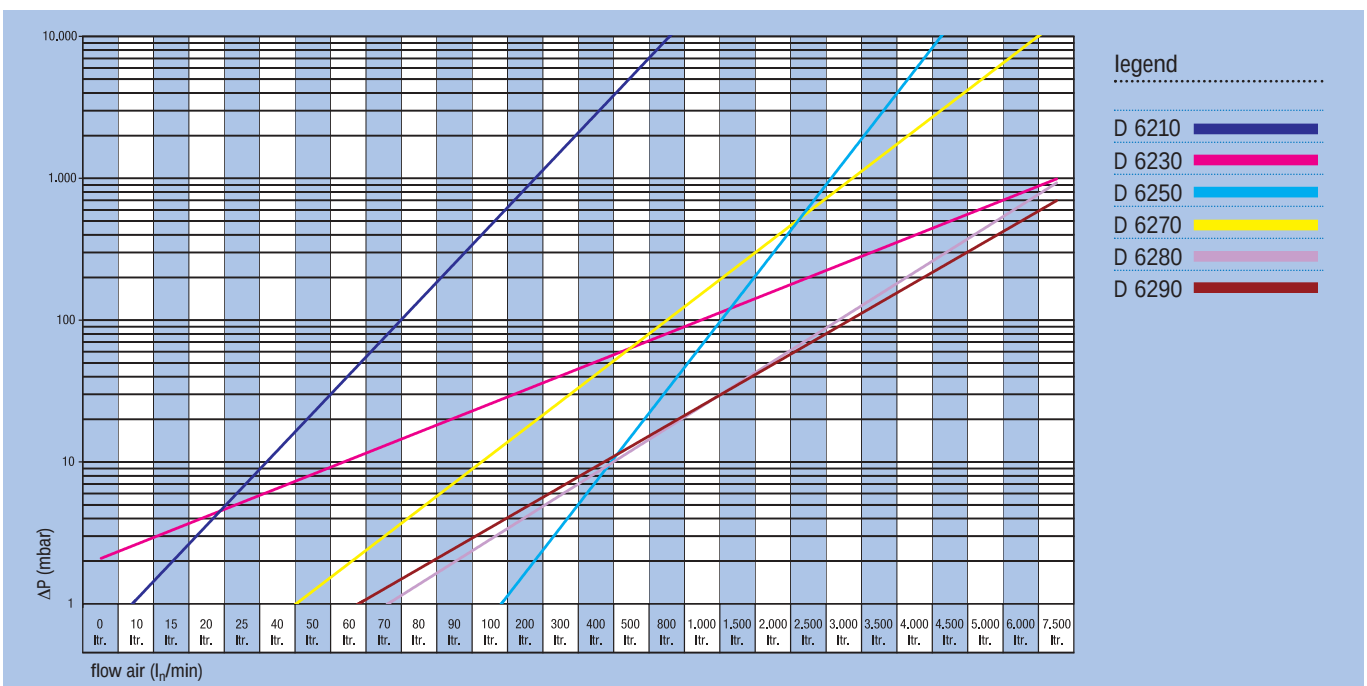

Model Number Identification

Options and Model Numbers MASS-STREAM®

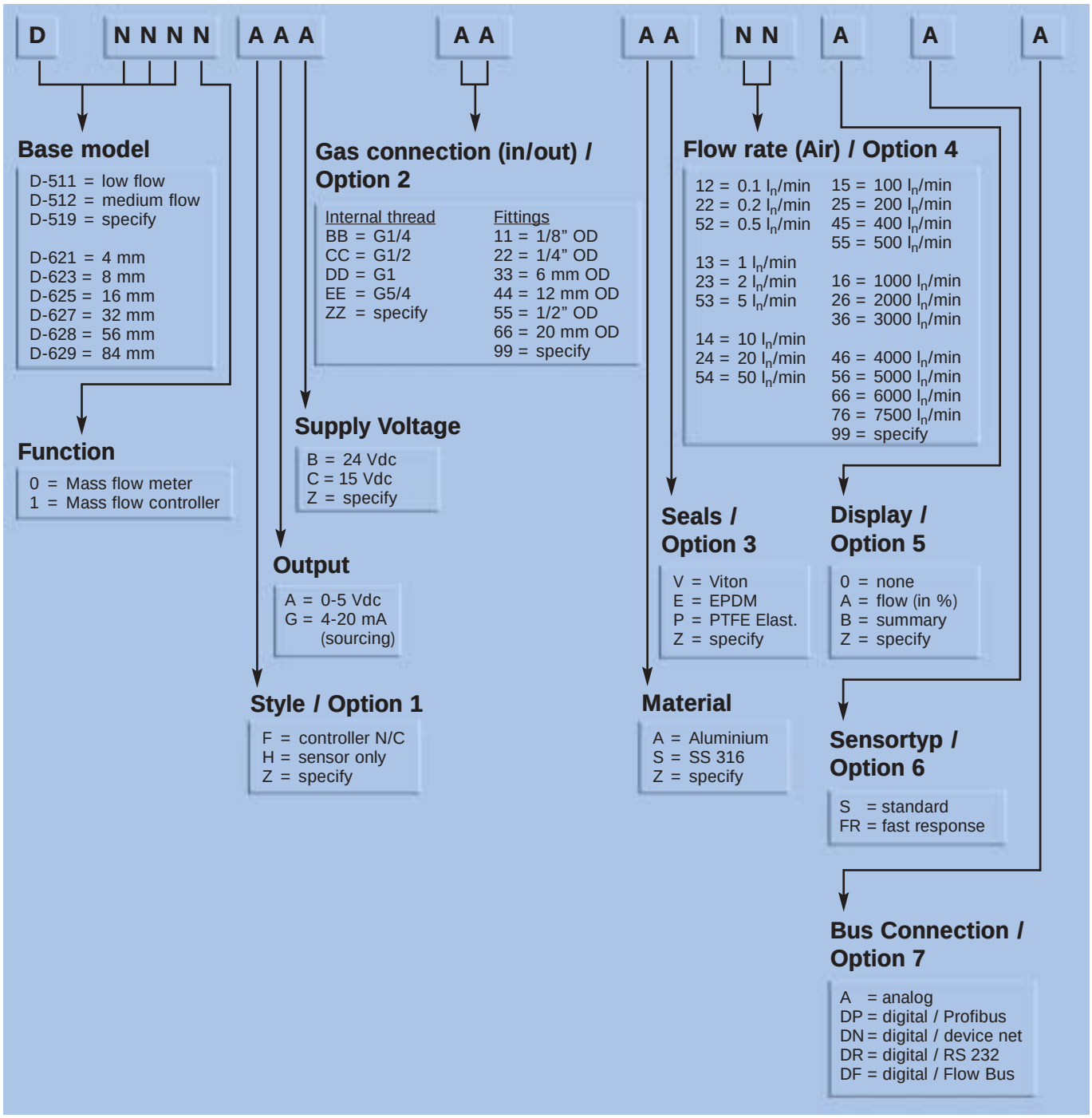

Enquiry and Ordering Information

In order to supply the correct instrument for your application we request you to state: type of gas, flow range, operating temperature and pressure (for controllers supply pressure and back pressure), electrical connection, desired output signal, type of process connection and seals.

Based on this information we perform the following actions/ calculations:

- Convert the desired flow to Air-equivalent flow, i.e., divide the desired flow by the conversion factor.
- Only for controllers, check if the pressure differential across the valve (ΔP) is within the limits.
- Only for controllers, check if the calculated Kv-value is within the specifications allowed.

Technical Specifications

Measurement System

Accuracy (based on air calibration)	± 3% FS incl. non-linearity (better one's on request)
Repeatability	± 0.5% FS (better one's on request)
Time constant (63.2%)	τ = 0.7 sec (standard, better one's s. p. 10)
Pressure sensitivity	0.2% / bar typical (air)
Attitude sensitivity	± 0.1% °C
Leak integrity	< 2 x 10^{-9} mbar l/s He
RFI	According to CE

Operating Limits

Range	3...100%
Type of gases	All gases compatible with materials chosen
Temperature	0...70°C
Pressure	10 bar; higher on application
Warming up time	30 min for optimum accuracy;
	within 30 sec for accuracy ±4% FS
Installation	
Series D-5100...	10 D straight pipe upstream
Series D-6200...	Unrestricted

Mechanical Part

Sensor	AISI 316L
Body	AISI 316L or Aluminium (anodised), please specify
Sieves / rings	Stainless steel / teflon
Protection	IP40 (IP 65 on application)

Electrical Properties

Supply voltage	24 Vdc ±10% or 15 Vdc ±10%	
Current peak values		
Series D-5100...	75 mA max.	
Series D-6200...	Inrush current	250 mA max.
	No flow	75 mA max.
	100% flow	175 mA max.
Control valve, if applicable	Add 250 mA max.	
Output signal	0...5 Vdc or 4...20 mA	
Cable	6-wire DIN or 15-wire SUB-D	

Ultra-Fast Sensor

"Fast response" version

M+W Instruments Mass Flow Meters and Controllers are used for a wide variety of applications and for this reason the sensor has been set up with "smooth-response" characteristics thereby avoiding any possible overshoot of the setpoint.
There are, however, applications where the response time of the sensor or the control valve is the decisive factor and for these applications M+W Instruments has developed a sensor with the following features:

Response time (5τ): up to <100ms

When using this sensor in connection with a flow controller the following response times are possible:

Response time (5τ): up to <1,5s

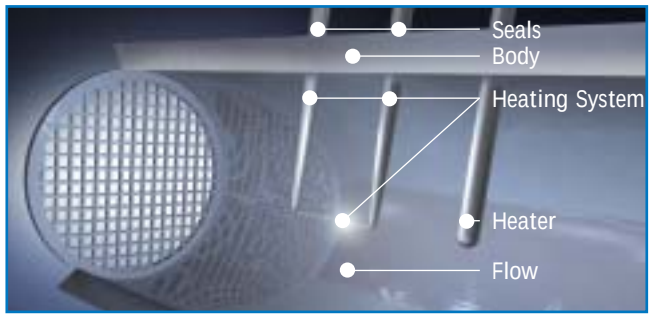

If even faster times are required then we would recommend using this sensor in conjunction with our digital pc-board. Further information is available within the section headed "Digital version".

Dimensions as standard, s. p. 4/5
Model number identification, s. p. 8

Digital version

All our standard products are equipped with an analog pc-board, a feature that ensures that they are very economically priced. However, our well thought-out modular system allows us to offer a digital pc-board as well thereby giving the options of analog voltage or current output together with Profibus DP, Device Net, RS 232 or Flowbus protocols.

Flow Controller response times down to 0.5 sec and less are possible when using the "fast response" sensor.

Readout Systems
with integrated Power Supply

General

This series comprises standard types for use with analog mass flow meters and controllers. The most commonly used functions are offered in compact single channel table top housing, DIN panel mount cassette and multi-channel versions in 1/2 19" or 19" table top or rack housing.

Functions

- Power Supply for MFM/MFC
- Indication of flow rate
- Totalization
- Setpoint-potentiometer

Electrical data

- Power supply 110 or 230 Vac, 50/60 Hz.
- Suitable for connection of instruments with output signal 0...5 Vac
- Sub-D socket for instrument connection
- Max. power +24 Vac, 0.5 A per channel

Model number identification

Code			Housing	
D - 11			1/2 19" table top	42 TE
D - 12			19" table top	84 TE
D - 13			1/2 19" rack	42 TE
D - 14			19" rack	84 TE
D - 15			Table top cassette	14 TE
D - 16			Panel mount cassette	14 TE
D - 19			Other/specify	
	Code		Supply voltage	
	- 00		100...240 Vac	
	- 10		230 Vac	
	- 20		110 Vac	
		Code	Modules with blind front (14TE)	
		- 00	Rearpanel with power supply + mains entry (incl. cable)	
		- 01	Rearpanel with power supply / sub D connector	
		- 02	Rearpanel with Sub D connector	
		- 03	Rearpanel blind	
		Code	Modules with flow indication (actual display) (14TE)	
		- 10	Rearpanel with power supply + mains entry (incl. cable)	
		- 11	Rearpanel with power supply / sub D connector	
		- 12	Rearpanel with Sub D connector	
		- 13	Rearpanel blind	
		Code	Modules with indication of totalised flow (14TE)	
		- 20	Rearpanel with power supply + mains entry (incl. cable)	
		- 21	Rearpanel with power supply / sub D connector	
		- 22	Rearpanel with Sub D connector	
		- 23	Rearpanel blind	
		Code	Modules with flow indication + control (14TE)	
		- 30	Rearpanel with power supply + mains entry (incl. cable)	
		- 31	Rearpanel with power supply / sub D connector	
		- 32	Rearpanel with Sub D connector	
		- 33	Rearpanel blind	
		Code	Modules with total flow + control (14TE)	
		- 40	Rearpanel with power supply + mains entry (incl. cable)	
		- 41	Rearpanel with power supply / sub D connector	
		- 42	Rearpanel with Sub D connector	
		- 43	Rearpanel blind	

Model D-15

Model D-11

Model D-14

M+W Instruments is a member of Brookhurst group

Distributor:

Flow-Teknikk as

Olav Brunborgsv. 27, Postboks 244, 1377 BILLINGSTAD
Tlf.: 66 77 54 00 Fax: 66 77 54 01 E-post: mail@flow.no www.flow.no

M+W Instruments GmbH
Gutenbergstraße 7
D-85748 Garching
Tel.: +49 (0) 89 - 32 94 59-0
Fax: +49 (0) 89 - 32 94 59-85
www.mw-instruments.com
info@mw-instruments.com

M+W Instruments

OMRON

Digital fiberforstærker

E3X-DA-N

Brugervenlig og med tydeligt display

- Vælg imellem 3 tydelige display visninger:
  Digital 12 bit visning (0 til 4000)
  Digital procentvisning
  Analog visning
- Multifunktion og stort modelprogram. Bl.a. blå LED, BUS typer for nem fortrådning samt M8 IP66 model
- Beskyttelse mod gensidig interferrens
- Skalérbar 1 til 5v analog udgang

Programmeringsenhed

- Giver mulighed for fjernbetjent programmering
- Copy og paste funktion og 10 hukommelsesbanker
- Aflåsning af parametre beskytter mod uhensigtsmæssig betjening

Typeoversigt

■ Forstærkerenheder

Med kabel

Enhed	Udseende	Udgang	Model	
			NPN udgang	PNP udgang
Standard model	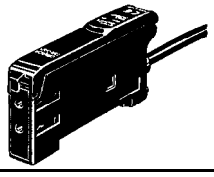	ON/OFF udgang	E3X-DA11-N	E3X-DA41-N
Med analog udgang		ON/OFF udgang Analog udgang	E3X-DA21-N	E3X-DA51-N
Mærkeaftaster med blå LED		ON/OFF udgang	E3X-DAB11-N	---

Til BUS forbindelse

Enhed	Udseende	Stik med kabel (Bestilles separat)		Udgang	Model	
					NPN udgang	PNP udgang
Standard model	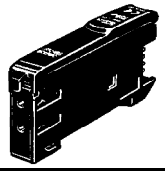	Master	E3X-CN11	ON/OFF udgang	E3X-DA6	E3X-DA8
		Slave	E3X-CN12			
Med analog udgang		Master	E3X-CN21	ON/OFF udgang Analog udgang	E3X-DA7	E3X-DA9
		Slave	E3X-CN22			

Med M8 stik og IP66 udførsel

Enhed	Udseende	Udgang	Model	
			NPN udgang	PNP udgang
Standard model	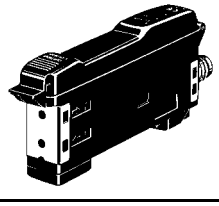	ON/OFF udgang	E3X-DA14V	E3X-DA44V

■ Stik med kabel til BUS model (Bestilles separat)

Enhed	Udseende	Kabel længde	Antal ledere	Model
Master stik	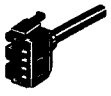	2 m	3	E3X-CN11
			4	E3X-CN21
Slave stik	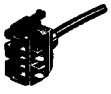		1	E3X-CN12
			2	E3X-CN22

■ Programmeringsenhed (Bestilles separat)

Udseende	Strømforsyning	Model	Bemærkning
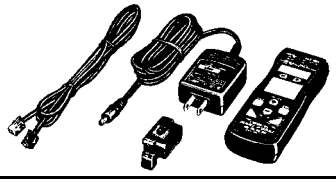	Genopladeligt batteri	E3X-MC11-EU	Komplet tilbehørspakke for trådløs programmering er inkluderet

■ Bestykning af fiberforstærker med BUS funktion

Eksempel hvis man ønsker BUS forbindelse mellem 5 forstærkere

Forstærker enheder		
Type	NPN	PNP
Standard model	E3X-DA6	E3X-DA8
Analog udgang model	E3X-DA7	E3X-DA9

+

Stik med kabel	
Master forbindelse	Slave forbindelse
E3X-CN11 (3-leder)	E3X-CN12 (1-leder)
E3X-CN21 (4-leder)	E3X-CN22 (2-leder)

Bestykning ved 5 sæt

Forstærker enheder 5 stk.	+	Master forbindelse 1 stk., Slave forbindelse 4 stk.

■ Fiber enheder

Separat sender/modtager

✂ Indikerer modeller, hvor det er tilladt at forkorte fiberen ved hjælp af den medfølgende saks.

: Super-lang-tasteafstand : Standard mode : Super-high-speed mode

Appli-kation	Egenskaber	Udseende	Forstærker	Tasteafstand (mm) (Værdier i parantes : ved anvendelse af E39-F1 linse)	Standard objekt *3 (mindste uigennem sigtige emne)	Model	Tilladelig bøjnings radius
Lang taste-afstand	M4	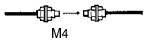 M4	E3X-DA□-N	1,660 (4,000) / 1,330 (3,200) / 490 (1,200)	1.4-mm dia. (0.02-mm dia.)	E32-T11L ✂	25 mm
			E3X-DAB11-N	150 / 120 / 75			
	3-mm dia.	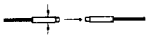 3-mm dia.	E3X-DA□-N	1,660 / 1,330 / 490	1.4-mm dia. (0.01-mm dia.)	E32-T12L ✂	
Lang taste-afstand	M3	 M3	E3X-DA□-N	500 / 440 / 180	0.9-mm dia. (0.01-mm dia.)	E32-T21L ✂	25 mm
	2-mm dia.	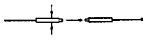 2-mm dia.	E3X-DA□-N	500 / 440 / 180		E32-T22L ✂	

Applikation	Egenskaber	Udseende	Forstærker	Tasteafstand (mm) (Værdier i parantes : ved anvendelse af E39-F1 linse)	Standard objekt *2 (mindste uigennemsigtige emne)	Model	Tilladelig bøjnings radius
Lang tasteafstand	M14, med linser, ideel til eksplosionssikre applikationer	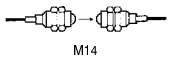 M14	E3X-DA□-N	20,000 *1 20,000 *1 9,800	10-mm dia. (0.01-mm dia.)	E32-T17L	25 mm
Almindelig brug	M4	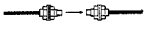 M4	E3X-DA□-N	950 (4,000) 760 280 (2,100)	1.0-mm dia. (0.01-mm dia.)	E32-TC200	25 mm
			E3X-DAB11-N	100 (700) 75 (550) 45 (350)			
	M3, mulighed for vinkelaftastning med E39-F5 vinkellinser	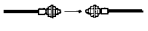 M3	E3X-DA□-N	850 680 250		E32-TC200A	
	M3	 M3	E3X-DA□-N	250 220 90	0.5-mm dia. (0.01-mm dia.)	E32-TC200E	
			E3X-DAB11-N	25 20 10			
Tynd fiber	2-mm dia.; små emner	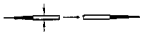 2-mm dia.	E3X-DA□-N	250 220 90	0.5-mm dia. (0.01-mm dia.)	E32-T22	25 mm
	ø1.2-mm, Bøjeligt metal fiberrør i enden	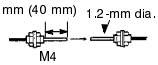 90 mm (40 mm) 1.2-mm dia. M4 ( ): E32-TC200B4	E3X-DA□-N	950 760 280	1.0-mm dia. (0.01-mm dia.)	E32-TC200B E32-TC200B4	
			E3X-DAB11-N	100 75 45			
	ø0.9-mm, Bøjeligt metal fiberrør i enden	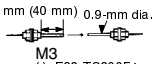 90 mm (40 mm) 0.9-mm dia. M3 ( ): E32-TC200F4	E3X-DA□-N	250 220 90	0.5-mm dia. (0.01-mm dia.)	E32-TC200F E32-TC200F4	
Fleksibel fiber	Kan bøjes som en ledning. Bøjningsradius=1mm	 M4	E3X-DA□-N	670 (4,000) 530 (3,700) 200 (1,400)	1-mm dia. (0.01-mm dia.)	E32-T11R	1 mm
		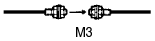 M3	E3X-DA□-N	150 130 50	0.5-mm dia. (0.01-mm dia.)	E32-T21R	
Fleksibel fiber. Meget hårdfør	Ideel til montage på kørende dele	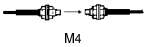 M4	E3X-DA□-N	850 (4,000) 680 (3,600) 250 (1,300)	1.0-mm dia. (0.01-mm dia.)	E32-T11	4 mm
Fleksibel fiber. Meget hårdfør	Ideel til montage på kørende dele	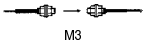 M3	E3X-DA□-N	220 200 80	0.5-mm dia. (0.01-mm dia.)	E32-T21	4 mm
		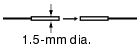 1.5-mm dia.	E3X-DA□-N	220 200 80		E32-T22B	
Vinkelaftastning	Lang tasteafstand; pladsbesparende	 3-mm dia.	E3X-DA□-N	570 460 170	1.0-mm dia. (0.01-mm dia.)	E32-T14L	25 mm
			E3X-DAB11-N	50 40 25			
	Til små emner	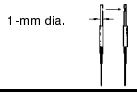 1-mm dia.	E3X-DA□-N	150 130 55	0.5-mm dia. (0.01-mm dia.)	E32-T24	

Note: 1. Størrelsen på standardobjektet er den samme som fiberens diameter (anvendes linse, er det linsediameteren).

2. Det mindst aftastbare emne med sender/modtager er fundet, når fotoaftasteren i digital 12 bits visning er indstillet til at modtage lys, der overstiger værdien 1000 på displayet.

*1 Fibrene på E32-T17L er 10 m.

*2 Indikerer værdier for standard mode.

Applikation	Egenskaber	Udseende	Forstærker	Tasteafstand (mm) (Værdier i parantes : ved anvendelse af E39-F1 linse)	Standard-objekt *4 (mindste uigennemsigtige emne)	Model	Tilladelig bøjnings radius
Modstår kemikalier og andre hårde miljøer	**Teflon belagt*1; (Omgivelsestemperatur imellem -30°C til 70°C)**	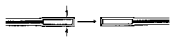 5-mm dia.	E3X-DA□-N	3,800 3,000 1,100	4.0-mm dia. (0.01-mm dia.)	**E32-T12F**	40 mm
	Teflon belagt*1; vinkelaftastning (Omgivelsestemperatur imellem -30°C til 70°C)	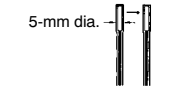 5-mm dia.	E3X-DA□-N	500 400 150	3.0-mm dia. (0.01-mm dia.)	**E32-T14F**	
Varmebestandig	**Modstår 200°C; fleksibel; Teflon belagt*1 (Omgivelsestemperatur imellem -40°C til 200°C)**	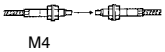 M4	E3X-DA□-N	350 280 100	1.0-mm dia. (0.01-mm dia.)	**E32-T61R**	10 mm
	Modstår 150°C*2; (Omgivelsestemperatur imellem -40°C til 150°C)	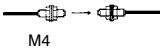 M4	E3X-DA□-N	950 760 280	1.5-mm dia. (0.01-mm dia.)	**E32-T51**	35 mm
	Vinkelaftastning;modstår 150°C*2; detektion af små emner; (Omgivelsestemperatur imellem -40°C til 150°C)	 2-mm dia.	E3X-DA□-N	290 230 80	1.0-mm dia. (0.01-mm dia.)	**E32-T54**	35 mm
Gaffel	**Ideel til aftastning af etiketter o.lign.**		E3X-DA□-N	10 10 10	4.0-mm dia. (0.16-mm dia.)	**E32-G14**	25 mm
			E3X-DAB11-N	10 10 10			
Lille spredning af lyskegle	**Aftastning af lille højdevariation**	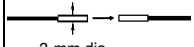 3-mm dia.	E3X-DA□-N	2,300 1,900 700	1.7-mm dia. (0.01-mm dia.)	**E32-T22S**	10 mm
	Vinkelaftastning; aftastning af lille højdevariation	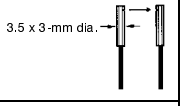 3.5 x 3-mm dia.	E3X-DA□-N	1,700 1,300 500	2-mm dia. (0.01-mm dia.)	**E32-T24S**	
Aftastning af areal	**4 følerhoveder for genkendelse af former og højder**	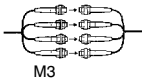 M3	E3X-DA□-N	700 610 250	2.0-mm dia. (0.01-mm dia.)	**E32-M21**	25 mm
	Taster i et område på 30mm	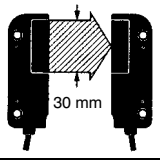 30 mm	E3X-DA□-N	2,300 1,800 660	(0.3-mm dia.) *2	**E32-T16W**	10 mm
Aftastning af areal	**Taster i et område på 10 mm; lang tasteafstand**	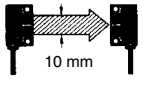 10 mm	E3X-DA□-N	3,500 2,800 1,000	(0.6-mm dia.)	**E32-T16**	25 mm
	Taster små emner i et område på 11 mm; IP50	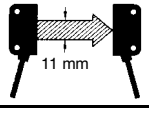 11 mm	E3X-DA□-N	1,400 1,100 420	(0.2-mm dia.) *2	**E32-T16P**	10 mm

Note: 1. Størrelsen på standardobjektet er den samme som fiberens diameter (anvendes linse, er det linsediameteren).

2. Det mindst aftastbare emne med sender/modtager er fundet, når fotoaftasteren i digital 12 bits visning er indstillet til at modtage lys, der overstiger værdien 1000 på displayet.

*1 Teflon er et registreret varemærke

*2 Maks. vedvarende temperatur er 130°C.

*3 Indikerer varmemodstanden på spidsen.

*4 Indikerer værdier i standard mode.

*5 Fibren er 2 m.

Typer for diffus reflektion

✂ Indikerer modeller, hvor det er tilladt at forkorte fiberen ved hjælp af den medfølgende saks.

■ : Super-lang-tasteafstand ■ : Standard mode □ : Super-high-speed mode

Applikation	Egenskaber	Udseende	Forstærker	Tasteafstand (mm) *1	Standard objekt (min. tasteemne *2: Guld tråd)	Model	Tilladelig bøjningsradius
Lang tasteafstand	**M6**	 M6	E3X-DA□-N	500 400 150	500×500 (0.01-mm dia.)	**E32-D11L** ✂	25 mm
			E3X-DAB11-N	44 35 22	(0.1-mm dia.)		
	3-mm dia.	 3-mm dia.	E3X-DA□-N	300 230 100	300×300 (0.01-mm dia.)	**E32-D12** ✂	25 mm
	M4	 M4	E3X-DA□-N	160 130 45	200×200 (0.01-mm dia.)	**E32-D21L** ✂	
	3-mm dia.	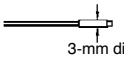 3-mm dia.	E3X-DA□-N	160 130 45		**E32-D22L** ✂	
Almindelig brug	**M6**	 M6	E3X-DA□-N	400 300 100	400×400 (0.01-mm dia.)	**E32-DC200** ✂	25 mm
			E3X-DAB11-N	32 25 16	(0.1-mm dia.)		
	M3	 M3	E3X-DA□-N	100 80 30	100×100 (0.01-mm dia.)	**E32-DC200E** ✂	
			E3X-DAB11-N	8 6 4	(0.2-mm dia.)		
Tynd fiber	**2.5-mm dia.; Bøjeligt metal fiberrør i enden**	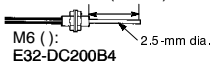 90 mm (40 mm) M6 ( ): E32-DC200B4 2.5-mm dia.	E3X-DA□-N	400 300 100	400×400 (0.01-mm dia.)	**E32-DC200B** **E32-DC200B4** ✂	25 mm
			E3X-DAB11-N	32 25 16	(0.1-mm dia.)		
	1.2-mm dia.; Bøjeligt metal fiberrør i enden	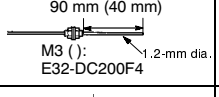 90 mm (40 mm) M3 ( ): E32-DC200F4 1.2-mm dia.	E3X-DA□-N	100 80 30	100×100 (0.01-mm dia.)	**E32-DC200F** **E32-DC200F4** ✂	
	0.8-mm dia.; præcis aftastning	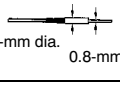 3-mm dia. 0.8-mm dia.	E3X-DA□-N	21 16 6	25×25 (0.01-mm dia.)	**E32-D33** ✂	
	0.5-mm dia.; præcis aftastning	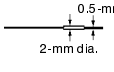 0.5-mm dia. 2-mm dia.	E3X-DA□-N	4 3 1		**E32-D331**	
Fleksibel	**Kan bøjes som en ledning. Bøjningsradius =1mm**	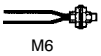 M6	E3X-DA□-N	220 170 80	300×300 (0.01-mm dia.)	**E32-D11R** ✂	1 mm
		 M3	E3X-DA□-N	40 30 10	50×50 (0.01-mm dia.)	**E32-D21R** ✂	

Flek-sibel fi-ber. Meget hårdfør	**Ideel til montage på kørende dele**	 M6	E3X-DA□-N	220 170 80	300 × 300 (0.01-mm dia.)	**E32-D11**	4 mm
		 M3	E3X-DA□-N	40 30 10	50 × 50 (0.01-mm dia.)	**E32-D21**	
		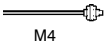 M4	E3X-DA□-N	90 70 25	100 × 100 (0.01-mm dia.)	**E32-D21B**	
		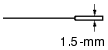 1.5-mm dia.	E3X-DA□-N	40 30 10	50 × 50 (0.01-mm dia.)	**E32-D22B**	

Note: 1. Værdien er opgivet for et standardobjekt.

2. Det kan være nødvendigt at udføre et- eller to-punkts teach for at opnå samme resultat.

*1 Tasteafstand ved hvidt papir

*2 Indikerer værdier i standard mode.

Applikation	Egenskaber	Udseende	Forstærker	Tasteafstand (mm) *1	Standard-objekt (min. tasteemne *5: Guld tråd)	Model	Tilladelig bøjnings radius
Coaxial fiber	**M6 coaxial; Stor aftastnings-nøjagtighed ved lang afstand**	 M6	E3X-DA□-N	400 300 100	500 × 500 (0.01-mm dia.)	**E32-CC200**	25 mm
			E3X-DAB11-N	32 25 16	(0.1-mm dia.)		
	3-mm dia. coaxial; Stor aftastnings-nøjagtighed	 3-mm dia.	E3X-DA□-N	200 150 50	300 × 300 (0.01-mm dia.)	**E32-D32L**	
	M3 coaxial; Stor aftastnings-nøjagtighed; muligt at montere linse for smalt spot (E39-F3A-5/F3B/F3C)	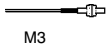 M3	E3X-DA□-N	100 75 25	25 × 25 (0.01-mm dia.)	**E32-C31**	
	M3 coaxial; Stor aftastnings-nøjagtighed; muligt at montere linse for smalt spot (E39-F3A-5/F3B/F3C)	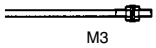 M3	E3X-DA□-N	45 35 10	50 × 50 (0.01-mm dia.)	**E32-C41**	
	2-mm dia. coaxial; Stor aftastnings-nøjagtighed; muligt at montere linse for smalt spot (0.1 til 0.6 dia) (E39-F3A)	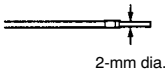 2-mm dia.	E3X-DA□-N	45 35 10	50 × 50 (0.01-mm dia.)	**E32-C42**	
	2-mm dia. coaxial; Stor aftastnings-nøjagtighed; muligt at montere linse for smalt spot (0.5 til 1 dia) (E39-F3A)	 2-mm dia.	E3X-DA□-N	100 75 25	100 × 100 (0.01-mm dia.)	**E32-D32**	
Vinkel-aftastning	**6-mm dia.; lang tasteafstand**	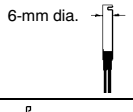 6-mm dia.	E3X-DA□-N	150 110 50	200 × 200 (0.01-mm dia.)	**E32-D14L**	25 mm
	2-mm dia.; små byggemål	 2-mm dia.	E3X-DA□-N	40 30 10	50 × 50 (0.01-mm dia.)	**E32-D24**	

Applikation	Egenskaber	Udseende	Forstærker	Tasteafstand (mm) *1	Standard-objekt (min. tasteemne *5: Guld tråd)	Model	Tilladelig bøjnings radius
Modstår kemikalier og andre hårde miljøer	**Teflon belagt*3; (Omgivelsestemperatur imellem -30°C til 70°C)**	 6-mm dia.	E3X-DA□-N	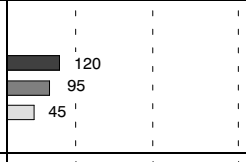 120 95 45	200×200 (0.01-mm dia.)	**E32-D12F**	40 mm
Varme-bestandig	**Modstår 150°C*2; (Omgivelsestemperatur imellem -40°C til 150°C)**	 M6	E3X-DA□-N	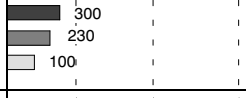 300 230 100	200×200 (0.01-mm dia.)	**E32-D51**	35 mm
	Modstår 300°C*4; med rustfri spiral fiberbeskyttelse (Omgivelsestemperatur imellem -40°C til 300°C)	 M6	E3X-DA□-N	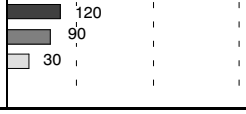 120 90 30		**E32-D61**	25 mm

Note: 1. Værdien er opgivet for et standardobjekt.

2. Det kan være nødvendigt at udføre et- eller to-punkts teach for at opnå samme resultat.

*1 Tasteafstand indikerer, værdier opnået med hvidt papir.

*2 Max. vedvarende temperatur er 130°C.

*3 Teflon er et registreret varemærke fra Dupont Company.

*4 Indikerer temperaturen målt på fiberspidsen.

*5 Indikerer værdier for standard mode.

Applikation	Egenskaber	Udseende	Forstærker	Tasteafstand (mm) *1	Standard objekt (min. tasteemne *2: Guld tråd)	Model	Tilladelig bøjnings radius
Aftastning af areal	**Taster i et stort område ud fra siden**		E3X-DA□-N	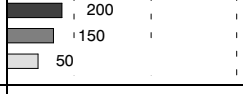 200 150 50	300×300 (0.01-mm dia.)	**E32-D36P1**	25 mm
Aftaster med refleksbrik	**Aftastning af transparente emner**	 M6 Reflektor E39-R3	E3X-DA□-N	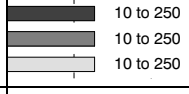 10 to 250 10 to 250 10 to 250	35-mm dia. (0.1-mm dia.)	**E32-R21 +E39-R3 (tilbehør)**	25 mm
	Aftastning af transparente emner; IP66	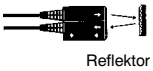 Reflektor E39-R1	E3X-DA□-N	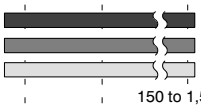 150 to 1,500	35-mm dia. (0.2-mm dia.)	**E32-R16 +E39-R1 (tilbehør)**	
Fast taste-afstand	**Positionering af glas**		E3X-DA□-N	 4 to 12	100×100	**E32-L56E1 E32-L56E2**	35 mm
	Aftastning af små højdeforskelle; (Omgivelsestemperatur imellem -40°C til 105°C); IP50		E3X-DA□-N	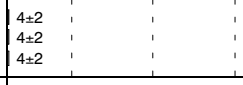 4±2 4±2 4±2	25×25 (0.01-mm dia.)	**E32-L24L**	10 mm
			E3X-DA□-N	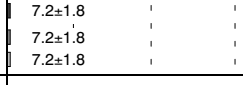 7.2±1.8 7.2±1.8 7.2±1.8		**E32-L25L**	
Fast taste-afstand	**Aftastning af små højdeforskelle; IP50**		E3X-DA□-N	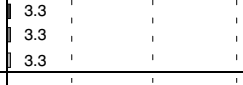 3.3 3.3 3.3		**E32-L25**	25 mm
			E3X-DA□-N	 3.3 3.3 3.3		**E32-L25A**	
Kontrol af væsker	**Montering på rør**		E3X-DA□-N	---	Væske	**E32-L25T**	10 mm

Note: 1. Værdierne for det mindste aftastbare objekt er opnået ved en ikke oplyst afstand.

2. Det kan være nødvendigt at udføre et- eller to-punkts teach, for at opnå samme resultat.

*1 Tasteafstand indikerer, værdier opnået med hvidt papir.

*2 Indikerer værdier for standard mode.

Specifikationer

■ Tekniske data

Fiberforstærker

Enhed		Standard model		Med analog udgang		Mærkeaftaster	Med M8 stik IP66
Udgangstype	NPN udgang	E3X-DA11-N	E3X-DA6	E3X-DA21-N	E3X-DA7	E3X-DAB11-N	E3X-DA14V
	PNP udgang	E3X-DA41-N	E3X-DA8	E3X-DA51-N	E3X-DA9	---	E3X-DA44V
Lyskilde (bølgelængde)		Rød LED (660 nm)				Blå LED (470 nm)	Rød LED (660 nm)
Strømforsyningsspænding		12 til 24 VDC ± 10%, ripple (p-p) 10% max.					
Strømforbrug		Normalt: 960 mW max. (strømforbrug: 40 mA max. ved 24 VDC forsyning) Eco Mode: 720 mW max. (strømforbrug: 30 mA max. ved 24 VDC forsyning) Display slået fra: 600 mW max. (strømforbrug: 25 mA max. ved 24 VDC forsyning)					
Kontrol udgang	**ON/OFF udgang**	NPN/PNP (afhængig af model) åben collector; belastningsstrøm: 50 mA max.; Restspænding: 1 V max.; Light ON/Dark ON kan vælges				NPN åben collector; belastningsstrøm: 50 mA max.; restspænding:1V max.; Light ON/Dark ON kan vælges	NPN/PNP (afhængig af model) åben collector; belastningsstrøm: 50 mA max.; Restspænding: 1 V max.; Light ON/Dark ON kan vælges
	Analog udgang	---		Belastning 1 til 5 VDC, 10 kΩ min.		---	---
Beskyttelse af kredsløb		Omvendt polaritet, kortslutning af udgang, gensidig påvirkning					
Responstid		Super-high-speed mode: 0.25 ms for drift eller reset Standard mode: 1 ms for drift eller reset Super-long-distance mode: 4 ms for drift eller reset					
Følsomhedsindstilling		Teach eller manual metode					
Funktioner	**Timer funktion**	Forsinket frafaldstimer: 0 til 200 ms; (0 til 20ms justeres i spring af 1 ms, og 20 til 200 ms i spring af 5 ms)					
	Automatisk strøm kontrol	Sikrer ensartet lysmængde i hele levetiden				---	Sikrer ensartet lysmængde i hele levetiden
	Zero-reset	Displayværdierne kan resettes til 0, hvis ønsket (negative værdier kan også vises)					
	Total reset	Mulighed for at stille tilbage til fabriksindstilling					
	Skalering af analog udgang	---		Øvre og nedre grænser kan skaleres i enheder af 100.		---	---
Display		Udgangsindikator (orange), 7-segment display (rød og grøn). Vælg mellem 3 visninger: 12 bit visning, procent visning eller analog bargraf visning					
Andre display visninger		Vælg mellem Normal/Peak høj/Peak lav visning					
Display orientering		Vælg mellem normal og omvendt visning					
Justering af optiske akser		Mulighed for at indstille optiske akser ved hjælp af hyper-flashing funktion					
Omgivende belysning		Glødelampe: 10,000 lx max.; Sollys: 20,000 lx max.					
Omgivelsestemperatur		Drift: I gruppe med 1 til 3 forstærkere: −25°C til 55°C I gruppe med 4 til 11 forstærkere: −25°C til 50°C I gruppe med 12 til 16 forstærkere: −25°C til 45°C (uden tilisning eller kondens) Opbevaring: −30°C til 70°C (uden tilisning eller kondens)					
Omgivende luftfugtighed		Drift og opbevaring: 35% to 85% (uden tilisning eller kondens)					
Insolationsmodstand		20 MΩ min. (ved 500 VDC)					
Stødspænding		1,000 VAC ved 50/60 Hz i 1 minut					
Vibrationsmodstand		10 til 55Hz, 1.5-mm dobbelt amplitude eller 300 m/s^2(ca.30G) i 2 timer i retning X, Y og Z					
Slagstyrke		500 m/s^2 (ca.50G) 3 gange i hver retning X, Y og Z					
Beskyttelsesgrad		IP50					IP66
Forbindelsesmetode		Kabel 2 m	Stik	Kabel 2 m	Stik	Kabel 2 m	M8 stik
Vægt i pakket tilstand		Ca. 100 g	Ca. 55 g	Ca. 100 g	Ca. 55 g	Ca. 100 g	Ca. 100 g
Materiale	**Hus**	PBT					
	Dæksel	Polycarbonate					
Tilbehør		Engelsk/Japansk instruktionsvejledning					

Grafiske Data

■ E3X-DA□-N

Parallelt aftastningsområde (typisk) ved max. følsomhed.

E32-TC200 (Sender/modtager)

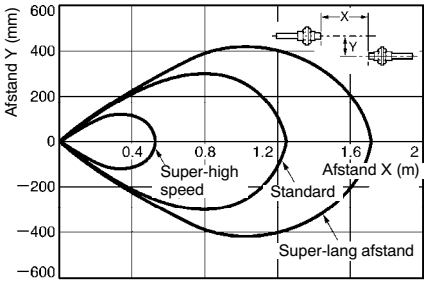

E32-T11R (Sender/modtager)

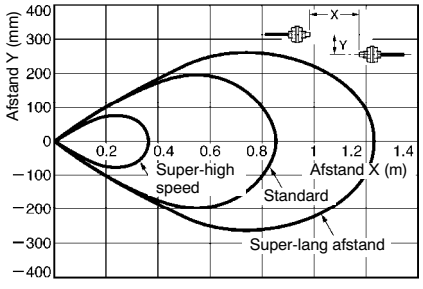

E32-T11 (Sender/modtager)

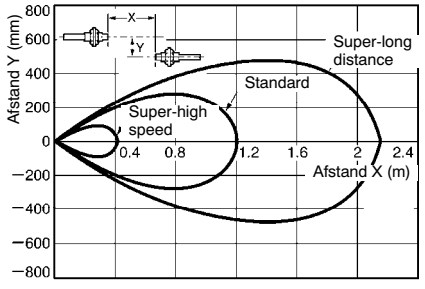

Driftsområde (typisk) standardobjekt aftastet ved max. følsomhed.

E32-DC200 (Diffus reflektion)

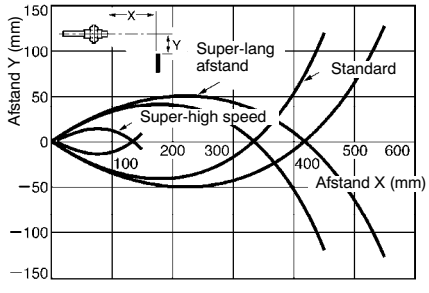

E32-D33 (Diffus reflektion)

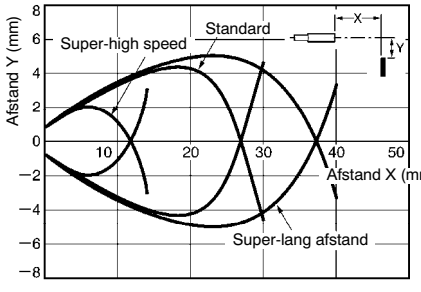

E32-L25L (Begrænset diffus reflektion)

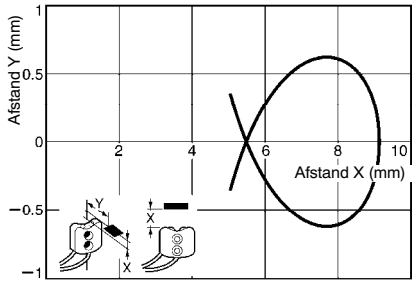

■ E3X-DAB11-N Parallelt aftastningsområde (typisk) Ved max. følsomhed.

E32-TC200 (Sender/modtager)

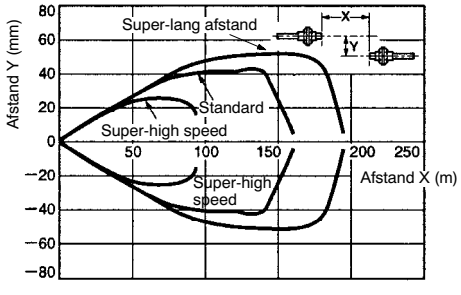

E32-TC200+E39-F1 (Sender/modtager)

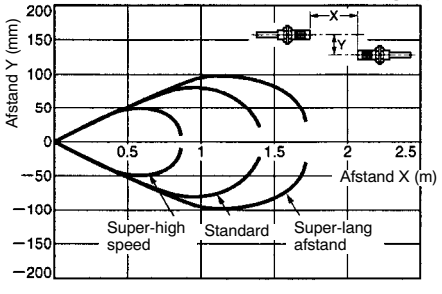

Driftsområde (typisk) Standardobjekt aftastet ved max. følsomhed.

E32-DC200 (Diffus reflektion)

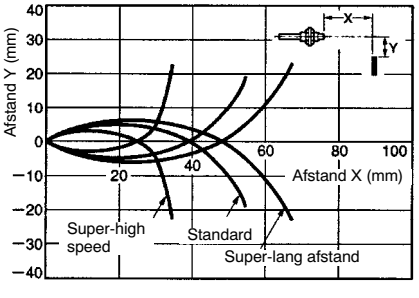

E32-CC200 (Diffus refleksion)

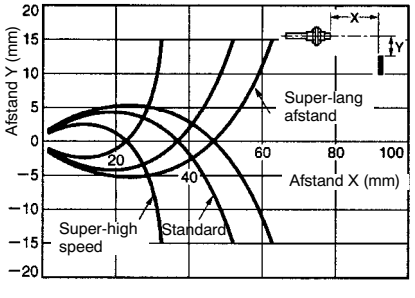

E32-D11L (Diffus reflektion)

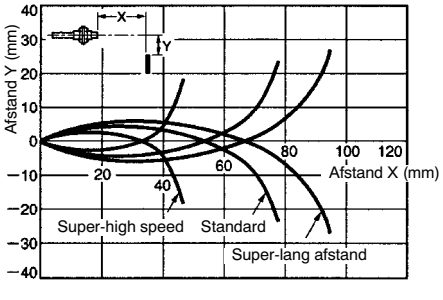

Drift

■ Udgangskredsløb

Udgang	Model	Driftmåde vælger	Tidssekvensdiagram	Udgangs status	Udgangskredsløb
NPN	E3X-DA11-N E3X-DAB11-N E3X-DA6 E3X-DA14V	LIGHT ON (L/ON)	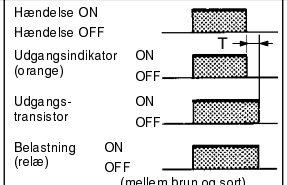	Light ON	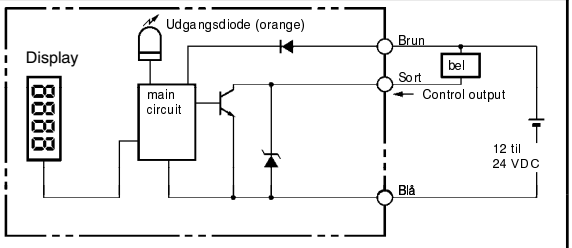
		DARK ON (D/ON)	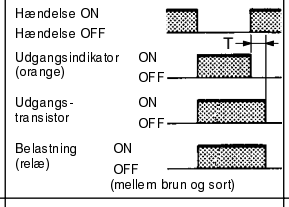	Dark ON	
	E3X-DA21-N E3X-DA7	LIGHT ON (L/ON)	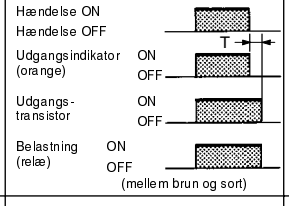	Light ON	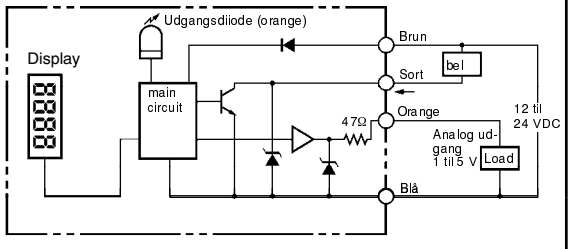
		DARK ON (D/ON)	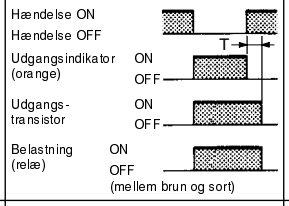	Dark ON	**Note:** Belastningsmodstand: 10 kΩ min.
PNP	E3X-DA41-N E3X-DA8 E3X-DA44V	LIGHT ON (L/ON)	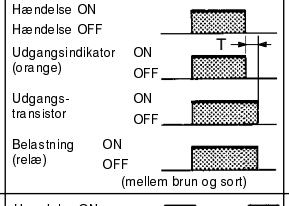	Light ON	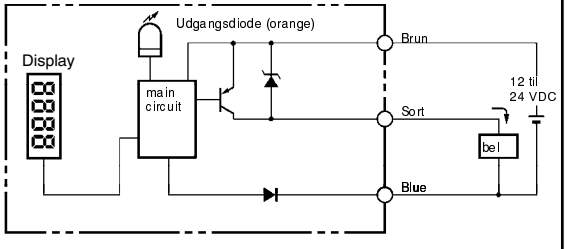
		DARK ON (D/ON)	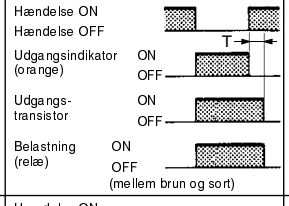	Dark ON	
	E3X-DA51-N E3X-DA9	LIGHT ON (L/ON)	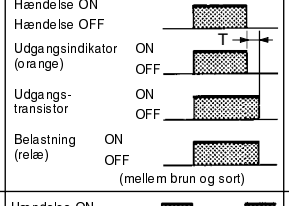	Light ON	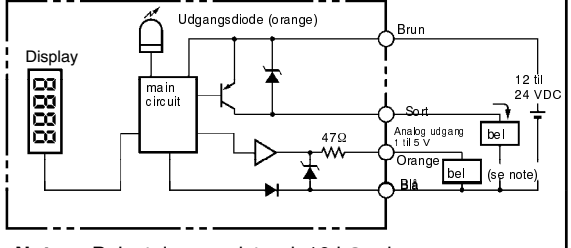
		DARK ON (D/ON)	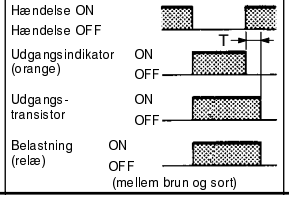	Dark ON	**Note:** Belastningsmodstand: 10 kΩ min.

Drift

Nem at anvende

Display visninger i RUN Mode

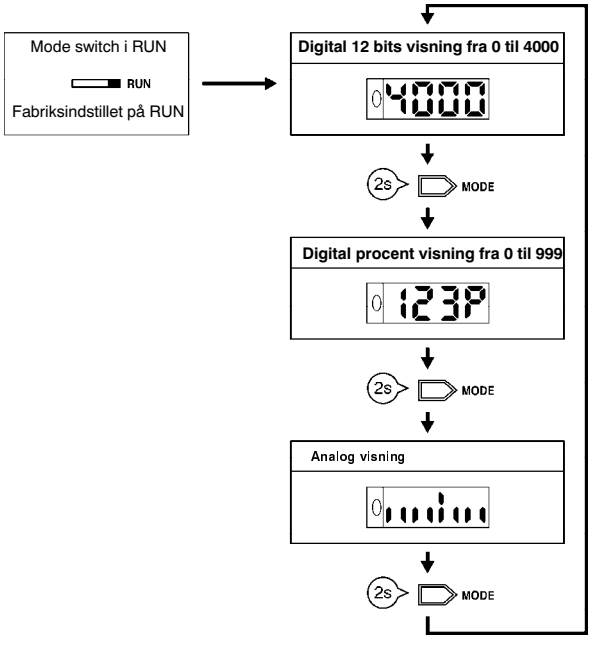

Manual indstilling i ADJ Mode. (Piletaster anvendes til fin-indstilling)

Manuel indstilling eller fin-indstilling efter Teaching

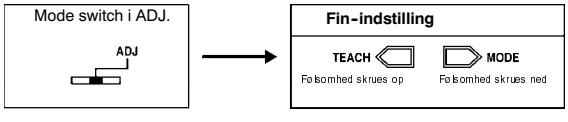

Visning i ADJ mode er forskellig fra visning i RUN mode.

RUN mode		ADJ mode
Digital 12 bit aktuel værdi	→	Digital 12 bit indstillet værdi
Digital procent aktuel værdi	→	Digital procent aktuel værdi
Aktuel analog værdi	→	Aktuel analog værdi

Zero-reset (RUN Mode)

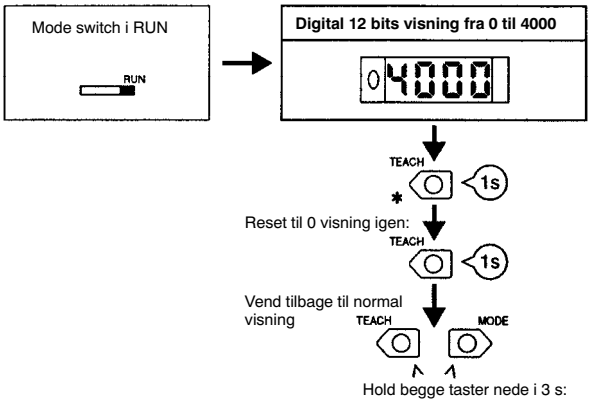

Note: Zero-reset kan udføres, så ofte man ønsker

Reset til fabriksindstilling (SET Mode)

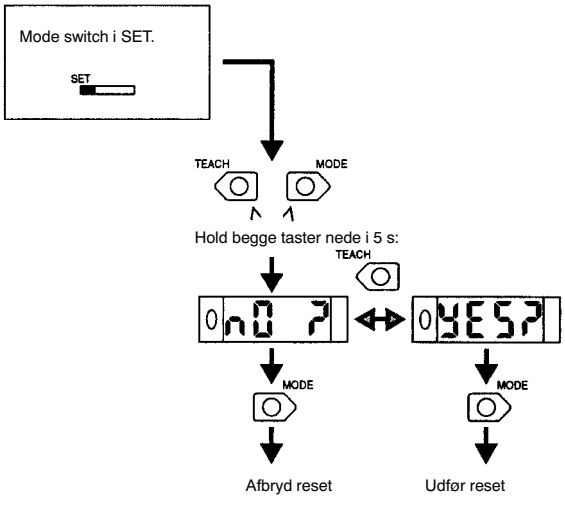

Nem at anvende

Indstillinger i SET Mode

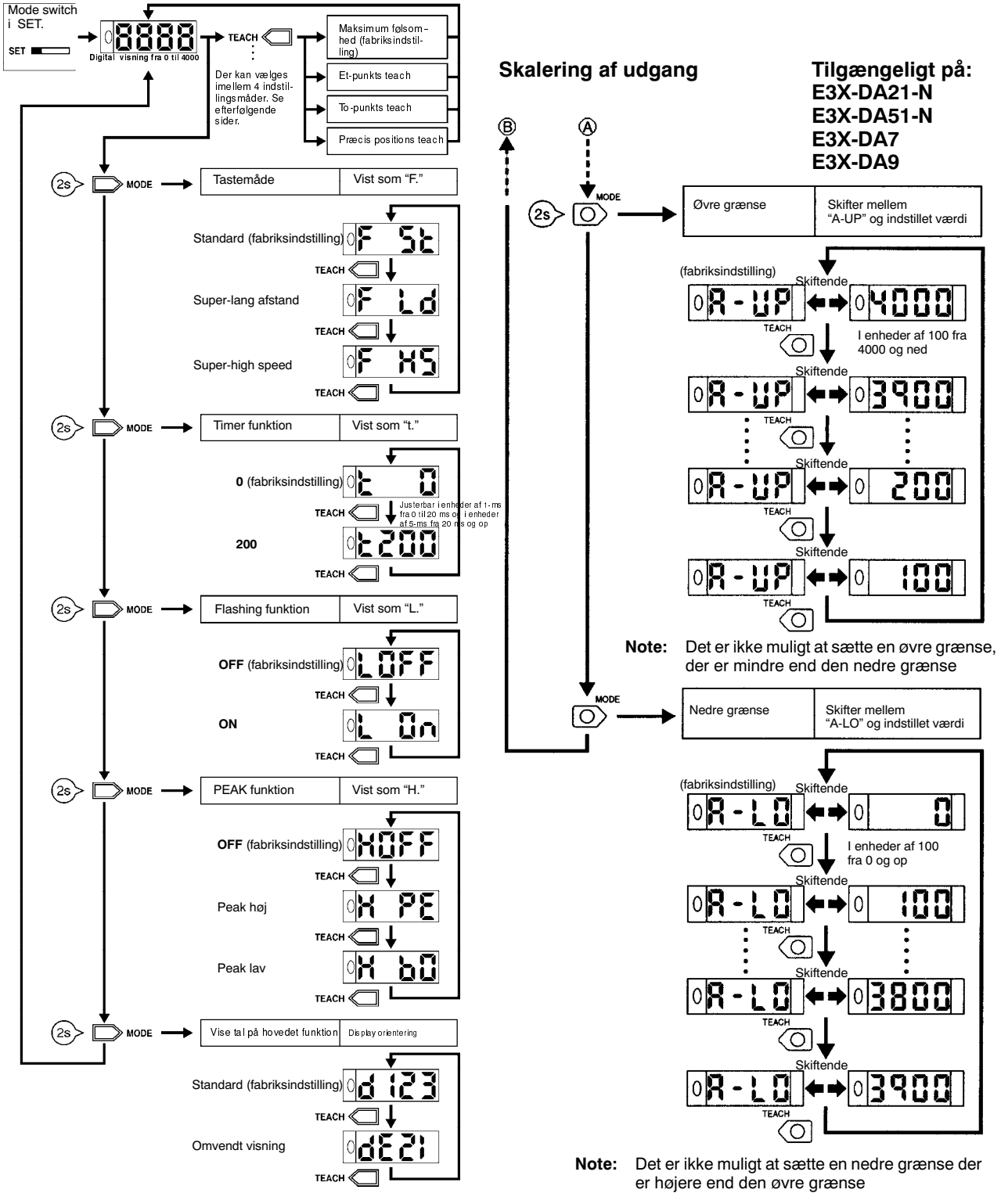

Skalering af udgang

Tilgængeligt på:
E3X-DA21-N
E3X-DA51-N
E3X-DA7
E3X-DA9

Note: Det er ikke muligt at sætte en øvre grænse, der er mindre end den nedre grænse

Note: Det er ikke muligt at sætte en nedre grænse der er højere end den øvre grænse

■ Følsomhedsindstilling/Teach (SET Mode)

Der er 4 måder at udføre Teach på

Når Teach er udført, vil forstærkeren fungere med den indlærte værdi. Hvis displayet blinker, er der sket en fejl under Teach, og proceduren skal gentages.

Indstil mode switch i SET for at påbegynde Teach.

Maximal følsomhed

1. Sæt mode switchen på SET.

2. Tryk på TEACH knappen i minimum 3 sekunder.

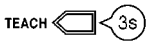

3. Teach er udført, når niveau displayet skifter fra rød til grøn. Niveau displayet vil vise den aktuelle værdi senere.

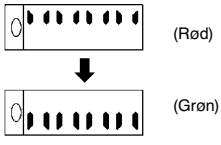

4. Sæt mode switchen tilbage på RUN

Et-punkts Teach uden emne

1. Sæt mode switchen på SET.

2. Tryk på TEACH knappen i ca. 1 sekund.

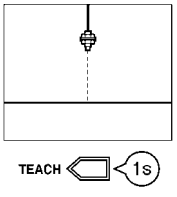

3. Teach er udført, når niveau displayet skifter til rød. Niveau displayet vil vise den aktuelle værdi senere.

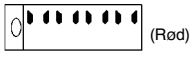

4. Sæt mode switchen tilbage på RUN.

5. Indstillingsværdien bliver automatisk indlært, når næste emne passerer fiberen.

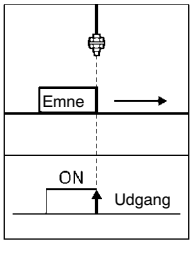

Note: Hvis et-punkts teach ikke kan udføres, er forskellen mellem emnet og baggrund for lille. Prøv da to-punkts teach.

Light ON/Dark ON omskifter

Funktionsmåde		Indstilling
Light ON	L• ON	L (Fabriksindstilling)
Dark ON	D• ON	D

To-punkts Teach (med og uden emne)

1. Sæt mode switchen på SET.

2. Tryk på TEACH knappen i ca. 1 sekund, når emnet er i tasteposition.

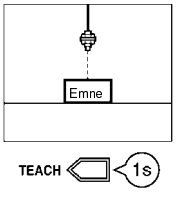

3. Niveau displayet lyser rødt.

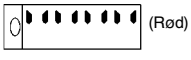

4. Tryk på TEACH knappen i ca. 1 sekund uden emne.

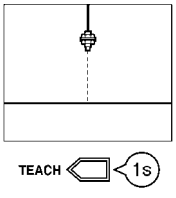

5. Teach er udført, når niveaudisplayet skifter fra rød til grøn. Niveau displayet vil vise den aktuelle værdi senere.

6. Sæt mode switchen tilbage på RUN.

Note: Om man udfører Teach med emnet først eller emnet sidst, betyder intet.

Præcis positions Teach

1. Sæt mode switchen på SET.

2. Tryk på TEACH knappen i ca. 1 sekund uden emne.

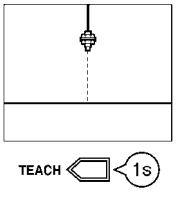

3. Niveau displayet lyser rødt.

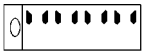

4. Anbring emnet i den ønskede position, og tryk på TEACH knappen i min. 3 sekunder.

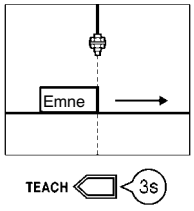

5. Teach er udført, når niveau displayet skifter fra rød til grøn. Niveau displayet vil vise den aktuelle værdi senere.

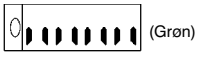

6. Sæt mode switchen tilbage på RUN.

Dimensioner

Note: Alle enheder er angivet i millimeter, hvis ikke andet angivet.

■ Forstærker

Forstærker med kabel og monteringsbeslag

E3X-DA11-N
E3X-DA21-N
E3X-DAB11-N
E3X-DA41-N
E3X-DA51-N

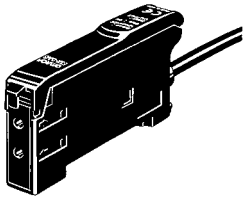

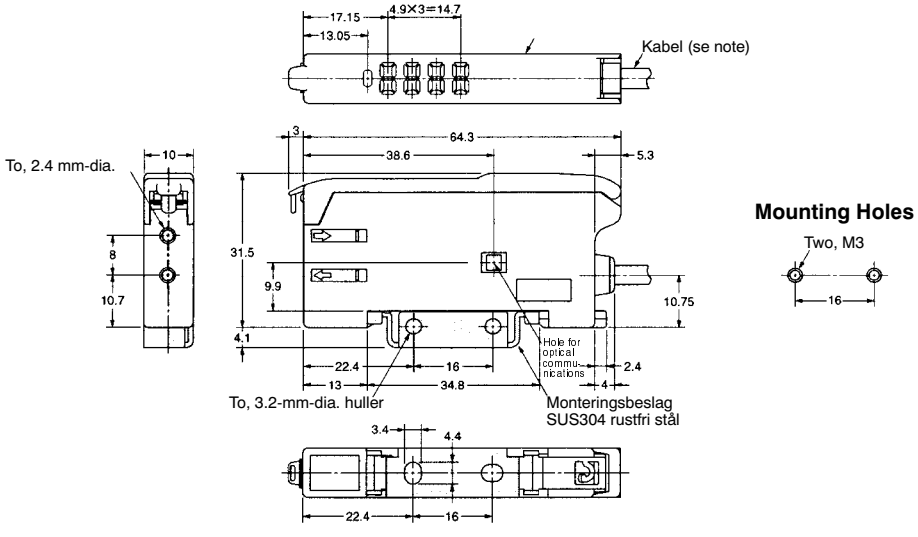

Mounting Holes

Note: På E3X-DA11-N/DA41-N/DAB11-N, anvendes ø4, 3-leder PVC kabel med et ledertværsnit på 0.45 mm^2
På E3X-DA21-N/DA51-N, anvendes ø4, 4-leder PVC kabel med et ledertværsnit på 0.2 mm^2